PONTIFICIA UNIVERSIDAD CATOLICA DE CHILE
ESCUELA DE INGENIERÍA

INFLUENCE OF THE MECHANICAL PROPERTIES OF FRICTION DAMPERS ON THE SEISMIC RESPONSE OF STEEL FRAME STRUCTURES

MATHIAS NICOLAS GELB ACEVEDO

Thesis submitted to the Office of Research and Graduate Studies
in partial fulfillment of the requirements for the degree of
Master of Science in Engineering

Advisor:
DIEGO LÓPEZ-GARCÍA

Santiago de Chile, December, 2014

© MMXIV, MATHIAS NICOLAS GELB ACEVEDO

PONTIFICIA UNIVERSIDAD CATOLICA DE CHILE
ESCUELA DE INGENIERÍA

INFLUENCE OF THE MECHANICAL PROPERTIES OF FRICTION DAMPERS ON THE SEISMIC RESPONSE OF STEEL FRAME STRUCTURES

MATHIAS NICOLAS GELB ACEVEDO

Members of the Committee:
DIEGO LÓPEZ-GARCÍA
MATÍAS HUBE GÍNESTAR
GERARDO ARAYA LETELIER
LUCIANO CHIANG SÁNCHEZ

Thesis submitted to the Office of Research and Graduate Studies
in partial fulfillment of the requirements for the degree of
Master of Science in Engineering

Santiago de Chile, December, 2014

© MMXIV, MATHIAS NICOLAS GELB ACEVEDO

To Andrea, my parents, my family

and my friends. Thank you.

ACKNOWLEDGEMENTS

I wish to thank my advisor, Professor Diego López-García for his guidance, support and help during this study. I am thankful for the time he spent advising me and helping me conduct this thesis, as well as for how he has helped me improve as a professional and as a person. I also wish to thank the following professors who have shown interest and advice throughout the elaboration of this thesis: Matías Hube, Rafael Riddell, Gerardo Araya and Luciano Chiang. A special thanks to Professor Robert Levy, who during his visit at the Pontificia Universidad Católica de Chile, provided useful advice and support.

I wish to extend my gratitude to my fellow postgraduate students at the Structural and Geotechnical Engineering Department, who not only helped make a pleasant environment, but also provided support and helpful advice: Felipe Rubilar, Felipe Toro, Alix Becerra, Antonio Salazar, Javier Pardo, María de los Ángeles Jordán, Álvaro Muñoz, Stalin Alcívar, Marcelo Semblantes, Felipe Quitral, Daniel González, Sebastián Castro, Felipe Sanz and Emmanuelle Sallin. As well, thank you to the staff of the department: Jenifer Flores, Josefina Uribe, Carlos Abarca and Luis.

Finally, I thank my friends and my family: my parents, my siblings and my cousins for the strength and support, which allowed me to succeed in this endeavor. A very special thanks to Andrea Kam, who has shown nothing but love and support throughout this study, helping me weather the hardships and rough times. I am infinitely thankful and blessed to be surrounded by people who constantly encourage and help me improve.

This thesis was supported by the National Research Center for Integrated Natural Disaster Management CONICYT/FONDAP/15110017. This support is gratefully acknowledged.

TABLE OF CONTENTS

LIST OF FIGURES

LIST OF TABLES

RESUMEN

El objetivo de esta tesis consiste en identificar y cuantificar la influencia de las propiedades mecánicas de disipadores de fricción sobre la respuesta sísmica de marcos de acero. Un disipador de fricción puede ser modelado como una arriostra, caracterizada por su rigidez elástica, en serie con un dispositivo de fricción de Coulomb, caracterizado por su fuerza de activación. Se consideraron tres marcos realistas de acero de 3, 6 y 9 pisos. Se analizó la respuesta sísmica de estas estructuras equipadas con arriostras de distintas rigideces y con dispositivos de fricción de distintas fuerzas de activación. La respuesta sísmica fue obtenida mediante análisis tiempo-historia no-lineal utilizando como excitación sísmica registros reales. También se analizó la posible influencia del número de pisos, de la distribución en altura de las propiedades mencionadas, y de las características de los registros sísmicos. Los resultados obtenidos indican que la reducción de la respuesta de desplazamiento de entrepiso del marco de 3 pisos es principalmente controlada por la rigidez de las arriostras, mientras que la reducción de la misma respuesta en los marcos de 6 y 9 pisos es controlada tanto por la rigidez de las arriostras como por los dispositivos de fricción. También se encontró que una distribución en altura uniforme de la fuerza de activación de los dispositivos de fricción resulta en menores fuerzas axiales en las columnas y en menores aceleraciones de piso que aquéllas que resultan cuando la distribución en altura es variable. Finalmente, el estudio también indica que la distribución en altura de la rigidez de las arriostras y las características de la fuente sismogénica de los registros sísmicos no son de mayor relevancia.

Palabras claves: disipadores de fricción, análisis tiempo-historia no lineal, marcos de acero

ABSTRACT

The objective of this thesis consists of identifying and quantifying the influence of the mechanical properties of friction dampers on the seismic response of steel frames. A friction damper can be modeled as an elastic brace, characterized by its stiffness, in series with a Coulomb friction device, characterized by its activation force. Three realistic steel frames of 3, 6 and 9 stories were considered. In order to observe the influence of each of the aforementioned properties on the seismic response, the structures were equipped with braces of varying stiffness and with friction devices of varying activation forces. The seismic response was obtained through nonlinear time-history analysis using real seismic records as the ground motion input. Other relevant properties such as the number of stories, the height-wise distribution of the properties and the characteristics of the seismic input were also analyzed. The study concludes that the reduction of the inter-story drift response of the 3-story structure is mainly controlled by the stiffness of the braces, while that of the 6- and 9-story structures is roughly equally controlled by both the friction devices and the braces. It was also found that a uniform height-wise distribution of the activation force of the friction devices results in lower axial forces in the central columns and lower floor accelerations with respect to those obtained with a varying height-wise distribution. Finally, the study also concludes that neither the height-wise distribution of the brace stiffness nor the seismic source of the ground motion records are of significant relevance.

Keywords: friction dampers, nonlinear time-history analysis, steel structures.

1. INTRODUCTION

Conventional seismic design codes allow for structures to be designed in such a way that the forces induced during strong earthquakes may exceed the elastic capacity of the building. This inelastic behavior is the mechanism through which typical constructions dissipate energy, and although it achieves the principal objective of avoiding collapse, it can ultimately lead to heavy structural damage that may be as expensive to repair as to replace a collapsed structure (Pall and Marsh, 1982). Two of the preferred lateral force resisting configurations for steel frames are the moment-resisting frames (MRF) and the braced moment-resisting (BMR) frames (Pall and Marsh, 1982). Damage observed in the 1994 Northridge earthquake ($M_w = 6.7$), however, questioned the ability of these types of framed systems to perform reliably during strong ground motions (Youssef et al., 1995). This led to the need of alternative types of lateral resisting systems that are less prone to earthquake damage. One alternative that developed from this need consists of equipping moment-resisting frames with passive energy dissipation devices such as viscous dampers or friction dampers.

Friction dampers such as the ones proposed by Pall and Marsh (1982) and Fitzgerald et al. (1989) are a valid alternative for the reduction of the seismic response of various types of structures, as previous studies have shown (Filiatrault and Cherry, 1988, Pall and Marsh, 1982). The behavior of braced friction dampers that do not require inelastic buckling can be theoretically described as conceptually similar to that of a mechanical system made up of two components in series: a component that behaves as an elastic spring, characterized by its stiffness, and a component that behaves as a purely frictional device, characterized by an activation force (Grigorian et al., 1993, Moreschi and Singh, 2003). The objective of this thesis is to determine the individual influence of each of these two components on the seismic response of steel frames.

The general objective of this study consists of identifying and quantifying the influence of the mechanical properties of friction dampers on the seismic response of steel frames.

The mechanical properties of interest are the stiffness of the bracing of the dampers and the activation force of the friction device. The response quantities considered are: maximum and residual inter-story drift ratio, absolute floor acceleration, and axial force in the columns at the bay where the friction dampers are located. A more specific objective is to determine how the seismic response of steel moment frames equipped with friction dampers is influenced by: 1) the number of stories of the structure; 2) the height-wise distribution of the mechanical properties of the friction dampers ; and 3) the characteristics of the seismic excitation.

The expected results of this thesis are: a) identification of the influence of each of the mechanical properties of the friction dampers (the stiffness component and the friction component) on the seismic response of steel frames; b) identification of the optimal properties of friction dampers; and c) development of practical design criteria for steel frames equipped with friction dampers. Identification of the optimal properties by means of practical procedures is valuable in the sense that it can lead to applicable design criteria where the properties of the friction dampers are optimal, understanding by optimal the values of the properties which in some way maximize one or more desirable properties of seismic resistant structures (i.e., lesser structural damage, lesser non-structural damage, higher reliability, etc.), or minimize certain responses (i.e., floor acceleration, inter-story drifts).

To achieve these objectives, the seismic response of three benchmark structures of 3, 6 and 9 stories, with and without friction dampers, was thoroughly evaluated. The 3- and 9-story structures are described in Ohtori et al. (2004), and the 6-story structure is described in Hall (1995). The response of the base structures (i.e., the structures without friction dampers) is the benchmark response versus which the performance of the same structures but equipped with friction devices are compared. Several different combinations of the mechanical properties of the dampers were considered. Numerical simulations consisting of nonlinear time-history analysis were carried out for each combination. These dynamic analyses were performed using the open source software OpenSEES (Mazzoni et al., 2006). The seismic excitations considered in these simulations corresponds to two sets of recorded seismic ground motions. The first set consists of 40 ground motions recorded in the 2010 Maule earthquake (www.renadic.cl). The second set is the FEMA P-695 Far Field set (FEMA P-695, 2009), which is made up of 44 ground motions. In both cases, the seismic response was taken equal to the median of the responses to each individual ground motion.

A review of previous studies on friction damper behavior and implementation is given in Chapter 2, along with an overview of the literature relevant to the desired objectives. Chapter 3 describes the seismic records used in the analysis, the structures chosen for this study, the range of values of the mechanical properties of the friction dampers, and the modeling of these components. Chapter 4 describes the results obtained from the numerical simulations mentioned in Chapter 3, as well as a summary and a comparison between the results for each of the three structures. Finally, Chapter 5 contains the conclusions obtained from the analysis as well as recommendations for future research.

2. DESCRIPTION OF PREVIOUS INVESTIGATIONS

Previous research and studies on passive energy dissipation, specifically on the development and application of friction dampers for the reduction of the seismic response of structures, is discussed in this chapter. Background information on the typical lateral-force resisting systems is given, as well as an overview of dry friction as a source of energy dissipation. Several proposed friction devices are discussed, and a summary of several studies, both analytical and experimental, that have been carried out on such devices is provided. Special attention is given to analytical studies on the seismic response of structures equipped with friction dampers modeled using an ideal Coulomb friction model.

2.1. Background information on friction damping in structural systems

Strong ground motions induce lateral forces on buildings. Such forces make buildings move in an oscillatory manner, and the amplitude of these oscillations is proportional to the input energy. Before energy dissipation devices were widely implemented, this input energy was dissipated almost in its entirety by the building through inelastic deformations in structural elements (Popov et al., 1993). This design criterion leads to permanent damage in many structural elements caused by the inelastic deformations which they must undergo in order to dissipate energy. The economic cost of repairing such extensive inelastic damage may be as high as that of replacing a collapsed structure (Pall and Marsh, 1982). In order to reduce the degree of inelastic deformations in structures, research on alternative energy dissipation methods became widespread (Christopoulos et al., 2006).

2.1.1. Lateral-force resisting systems

The two preferred lateral force resisting systems for steel structures are the Moment-Resisting Frames (MRFs) and the Braced Moment-Resisting (BMR) frames (Figure 2.1), which dissipate energy through inelastic deformations in their structural elements (Popov et al., 1993, Pall and Marsh, 1982). MRFs are advantageous due to their stable ductility behavior during cyclic loads, although the 1994 Northridge earthquake ($M_w = 6.7$) caused brittle failure in beam-to-column connections of several steel MRFs (Youssef et al., 1995). This undesirable response led to question the predictability of MRFs when subjected to strong ground motions. The Special Moment-Resisting Frame (SMRF), was adopted in several seismic codes as an improved, more predictable structure than the MRF under seismic loads, by imposing special requirements such as: the ability of the connections to develop the strength of the connected member, strong-column/weak-beam behavior, and other criteria that improved the behavior of the structure in intense cyclic loading (Hamburger et al., 2009).

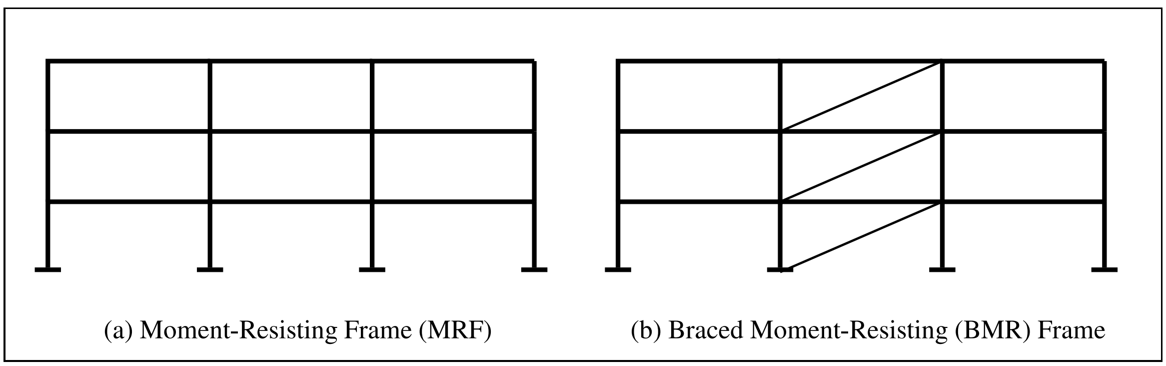

Figure 2.1: Traditional lateral-force resisting systems

On the other hand, BMR frames are preferred for their better performance under severe earthquakes, but are disadvantageous due to the fact that the braces respond very differently to tensile loads versus compressive loads, where the response is buckle-dominated (Pall and Marsh, 1982, Sabelli et al., 2003). The need for a system that can perform more predictably and in a more stable manner under cyclic reversing loads, and capable of limiting inter-story drifts by adding stiffness, led to the development of Friction Damped Braced (FDB) frames (Figure 2.2).

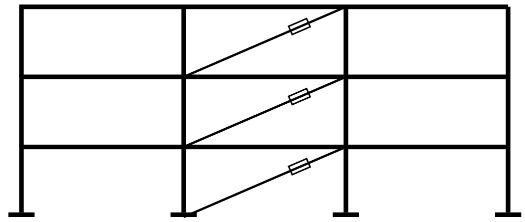

Figure 2.2: Friction-Damped Braced (FDB) Frame

2.1.2. Dry friction

Friction is an attractive mechanism for energy dissipation due to its non-destructive nature. In the context of a study on friction dampers intended to control the seismic response of structures, dry friction, i.e., the resisting force that arises due to the relative motion of two solid surfaces in contact, can be appropriately described by considering the case of two plates in contact subjected to the time-varying force $F(t)$ at their ends and the static normal force N (constant) perpendicular to the flat contact surface of the plates (Figure 2.3).

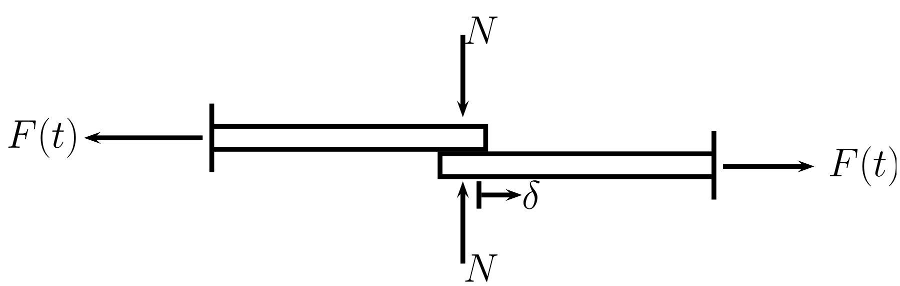

Figure 2.3: Sliding friction of two sliding plates in contact

As a result of dry friction, a friction force f_f that opposes $F(t)$ develops at the contact surface. The magnitude of the friction force f_f is given by

$$f_f \leq F_f = \mu N$$

where μ is the coefficient of friction (an adimensional quantity). In its most simple characterization, μ depends only on the type and condition of the materials of the surfaces in contact, and does not depend neither on the velocity of the plates relative to each other nor on the magnitude of N. This characterization is known as Coulomb friction, and it will be shown later that it is indeed appropriate to reasonably describe the behavior of friction dampers, even though it is actually an ideal model. Hence, if the friction between the plates shown in Figure 2.3 is of the Coulomb type, F_f has a constant value, and relative motion between the plates occurs only when $F(t)$ exceeds F_f. If the displacement of the plates relative to each other is denoted by δ, the f_f vs. δ relationship is characterized by the perfectly rectangular hysteresis loops shown in Figure 2.4.

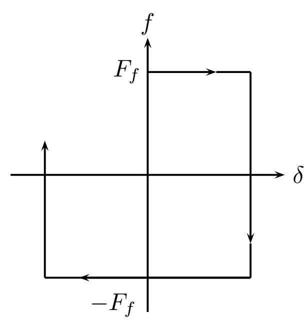

Figure 2.4: Idealized hysteresis loop for Coulomb friction

Testing of different flaying surfaces reported by Pall and Marsh (1982) has shown that stable hysteresis loops similar to that of the ideal Coulomb model can be achieved by many materials in contact to each other. Although some materials, like steel on steel, produce less stable results as shown in Grigorian et al. (1993), this research also indicates that steel on brass produce hysteresis loops that are very similar to the idealized Coulomb friction loop. Experiments by Constantinou et al. (1990) have shown that polished steel on Teflon® also produce hysteresis loops that closely resemble those of ideal Coulomb friction.

2.2. Description of existing friction damper devices

The non-destructive nature of dry friction provides an attractive energy dissipating mechanism. Previous researchers have developed and studied the behavior and application of a variety of passive energy dampers which use friction to dissipate energy.

2.2.1. Pall and Marsh device

The device described in Figure 2.5 was proposed by Pall and Marsh (1982). The device is a cross-brace friction damper that is designed to slip only when subjected to severe seismic loads, and before yielding occurs in the rest of the frame. Since the braces are designed to work only in tension, the novelty of the device is that slip occurs simultaneously along both braces (i.e., the one in tension and the one in compression). When the device is subjected to a lateral load, the brace in compression buckles, and the braking pads slip before the brace in tension yields, which through the four links of the device, activate the friction devices of both braces (Figure 2.6). The buckled brace will then straighten out when the cycle reverses (Filiatrault and Cherry, 1987).

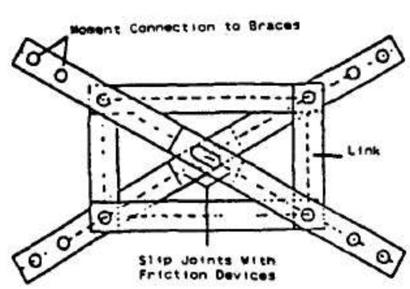

Figure 2.5: Device proposed by Pall and Marsh (1982)

Despite its effectiveness, its major disadvantage lies in the fact it requires inelastic buckling in the braces (Fitzgerald et al., 1989). Further, the activation force of the device is relatively small, which means that several devices are needed when slippage is to be prevented under lateral loads that are not of seismic nature, such as wind loads (Filiatrault and Cherry, 1987).

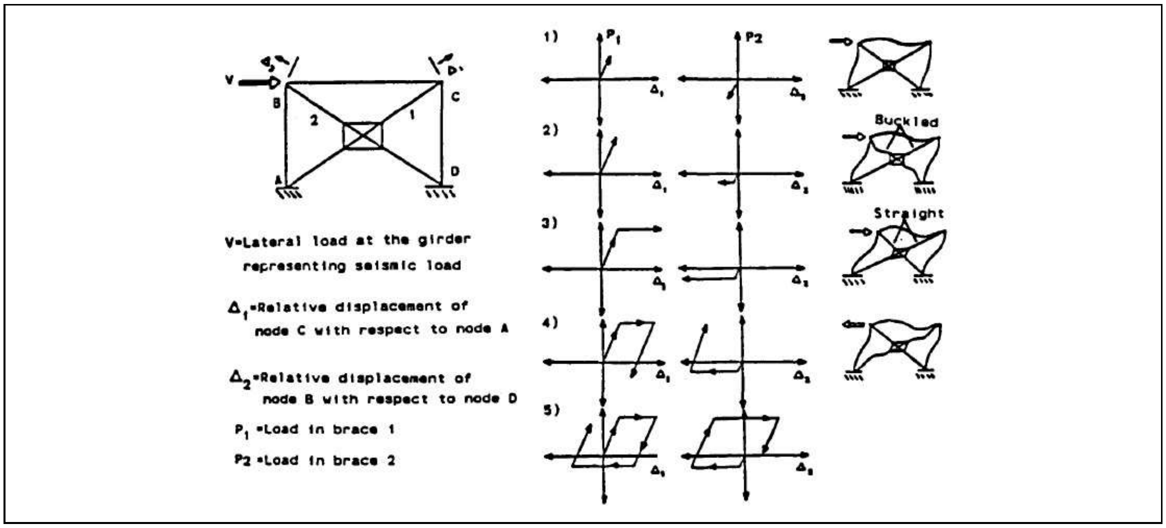

Figure 2.6: Friction Device: slips in tension before yield loads, buckles in compression (Filiatrault and Cherry, 1987)

2.2.2. Slotted Bolted Connections

The previously mentioned limitations of the Pall and Marsh device, i.e., low activation force and inelastic buckling of the braces, led to the development of devices based on Slotted-Bolted Connections (SBC). For instance, the SBC device proposed by Fitzgerald et al. (1989) uses friction as the dissipating mechanism but without the need of inelastic buckling in the braces. The construction of SBC devices does not require exotic materials nor precision manufacturing, an advantage over several alternatives (Grigorian et al., 1993). A SBC device is typically located at an end of a conventional brace (Figure 2.7) and slippage occurs at the connection between the device and the gusset plate of the brace. The relative motion between the two sliding members produces the friction through which seismic energy is dissipated. The slot of the device and the slot of the gusset plate are initially aligned, and linked to each other through bolts located at the center of the slots. The axes of the slots coincide with the axis of the brace. Slippage along the slots occurs when the axial force in the brace exceeds the activation force of the SBC device (Figure 2.8).

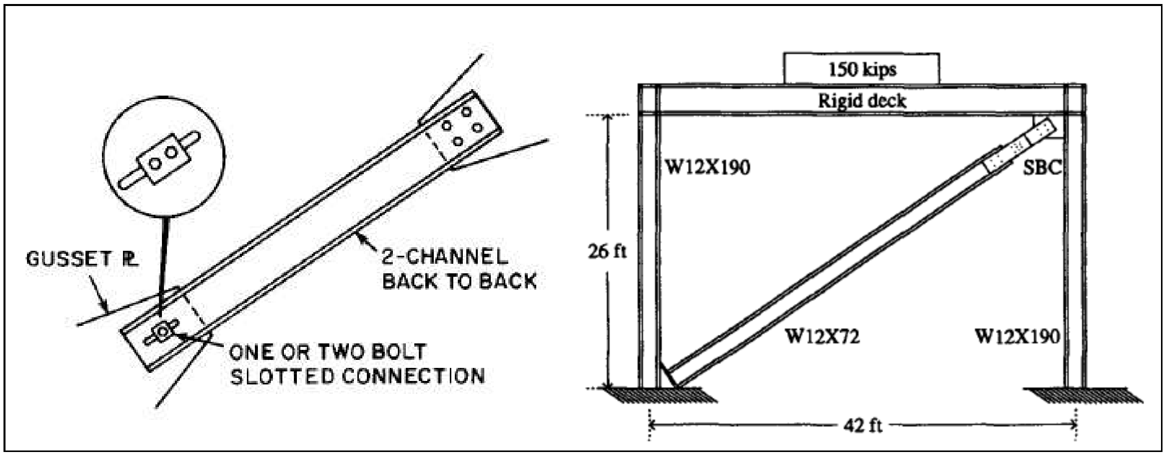

Figure 2.7: Slotted-bolted connection device, and implementation (Fitzgerald et al., 1989, Grigorian et al., 1993)

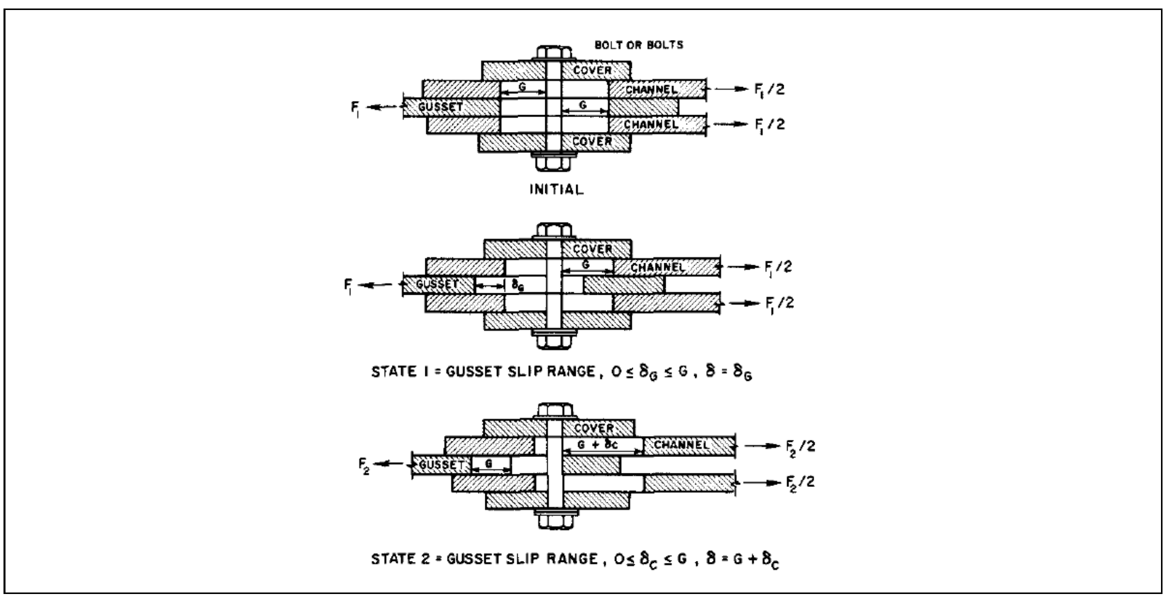

Figure 2.8: The first slip occurs at the gusset plate and the second when the cover plate slips (Fitzgerald et al., 1989)

2.2.3. Sumitomo Friction Damper

Another commercially available friction damper was designed and developed by Sumitomo Metal Industries, Ltd.. This cylindrical device contains copper alloy friction pads which slide directly upon the steel surface of the inner case (Towashiraporn et al., 2002). In the implementation proposed by Aiken et al. (1993), the axis of the device is parallel to the axis of the beams (i.e., horizontal), one end of the device is connected to a beam, and the other end is connected to a stiff chevron bracing (Figure 2.9).

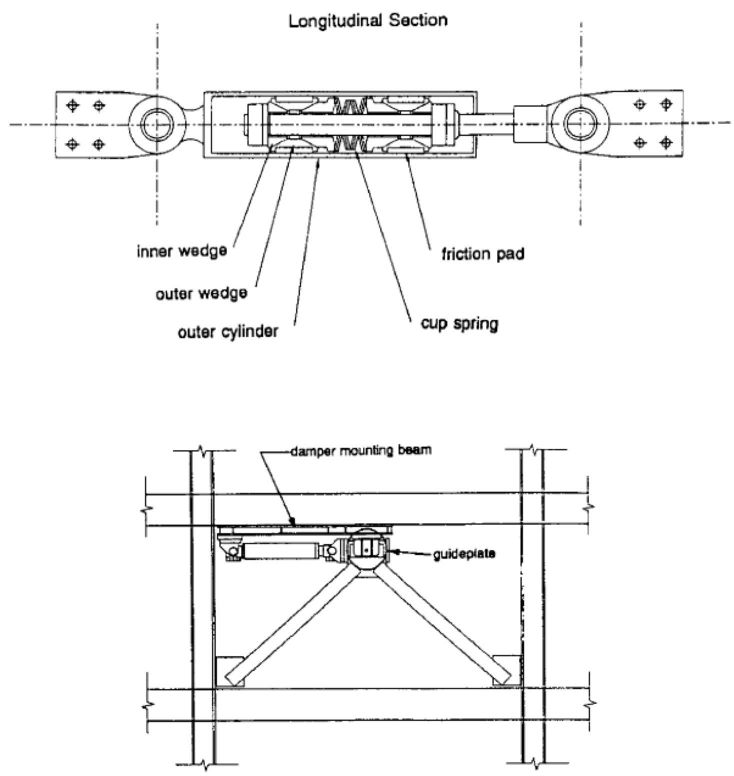

Figure 2.9: Friction damper developed by Sumitomo Metal Industries, Ltd. Japan (Aiken et al., 1993)

This device was originally implemented in railway applications, but was later used in multi-story office and residential buildings in Japan, such as the Sonic City Office Buidling in Omiya City and the Asahi Beer Azumabashi Building in Tokyo (Constantinou and Symans, 1992).

2.3. Experimental studies on friction dampers

Prototypes of the previously described friction dampers have been studied in order to characterize their dynamic behavior as well as their hysteresis loops. Other experiments were carried out in order to determine the effect of friction devices on the seismic response of structures.

2.3.1. Cyclic loading of prototypes and hysteresis behavior of friction dampers

Cyclic load tests were carried out on prototypes based on the friction damping mechanism proposed by Pall and Marsh (1982) using standard testing apparatus (Filiatrault and Cherry, 1987). One end of the diagonal link of the friction damper was bolted to a rigid testing bench, and the other was attached to a vertical hydraulic actuator. Results showed stable hysteresis loops, almost perfectly rectangular, with very little slip force degradation. Imperfections were noted at opposite corners of the loops (Figurre 2.10) due to fabrication tolerances between: (a) the bolts and the four corner holes of the mechanism; and (b) the central clamping bolt and the corresponding slot in the brake lining pads. If these are minimized, the hysteresis loop becomes even more similar to the ideal rectangular loop.

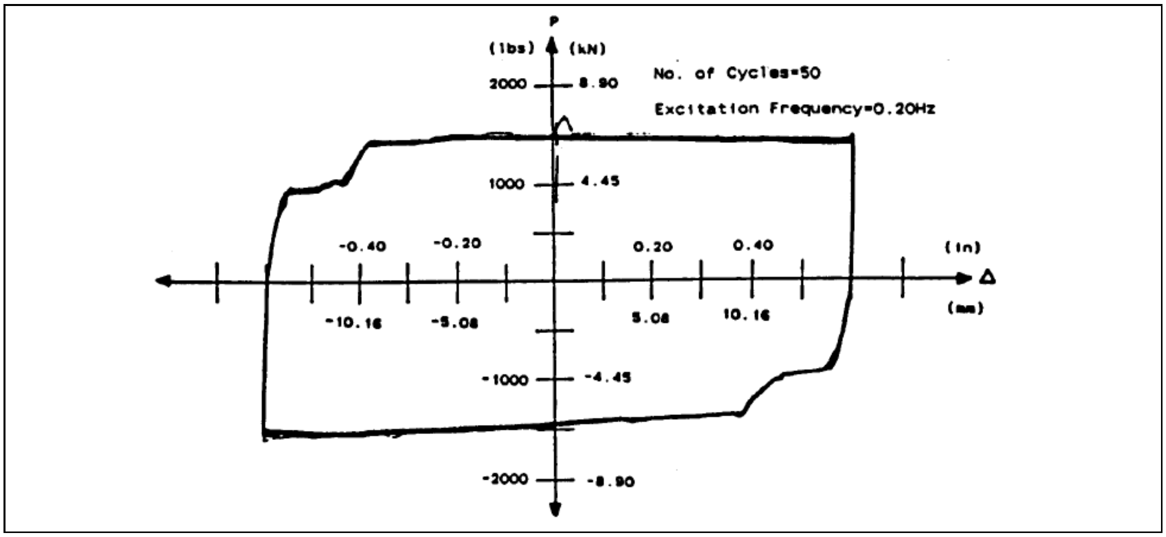

Figure 2.10: Experimental hysteresis loop of prototype Pall and Marshall friction device (Filiatrault and Cherry, 1987)

Laboratory tests of several configurations of SBC devices were also carried out to determine which configurations have the most stable hysteresis loops and the least loss of bolt tension. Venuti (1976) utilized a configuration consisting of hardened, load-indicating washers under the bolt head, as well as both plate washers and hardened, load-indicating washers under the nut. Experimental testing on said configuration showed that degradation of frictional slip load was low, but the initial tension of the bolts was lost with repeated cycles. Laboratory experiments by Fitzgerald et al. (1989), performed using SBCs with three single bolt ”S”series, and three double bolt ”D”series and with solon washers, showed that such configuration exhibits much more stable hysteresis loops, and lesser loss of tension in the bolts (Figure 2.11).

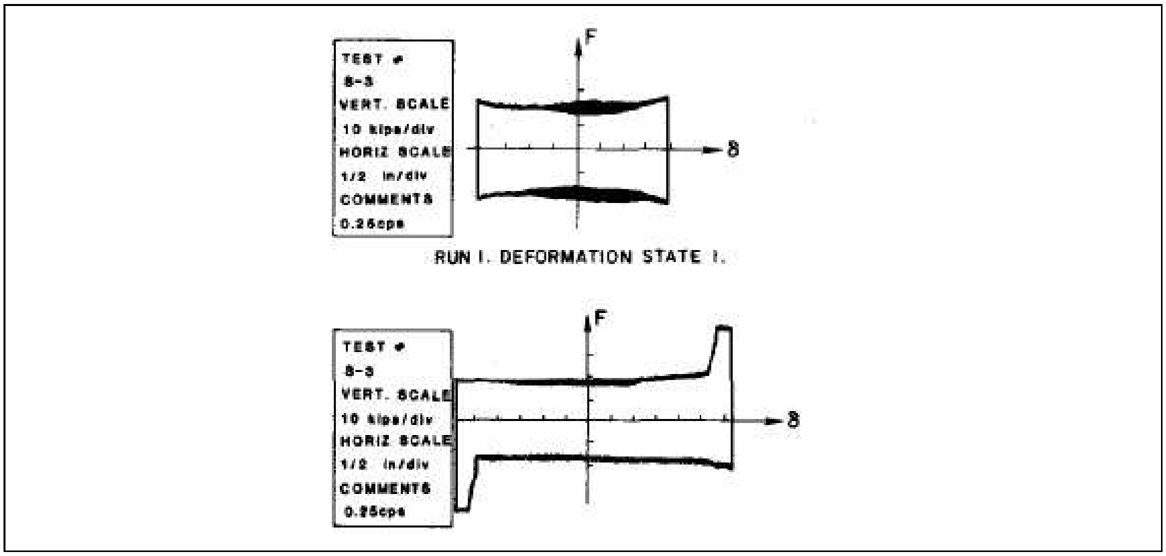

Figure 2.11: The first state is achieved when the gusset plate slips, while the second occurs when the cover plates slip (Fitzgerald et al., 1989)

Similar SBC specimens with Belleville washers were tested by Grigorian et al. (1993) considering two different contact surfaces: steel on steel, both cleaned to clean mill scale condition, and brass on steel. These experimental tests showed that steel on brass produced more stable hysteresis loops with almost negligible slip force degradation (Figure 2.12).

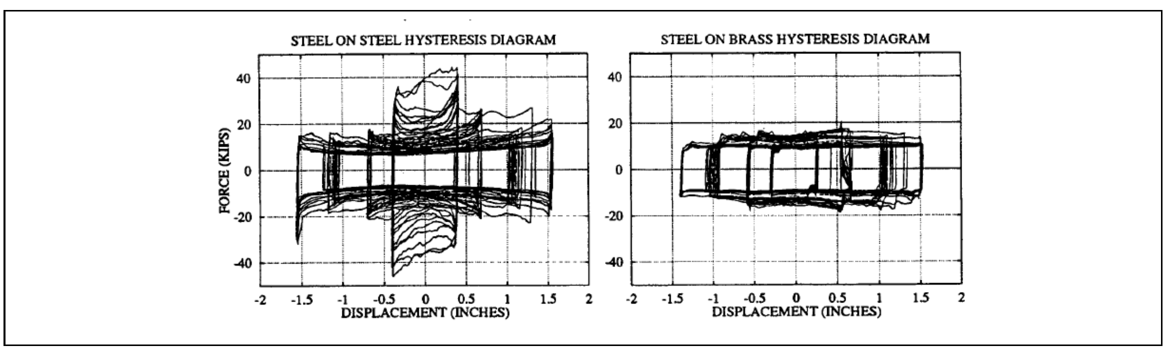

Figure 2.12: Hysteresis diagrams for SBC devices using steel on steel and steel on brass (Grigorian et al., 1993)

Grigorian et al. (1993) added a SBC configuration with brass inserts to a 1-story steel frame, and subjected the structure to four real earthquake records in a shaking table. The tests demonstrated the validity of the assumption of elastic, perfectly-plastic behavior of SBCs with brass inserts.

Experimental testing on scaled 9-story structures equipped with various types of dampers was carried out by Aiken et al. (1992). Among the various types of damping systems tested were Sumitomo friction dampers. The 9-story structure was subjected to several real seismic records on a shaking table, and hysteresis loops of the dampers were obtained. The test results for the structure subjected to the Llolleo record of the 1985 Chile earthquake were excellent (Figure 2.13). The hysteresis loop of the friction damper shows almost no variation in the slip load (Aiken et al., 1992).

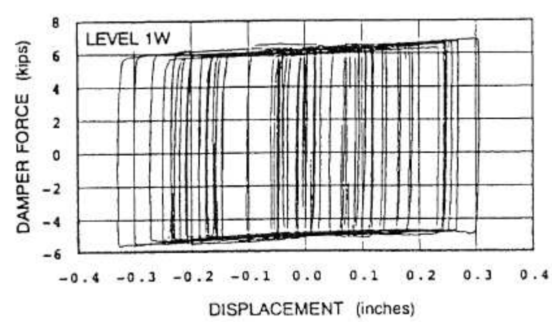

Figure 2.13: Hysteresis loops for Sumitomo friction dampers implemented in a scaled 9-story steel structure subjected to the Llolleo, Chile 1985 record (Aiken et al., 1992)

2.3.2. Experimental testing of structures implemented with friction dampers

Several experimental studies on the seismic response of frame structures equipped with the friction device proposed by Pall and Marsh (1982) were carried out. A study on one-third scale models of a 3-story frame structure was carried out on a shaking table using several earthquake records of varying intensities (Filiatrault and Cherry, 1987). The frame structure was tested without friction dampers in both MRF and BMR frame configurations, and with friction dampers in a FDB frame configuration. This study concluded that the FDB frame sustained no damage in any of its elements, whereas the MRF suffered damage in its beams at the first and second floors, and the BMR frame suffered inelastic buckling in the diagonal braces. Further, both deflections and accelerations were significantly smaller in the FDB frame (Figure 2.14).

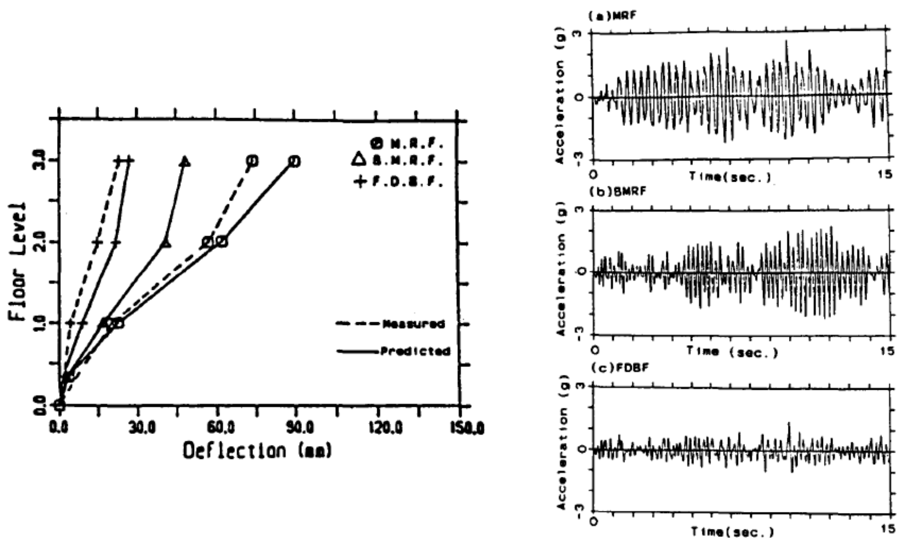

Figure 2.14: Experimental deflection and third-story absolute acceleration of tested frames equipped with Pall and Marsh friction devices (Filiatrault and Cherry, 1987)

A study by Aiken et al. (1988) on a scaled model of 9-story steel MRF, modified to include friction dampers as proposed by Pall and Marsh (1982), also demonstrated the superior seismic performance of FDB frames. The MRF and FDB frame were subjected to several seismic excitations on a shake table, and their responses were compared to each other. The total energy dissipated by the friction devices was observed to be equal to approximately 70 % of the input energy. The peak story acceleration and peak story drift profiles were greatly reduced in the FDB frame with respect to those in the original MRF (Figure 2.15).

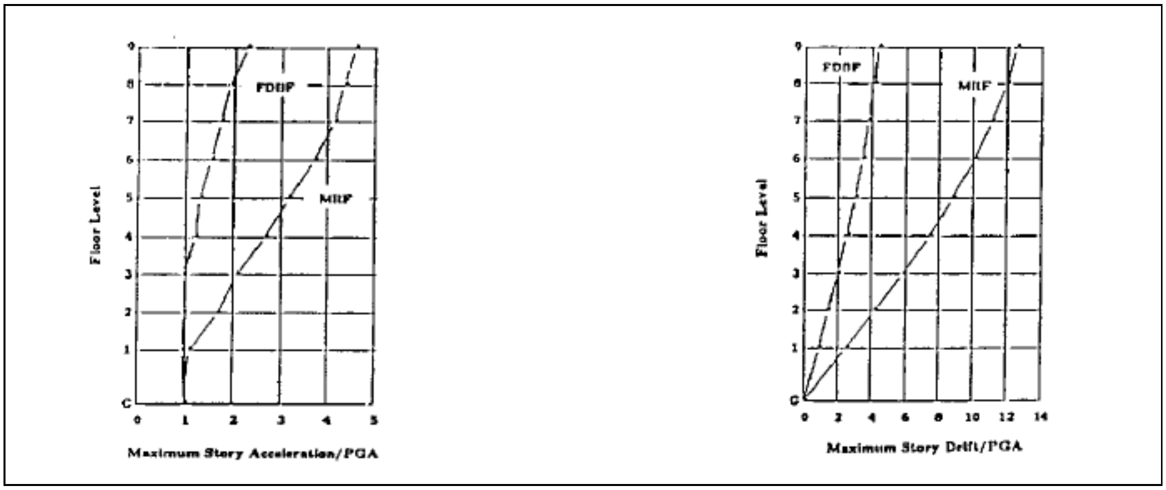

Figure 2.15: Peak story drift and peak story acceleration profiles for scaled 9-story structure equipped with Pall and Marsh friction devices(Aiken et al., 1988)

Aiken et al. (1993) reported a study on Sumitomo dampers implemented in a scale model of a 9-story MRF. The original (i.e., without friction dampers) MRF and the same structure equipped with Sumitomo dampers (i.e., a FDB frame) were tested at a shaking table considering various input seismic records. Results showed that the drift response of the FDB frame was 10 to 60 % less than that of the MRF, and floor accelerations were 25 to 60 % less than those of the MRF. These large variations showed that the reduction is highly dependent on the input motion. Another interesting result of this study is that if optimum performance is desired, the activation force of devices located at different stories should be selected based on results given by nonlinear dynamic analysis.

2.4. Analytical studies of friction dampers

2.4.1. Analytical modeling and implementation of friction dampers

Analytical studies on FDB frames using the Pall and Marsh devices have shown that the reduction of the roof displacement response can be as high as 40 % with respect to that of a MRF, and as high as 50 % with respect to that of a BMR frame (Pall and Marsh, 1982). This same study showed that the seismic performance of FDB frames is better in terms of lesser inelastic deformation and reductions of up to 80 % of the base shear response. Studies by Filiatrault and Cherry (1987), which used an improved analytical model, confirmed the superior seismic performance of FDB frames over those of MRF and BMR frames, but their results differed by as much as 30 % with respect to those given by the approximate model used by Pall and Marsh (1982).

Colajanni and Papia (1995) compared the seismic behavior of ordinary cross-bracing systems with that of the same systems equipped with friction devices. The response of both systems was evaluated in terms of adimensional quantities, which allowed for a direct comparison between the behavior of both systems. Results showed that the systems with friction dampers have greater available ductility and a better performance due to the stability of the hysteresis of the overall force-deformation relationship.

Similar studies were carried out considering FDB frames with SBC devices. Grigorian et al. (1993) analyzed the seismic response of a 1-story FDB frame equipped with a SBC device subjected to several real earthquake records. It was estimated that the SBC device dissipated approximately 85 % of the total input energy. The analytical force-deformation hysteresis loops were satisfactorily replicated by a companion experimental study, confirming that the behavior of SBC devices is close to that of an ideal Coulomb friction device.

Results given by nonlinear time-history analysis of a scaled 9-story friction-damped structure showed good agreement with those obtained in shake table tests (Aiken et al., 1992). While the analytical response of the equivalent cross-braced frame and MRF indicated yielding in some members, results indicated no yielding in the members of the friction-damped structure.

2.4.2. Influence of the mechanical properties of friction dampers on seismic response of Single Degree of Freedom systems

The studies previously mentioned in Section 2.3.1 indicate that the real behavior of actual friction devices can be reasonable approximated by using a relatively simple Coulomb friction model (Figure 2.4). As shown in previous studies, when the friction device mechanism is attached to a diagonal brace, the brace-device system can be modeled as an elastic spring in series with a Coulomb friction element. The hysteresis loop of such a system is represented in Figure 2.16, where F_f is the activation force of the friction device (sometimes also called slip load or slip force) and k_b is the stiffness of the brace. This approach considers that the behavior of a brace-device system is analogous to that of an elastic, perfectly-plastic element (Moreschi and Singh, 2003).

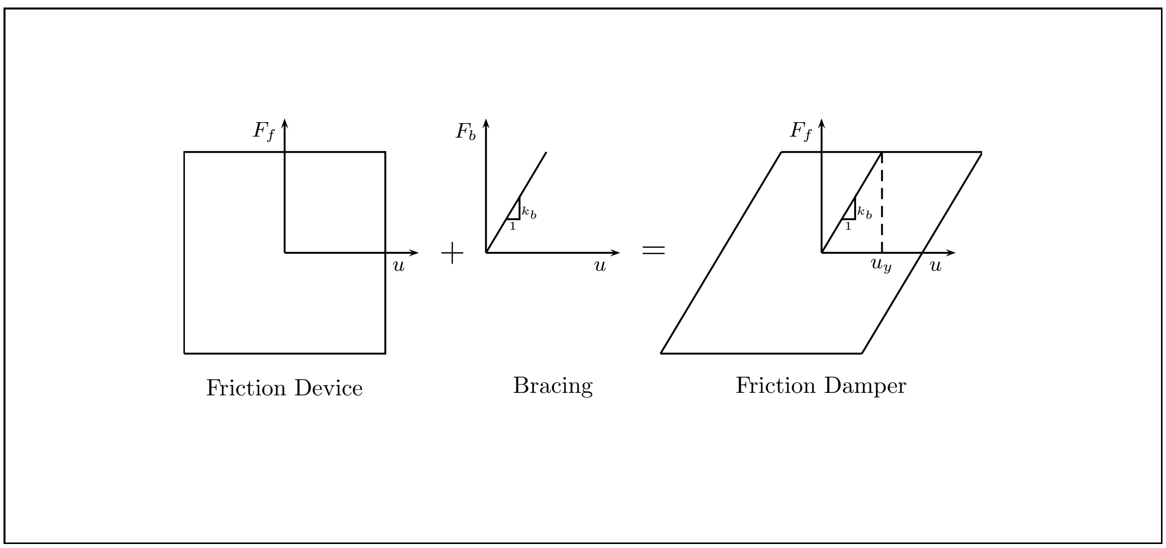

Figure 2.16: Hysteresis curve of an idealized friction device (Moreschi and Singh, 2003)

Vergara (2012) studied the response of single degree of freedom (SDOF) structures, both unbraced and braced, and in the latter case with and without friction dampers. The main objective of the research was to characterize the response of SDOF systems with friction dampers considering different levels of brace stiffness k_b and slip displacement u_y, thus determining the influence of each of these properties on the seismic response. The friction devices were modeled as elastic, perfectly-plastic devices.

The unbraced SDOF system was considered to have periods $T = [0.4, 0.6, 0.8, 1.0, 1.5, 2.0]sec$, and for each of these periods the SDOF system was subjected to 500 synthetic seismic records. The response was evaluated in terms of mean values of absolute acceleration and displacement, $a_o(T)$ and $u_o(T)$. Braced SDOF systems without friction dampers were then considered having an added stiffness k_b such that the braced period T_b is a fraction of the unbraced period T:

$$\frac{T_b}{T} = [0.05, 0.10, 0.15, ..., 0.9, 0.95]$$

Again, the response of the system was evaluated in terms of mean values of absolute acceleration and displacement, $a_e(T, T_b)$ and $d_e(T, T_b)$. Lastly, braced SDOF systems with friction devices were considered. The slip displacement u_y of the brace-device system was defined in terms of $u_e(T, T_b)$, which is the elastic deformation of the braced system, as follows:

$$\frac{u_y}{u_e} = [0.05, 0.10, 0.15, ..., 0.9, 0.95]$$

thus ensuring the activation of the friction device. As before, the response was evaluated in terms of the mean values of absolute acceleration and displacement, $a(T, T_b, u_y)$ and $u(T, T_b, u_y)$. The response of the braced SDOF with friction devices was normalized with respect to that of the unbraced SDOF system, which led to the following response ratios:

$$r_u = \frac{u}{u_o}(T, T_b, u_y) \quad r_a = \frac{a}{a_o}(T, T_b, u_y)$$

From the analysis of values of factors r_u and r_a, Vergara (2012) determined that the displacement response of an elastic, braced SDOF system equipped with a friction device is always less than that of the corresponding elastic, unbraced SDOF system. For example, when an unbraced SDOF system with $T = 1.0sec$ is braced in such a way that the period of the braced SDOF system is $T_b = 0.8sec$, the corresponding normalized displacement response ratio is $r_u \approx 0.8$. Vergara (2012) showed that the displacement response decreases with the braced period T_b, but at the expense of increasing absolute accelerations, up to the point where $r_u \approx 1.2$. If an optimally designed friction device is then added to the braced SDOF system, a slight reduction in displacement response is attained, but more importantly a considerable reduction in the absolute acceleration response is obtained.

Vergara (2012) concluded that the displacement response of a braced SDOF system with a friction device is mostly determined by the level of the brace stiffness k_b. In other words, the response of a braced SDOF system with an optimally designed friction device is only marginally smaller than that of a braced SDOF system without a friction device. However, the acceleration response of a braced SDOF system with an optimally designed friction device is indeed much smaller than that of a braced SDOF without a friction device. In general, the absolute acceleration response decreases with the activation force. It is important to note that the limitation of the study carried out by Vergara (2012) is that it concentrates only on SDOF systems. It is impossible then to generalize the results obtained to higher number of DOF without further studies.

A similar numerical study, conducted considering concrete frames equipped with various types of dampers, obtained similar conclusions for the case of friction dampers (Vulcano and Mazza, 2000). This study concluded that the response of structures equipped with friction dampers is more sensitive to the value of the activation force when the period of the unbraced structure is relatively low.

3. DESCRIPTION OF THE ANALYSIS PROCEDURE

To properly quantify the influence of each property of friction dampers (brace stiffness and activation force) on the seismic response of structures, a thorough numerical analysis of the seismic performance of various structures having different values of those properties was undertaken. Three benchmark steel structures were considered as the base structures. The response of these base structures was compared against the response of the base structures equipped with elastic braces of stiffness k_b, and against the response of the braced structures equipped with a friction device of activation force F_f. The seismic response was obtained through nonlinear time-history analysis using different sets of seismic records.

3.1. Selection and scaling of ground motion records

Seismic records from real earthquakes were chosen as the source of seismic excitation for the numerical simulations. The focus of this thesis is on the impact of the mechanical properties of friction dampers, therefore to properly assess this influence, two sets of seismic records were chosen in order to evaluate possible ground motion dependency. Since Chilean ground motions are of particular interest in this thesis, a set of seismic records was chosen from the available set of acceleration ground histories recorded during the 2010 Maule earthquake. In order to evaluate whether the influence of the properties of friction dampers depend on the characteristics of the seismic excitation, a second set of records made up of the acceleration ground histories included in the FEMA P-695 (2009) Far-Field set was considered as well.

3.1.1. Seismic records of the Maule Earthquake

The Maule Earthquake occurred on February 27^{th}, 2010, and had a moment magnitude $M_w = 8.8$. It was produced by the sudden displacement of the Nazca plate subducting into the Southamerican plate, with a rupture area of 450 km in the longitudinal (north-south) direction, and 150 km in the east-west direction (Barrientos, 2010). Seismic records are available from 31 stations, however those of Copiapó and Vallenar were discarded due to the fact that their Peak Ground Acceleration (PGA) are lower than 0.1 g, thus considered to have no engineering significance. The 29 remaining stations are spread throughout Chile in a region roughly limited by Santiago in the north (-30.5,-70.58) and Valdivia in the south (-39.83,-73.24), which is approximately requal to the whole longitudinal extension affected by the earthquake (Figure 3.1) (Barrientos, 2010).

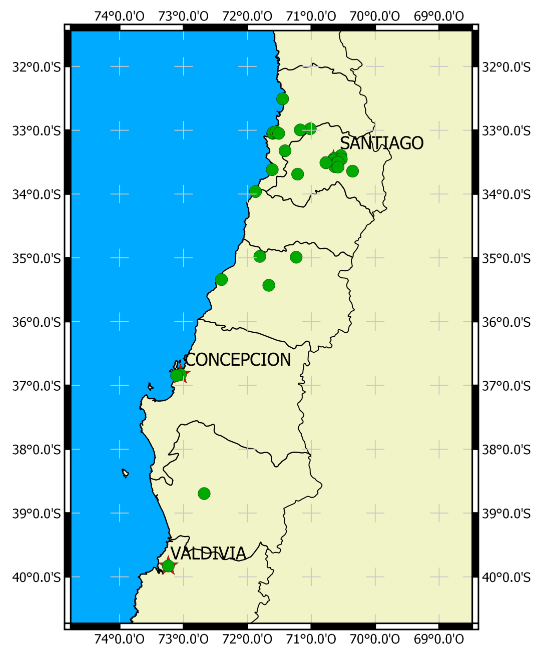

Figure 3.1: Location of the stations where ground motions were recorded during the 2010 Maule earthquake

The seismic records from the Maule earthquake were obtained through RENADIC (www.renadic.cl), the national network of accelerometers set up and maintained by the science and physics faculty of the Universidad de Chile. Each seismic record is made up of two horizontal components, and one vertical component which is not considered in this study, whose orientation depend on the station. Each component will be individually applied to the different structures being considered. The records are not classified by soil types, they are all grouped together independently of site location. Great dispersion was observed in characteristics of the seismic records such as duration and PGA, as well as in the elastic, 5 %-damped pseudo-acceleration response spectra (Figure 3.2a). Such dispersion is also a consequence of the differences in the characteristics of the soil at which each record was measured.

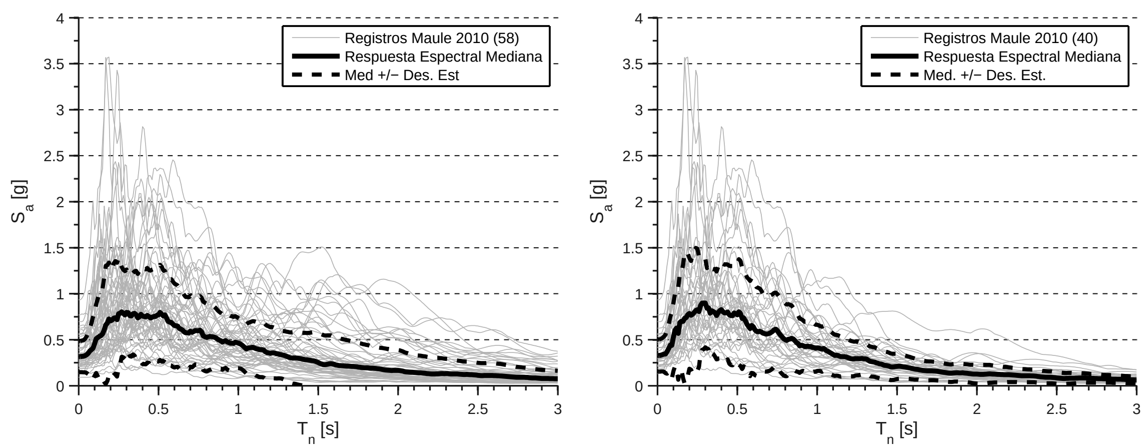

(a) All components of Maule Earthquake

(b) Selected components of Maule Earthquake

Figure 3.2: Response spectra of Maule earthquake records

Since two different sets of records are considered, it was decided that both sets have a similar number of records. In order to achieve this objective, it was decided to select 20 records from the complete set of records of the Maule earthquake, reducing the number of individual components from 58 to 40. The records chosen are shown in Appendix B. As the interest of this investigation is centered on simulating the seismic response of 3-, 6-, and 9-story buildings to the selected seismic records, the criterion chosen to reduce the number of records consists of eliminating those records having higher spectral ordinates at long periods, i.e., at periods greater than 1.5 seconds. For this, a frequency content factor of each spectrum was calculated by multiplying each spectral ordinate by the corresponding period, and then a factor of each record was calculated by combining the factors of the corresponding horizontal components. The 9 records having the largest values of the combined factor were then eliminated. As it can be seen in (Figure 3.2b), the resulting set of records has a more homogeneous frequency content as a result of eliminating the records having an unusually large frequency content at long periods.

3.1.2. Seismic records of the FEMA P-695 far-field Set

The FEMA P-695 far-field set of records includes 22 records, i.e. 44 components, obtained from 14 different seismic events that occurred between 1971 and 1997. These events include earthquakes in California, Turkey, Japan, Taiwan and Italy. The events vary in M_w from 6.5 to 7.0, lesser than the $8.8 M_w$ of the Maule earthquake (FEMA P-695, 2009). Similarly to what was considered for the records of the Maule earthquake, the records are not separated by soil type nor by any other factor. The response spectra of this set (Figure 3.3) are similar to that of the Maule earthquake.

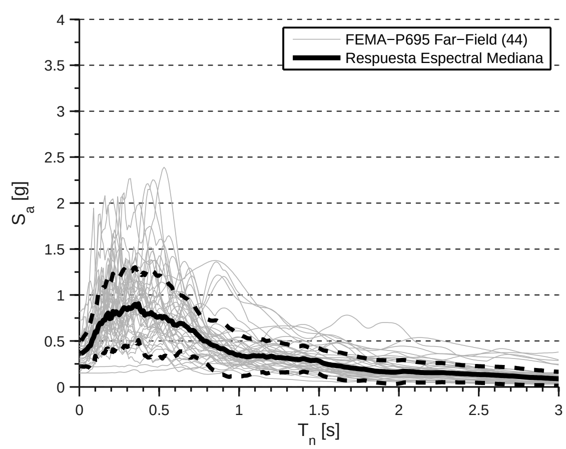

Figure 3.3: Response spectra of seismic records of the FEMA-P695 Far-Field Set

3.1.3. Scaling of the seismic records

Each record of each of the sets described before was scaled in accordance with the scaling procedure described in FEMA P-695 (2009). This methodology was chosen due to the fact that it results in median spectra that greatly resemble the Newmark-Hall spectral shape (Chopra, 1995). Further, the procedure proposed in FEMA P-695 removes variability between records due to differences in magnitude, distance from source and the source type (FEMA P-695, 2009).

The normalization factor NM$_i$ of the i^{th} record (it must be recalled that each record consists of two components, denoted here TH_1 and TH_2) is determined according to the peak ground velocity (PGV) of each record PGV$_i$, which is obtained from the geometric mean of the PGV values of the two components of the record (the geometric mean of two values is the square root of the product of the values). A value of PGV of the whole set PGV$_{set}$ is then obtained as the median of the PGV_i values. The normalization factor NM$_i$ of the i^th record is then set equal to the ratio of PGV_{set} to PGV_i. Scaled time histories $STH_{1,i}$ and $STH_{2,i}$ are then obtained by multiplying the components $TH_{1,i}$ and $TH_{2,i}$ of the i^{th} record by the corresponding normalization factor NM_i.

$$\mathrm{NM_i = PGV_{set}/PGV_i}$$

$$\mathrm{STH_{1,i} = NM_i TH_{1,i}}$$

$$\mathrm{STH_{2,i} = NM_i TH_{2,i}}$$

This process was carried out for both sets of seismic records being considered, the 20 records of the Maule Earthquake and the 22 records of the FEMA-P695 far-field set. Response spectra of the sets of scaled ground motions were obtained (Figure 3.4). As expected, the median spectra are similar to Newmark-Hall design spectra, but they are also surprisingly similar to each other even though the records have very different characteristics: the records of the Maule earthquake have a relatively large duration and were generated by a subduction type earthquake of very large magnitude, whereas the records of the FEMA P-695 far-field set have shorter durations and were generated by other types of earthquake having lesser magnitudes.

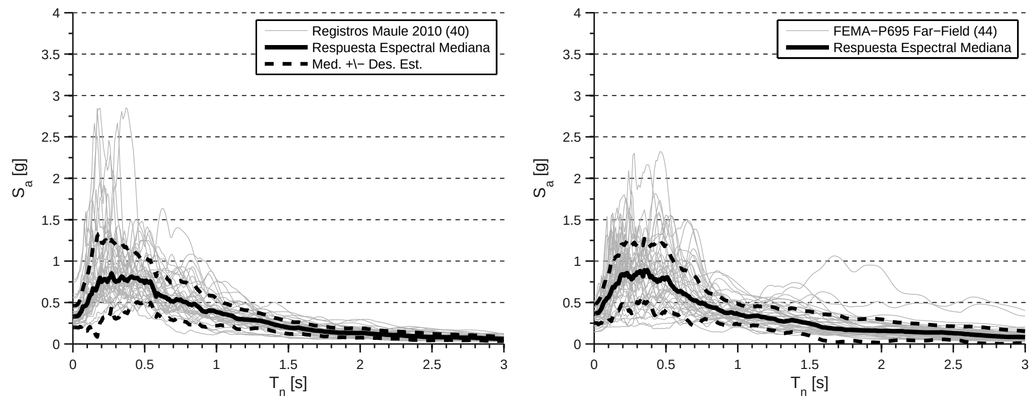

(a) 2010 Maule Earthquake (b) FEMA-P695 Far-Field Set

Figure 3.4: Normalized response spectra of the selected set of seismic records

3.2. Description of the structures and friction dampers

The structures considered in this study are steel MRF structures that have been previously presented and studied (for different purposes) in the literature. A total of three building structures were considered, having 3, 6 and 9 stories. All of them are realistic structures, and their main characteristics are described next.

3.2.1. Benchmark frames models for evaluation

The 3-story building was proposed as a benchmark structure by Ohtori et al. (2004). The building has a rectangular plan of 36.58 m by 54.87 m, with an elevation of 11.89 m. The plan consists of four bays in the north-south direction and six bay in the east-west direction. The interior bays of the structure consist of simple frames intended to carry gravity loads only. The floor system is a composite construction of concrete and steel. The lateral load-resisting system of the building is made up of perimeter MRFs oriented along the east-west orientation (Figure 3.5).

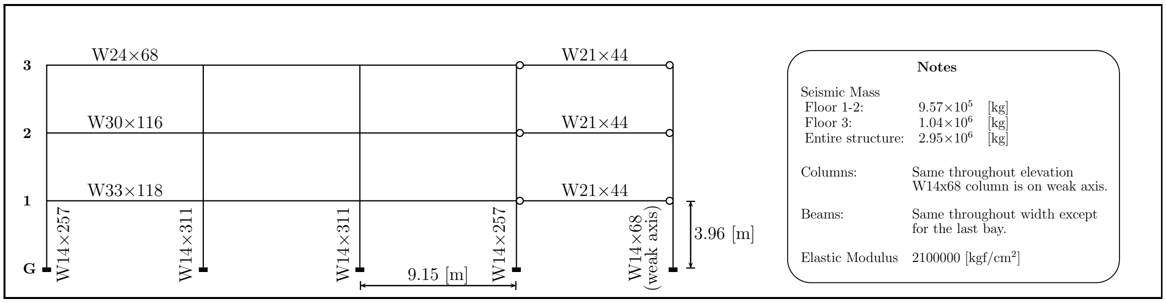

Figure 3.5: Three-story steel frame used in analysis (Ohtori et al., 2004)

The 6-story building was originally studied by Hall (1995). The building has a rectangular plan of 36.60 m by 21.90 m, with an elevation of 24.54 m. The plan consists of four bays in the north-south direction and three bays in the east-west direction. The interior bays of the structure consist of simple frames intended to carry gravity loads only. The floor system is a composite construction of concrete and steel. The lateral load-resisting system of the building is made up of perimeter MRFs. The 2D frame considered in this study is one of the perimeter MRFs oriented along the east-west orientation (Figure 3.6).

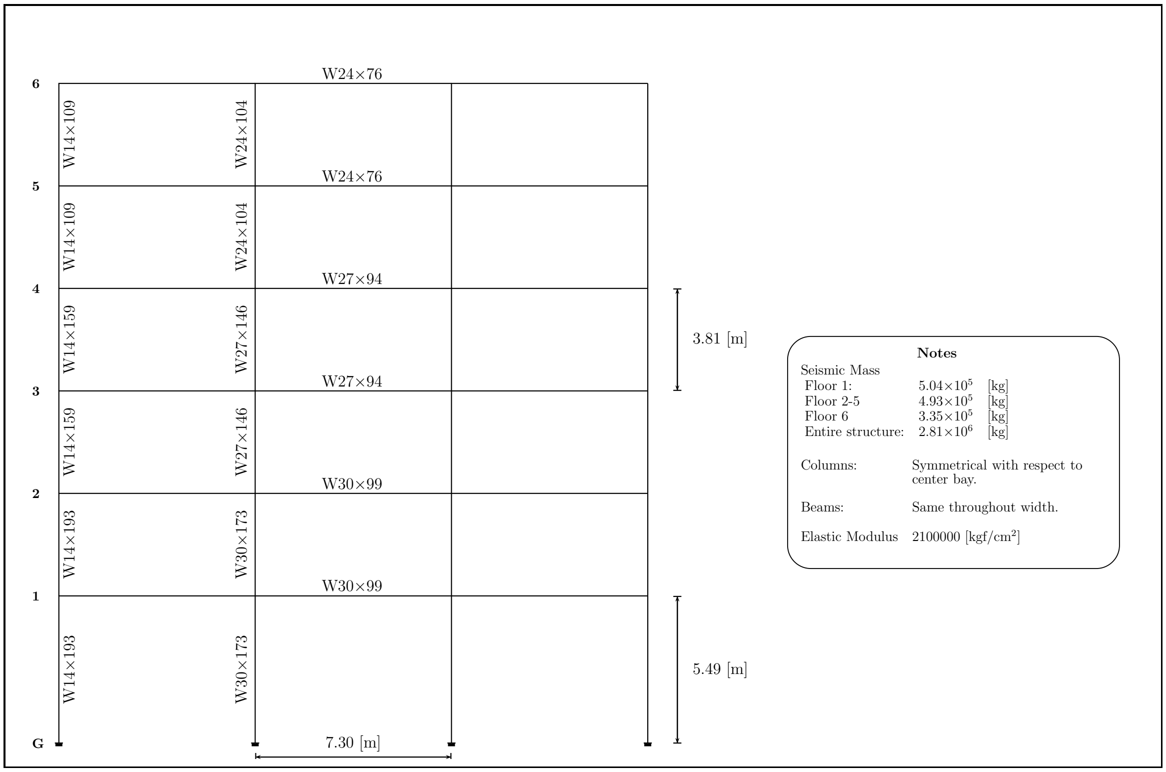

Figure 3.6: Six-story steel frame used in analysis (Hall, 1995)

The 9-story building was also proposed as a benchmark structure by Ohtori et al. (2004). The building has a rectangular plan of 45.73 m by 45.73 m, with an elevation of 37.19 m. The plan consists of five bays in the north-south direction and five bays in the east-west direction. The interior bays of the structure consist of simple frames intended to carry gravity loads only. The floor system is a composite construction of concrete and steel. The lateral load-resisting system of the building is made up of perimeter MRFs. The 2D frame considered in this study is one of the perimeter MRFs (Figure 3.7).

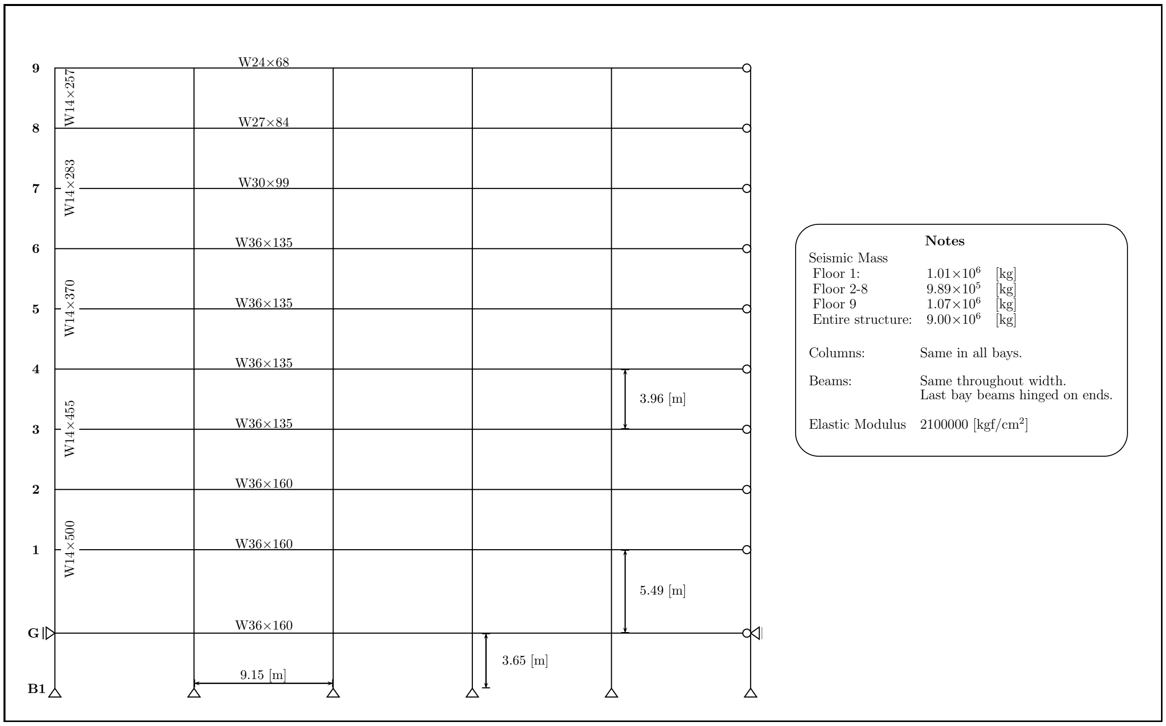

Figure 3.7: Nine-story steel frame used in analysis (Ohtori et al., 2004)

3.2.2. Modeling assumptions

For the analysis of the seismic response of the structures described above, several modeling assumptions were made. These assumptions were made in line with the focus of this study, which is to evaluate and compare the 2D seismic response of structures with and without elastic diagonal braces and friction devices.

Table 3.1: Modeling assumptions for the structures studied

	3-story Frame	6-story Frame	9-story Frame
Rigid diaphragm & Axially rigid beams	✓	✓	✓
Seismic mass half total mass of building	✓	✓	✓
Rigid beam-column connections	×	✓	×
Columns fixed to ground (first story)	✓	✓	×

The three structures have several similarities, and some minor differences in their modeling, which are noted in Table 3.1. The floor system is assumed to act as a rigid horizontal diaphragm, thus the seismic mass of the 2D MRFs considered was assumed equal to half of the total seismic mass of the building. This assumption has been shown to produce only minor modeling errors (Gupta and Krawinkler, 1999). Since the floor system is considered horizontally rigid and consists of composite construction (i.e. concrete and steel), the beams were modeled as rigid in their axial direction. For the 3 and 6 story building, all the columns are fixed at their base, i.e. ground level, while for the 9 story structure all columns are pinned at their base, i.e. basement level, while restricted from lateral motion at ground level. All beam-column connections were modeled as rigid, except for the 3 and 9 story structures, where the beams at the bay furthest right were modeled as hinged. These gravity columns in the 3 and 9 story structure, act as leaning columns (Geschwindner, 2002), and induce $P-\Delta$ effects, which have not been considered as it is deemed that this analysis escapes the focus of this study.

Based on the physical descriptions shown in Figure 3.5, Figure 3.6 and Figure 3.7, evaluation models were constructed using the open source software OpenSEES (Mazzoni et al., 2006). The models are 2D models that consider three Degrees-Of-Freedom (DOF) per node. The nodes are located at every beam-column joint as well as at the column-ground connections, and the mass of the structures has been lumped to the nodes using the tributary area method. The beam and columns were modeled as elastic frame members using elastic beam-column elements, and the connections between beams and column were modeled as rigid joints. The exceptions are the beams that are hinged. The beams of the 3-story structure that are hinged at both ends were modeled with truss elements. The beams of the 9-story structure that are hinged at one end were modeled with beam-column elements, and two nodes where defined at the hinged end (at the same location): one node is the end node of the hinged beam and the other node is the end node of the other members framing into the joint. These two nodes were then link by displacements constraints but were left free to rotate with respect to one another, thus behaving as an elastic hinge.

The inherent damping of the structures was assumed equal to 0.02 and was modeled as Rayleigh damping, setting 2 % damping at the first and third modes.

In order to determine the influence of the stiffness of the braces of a friction damper, the frames of the braced structures were modeled exactly as described in the former paragraph, except they were equipped with elastic braces of axial stiffness k_b located at their central bays. These elastic braces were modeled with elastic two-node axial links. In this study, such structures (i.e., the base structures with the addition of the braces) are referred to as braced structures (Figure 3.8).

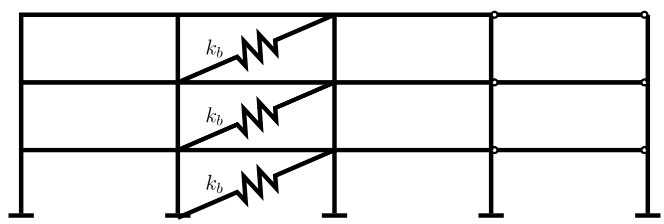

Figure 3.8: 3-story braced structure

The frames of the friction-damped structures were also modeled exactly as described before. Elastic, perfectly-plastic axial elements were added at the center bay of each story to model the friction dampers (Figure 3.9). The stiffness of these elements was set equal to the brace stiffness k_b, and the yield force was set equal to the activation force F_f. As previously shown in Section 2.4.2, the behavior of these elements (Figure 2.16) has been shown to correctly model the behavior of friction dampers.

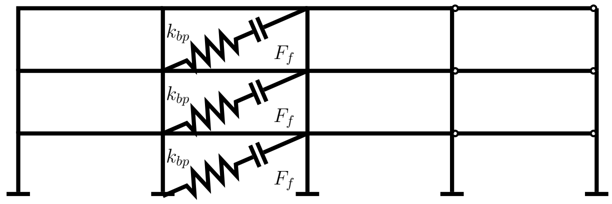

Figure 3.9: 3-story friction-damped structure

3.3. Analytical procedure: Parameters of interest and numerical simulations

For each set of seismic records, the structures described in Section 3.2.1 were analyzed considering three different cases: the base structure, the braced structure, and the friction-damped structure. The base structures are the structures described in Section 3.2.1. The braced structures are the base structures with the addition of elastic diagonal braces at the center of each story, and the axial stiffness of the braces is k_b. The friction-damped structures are the base structures with the addition of diagonal friction dampers ate the center bay of each story. The stiffness of the friction dampers is k_b (i.e., same as in the braced structure) and the activation force is F_f. The seismic response is evaluated in terms of the following quantities: inter-story drift ratio Δ, residual inter-story drift ratio Δ_r, floor acceleration a, and axial force c on the columns at the bay where the friction dampers are located (i.e., the center bay).

Each of the described structures were subjected to each individual component of the two sets of seismic records, the Maule earthquake set and the FEMA far-field set. The time-history nonlinear analysis was carried out using OpenSEES, with a time-step of 0.005 sec unless otherwise specified, and with the Krylov-Newton algorithm which uses a Krylov subspace accelerator to accelerate the convergence of the modified Newton Method (Mazzoni et al., 2006). The Newmark integrator was used with $\gamma = 0.5$ and $\beta = 0.25$. For each time-history analysis, the response history of the quantities mentioned in the former paragraph was recorded. The response to each ground motion was assumed equal to the maximum absolute response value over all the stories, and the response to each set of records was assumed equal to the median of the responses to each ground motion.

3.3.1. Analysis of the base structures

For the purposes of this study, the base structures are frame structures described in Section 3.2.1. The seismic response of these base structures is the benchmark response against which the response of the braced structures and the friction-damped structures will be compared. Modal analysis of the base structures were performed in order to determine the unbraced fundamental period T_o, which was used to determine the stiffness k_b of the braces of the braced structures. The fundamental periods T_o of the base structures are shown in Table 3.2.

Table 3.2: Unbraced fundamental periods

	3-story Frame	6-story Frame	9-story Frame
T_o	0.996 [s]	1.416 [s]	2.155 [s]

3.3.2. Analysis of the braced structures

The elastic component of a friction damper is characterized by the stiffness of the brace which connects the friction device to the structure. Such stiffness is called k_b in this study, as seen in Figure 3.8. In order to determine the values of k_b in an appropriate manner, the stiffness of the braces were determined by setting the fundamental period T_b of the braced structures equal to a fraction c_k of the fundamental period T_o of the corresponding base structures. Four values of c_k were considered, namely:

$$T_b = c_k T_o$$

$$c_k = [0.85, 0.70, 0.55, 0.40]$$

To achieve the desired periods T_b, the stiffness of the braces were calculated considering two possible height-wise distributions: uniform and variable. In the first case (uniform), all the braces have the same stiffness k_b, which was found by an iterative procedure. The resulting values of brace stiffness k_b are summarized in Table 3.3.

Table 3.3: Bracing stiffness k_b [kgf/cm] used for each frame (uniform height-wise distribution)

	$c_k = 0.85$	$c_k = 0.70$	$c_k = 0.55$	$c_k = 0.40$
3-Story Frame	4.618×10^4	1.274×10^5	2.964×10^5	7.250×10^5
6-Story Frame	4.658×10^4	1.435×10^5	4.605×10^5	1.631×10^8
9-Story Frame	1.046×10^5	3.528×10^5	1.470×10^6	4.418×10^{19}

In the case of the 9-story structure, the value of k_b necessary to achieve a period $T_b = 0.4T_o$ turned out to be unrealistically high. Because such stiff braces are not possible in practice, and also because such large stiffness values created numerical instabilities in the time-history analysis, the 9-story braced structure having a period $T_b = 0.4T_o$ was not considered in the analysis.

For the variable height-wise distribution of brace stiffness, the stiffness of the brace is different at each story. The stiffness of the brace at story p was set inversely proportional to the first mode inter-story drift of the base structure at the same story. Such height-wise stiffness distribution results in braced structures having a first modal shape very similar to a straight line (i.e., the first mode inter-story drifts are roughly the same at all stories). Hence the stiffness $k_{b,p}$ of the brace at each story p is given by:

$$k_{b,p} = \frac{\phi_{1n}}{\phi_{1p}} k_{b(p-1)}$$

where ϕ_{1n} is the first mode inter-story drift at the top story, and ϕ_{1p} is the first mode inter-story drift at story p. Since the stiffness of the brace at story p is related to the stiffness of the brace at the story below, it is then necessary to define the stiffness of the brace at first story $k_{b,1}$. This latter value was determined through an iterative procedure. The resulting values of brace stiffness are summarized in Tables 3.4,3.5 and 3.6.

Table 3.4: Bracing stiffness k_b [kgf/cm] in 3-story frame (variable height-wise distribution)

	$c_k = 0.85$	$c_k = 0.70$	$c_k = 0.55$	$c_k = 0.40$
1st Floor	5.368×10^4	1.527×10^5	3.623×10^5	8.686×10^5
2nd Floor	4.369×10^4	1.156×10^5	2.620×10^5	6.348×10^5
3rd Floor	4.369×10^4	1.156×10^5	2.620×10^5	6.348×10^5

Table 3.5: Bracing stiffness k_b [kgf/cm] in 6-story frame (variable height-wise distribution)

	$c_k = 0.85$	$c_k = 0.70$	$c_k = 0.55$	$c_k = 0.40$
1st Floor	9.692×10^4	2.468×10^5	6.159×10^5	1.931×10^8
2nd Floor	5.789×10^4	1.877×10^5	5.601×10^5	1.869×10^8
3rd Floor	2.878×10^4	1.121×10^5	4.131×10^5	2.239×10^8
4th Floor	1.490×10^4	6.308×10^4	2.796×10^5	2.351×10^8
5th Floor	9.495×10^3	4.075×10^4	2.017×10^5	2.352×10^8
6th Floor	9.495×10^3	4.075×10^4	2.017×10^5	2.352×10^8

Table 3.6: Bracing stiffness k_b [kgf/cm] in 9-story frame (variable height-wise distribution)

	$c_k = 0.85$	$c_k = 0.70$	$c_k = 0.55$	$c_k = 0.40$
1st Floor	1.810×10^5	4.704×10^5	1.2098×10^6	5.787×10^{18}
2nd Floor	1.630×10^5	4.754×10^5	1.4962×10^6	1.314×10^{19}
3rd Floor	1.334×10^5	4.359×10^5	1.6635×10^6	2.156×10^{19}
4th Floor	1.033×10^5	3.720×10^5	1.7086×10^6	2.909×10^{19}
5th Floor	7.632×10^4	2.937×10^5	1.6284×10^6	3.448×10^{19}
6th Floor	6.052×10^4	2.372×10^5	1.5274×10^6	3.767×10^{19}
7th Floor	4.363×10^4	1.726×10^5	1.3688×10^6	3.909×10^{19}
8th Floor	3.307×10^4	1.308×10^5	1.2474×10^6	3.949×10^{19}
9th Floor	3.307×10^4	1.308×10^5	1.2474×10^6	3.949×10^{19}

Again, in the case of the 9-story structure, the values of k_b necessary to achieve a period $T_b = 0.4T_o$ turned out to be unrealistically high. Hence, for the same reasons mentioned before, the 9-story braced structure having a period $T_b = 0.4T_o$ was not considered.

The modal shapes of the braced structures are shown in Appendix C. It is observed that when the stiffness of the braces is very high, the modal shape is essentially the same regardless of the height-wise distribution of brace stiffness k_b. Otherwise, the variable height-wise distribution of k_b leads, as expected, to modal shapes that are more similar to straight lines (Figures C.1, C.2, and C.3). It can also be seen that the influence of the height-wise distribution of k_b on the first modal shape increases with increasing number of stories.

In addition to the four response quantities mentioned before, the axial force demand f_e on each brace was also obtained from the numerical analysis of the braced structures. As it will be explained in the next section, force f_e was used to set the value of the activation force F_f.

3.3.3. Analysis of friction-damped structures

The braced structures described in the previous section were then equipped with Coulomb friction devices on the braces, which slip when the axial force on the brace exceeds the activation force F_f (Figure 3.9).

Two height-wise distributions of the activation force F_f are considered: uniform and variable. In the first case (uniform) the activation force is the same at all stories, and was set equal to a fraction c_f of the force demand f_e defined in the former section. A total of nine values of factor c_f were considered, namely:

$$F_f = c_f min(f_{ep})$$
$$c_f = [0.9, 0.8, ..., 0.2, 0.1]$$

where f_{ep} is the force f_e on the brace at story p of the corresponding braced structure, and min(f_e) is the least value (over all the stories) of f_{ep}. For the variable height-wise distribution, the activation force of the friction device at story p, F_{fp}, was set equal to c_f times the force f_{ep}, i.e:

$$F_{fp} = c_f f_{ep}$$

Both height-wise distributions of the activation force F_f were considered for each height-wise distribution of brace stiffness k_b. Hence, four friction-damped structures where then considered for each base structure. Sample values of the activation force F_f can be seen in Appendix A.

3.3.4. Parameters representative of the seismic response

As mentioned before, the response quantities of interest in this study are inter-story drift ratio Δ, residual inter-story drift ratio Δ_r, floor acceleration a, and axial force c on the columns at the bay where the friction dampers are located (i.e., the center bay). The response of the base structures is denoted Δ_o, Δ_{ro}, a_o and c_o, where, obviously, $\Delta_{ro} = 0$ because the base structures are assumed to behave in a linearly elastic manner. The response of the braced structures and of the friction-damped structures is denoted Δ_{fk}, Δ_{rfk}, a_{fk} and c_{fk} where f and k are the values of coefficients c_f and c_k, respectively. It must be noted that $f = 1$ indicates a braced structure, whereas $f < 1$ indicates a friction-damped structure. The response of the braced structures and of the friction-damped structures is then normalized by the response of the corresponding base structure, i.e.:

$$r_\Delta = \frac{\Delta_{fk}}{\Delta_o}, r_a = \frac{a_{fk}}{a_o}, r_c = \frac{c_{fk}}{c_o}$$

Naturally, the residual inter-story drift response is not normalized because $\Delta_{ro} = 0$. Values of r_Δ, r_a or r_c less than unity indicates that the response of the braced structure ($f = 1$) or the friction-damper structure ($f < 1$) is less than that of the corresponding base structure. Normalized response values for $f = 1$ indicate the sole influence of the brace stiffness on the response. Normalized response values for $f < 1$ indicate the influence of both the brace stiffness and the activation force on the response. A comparison between the latter and the former provides insight into the influence of the activation force.

4. EVALUATION OF THE SEISMIC RESPONSE OF FRICTION-DAMPED STRUCTURES

The seismic response of the 3-, 6- and 9-story structures was evaluated numerically following the methodology described in Chapter 3. In this section, the results are presented and critically examined.

4.1. Response of the 3-Story frames

The inter-story drift response of the 3-story structure is shown in Figure 4.1. It can be observed that this response quantity is controlled mainly by the stiffness of the braces, which are defined by factor c_k. For the braced structures, which is to say $c_f = 1.0$, it is observed that the response reduction is proportional (not necessarily in a linear manner) to the value of c_k. For lower values of c_k, which is to say increased brace stiffness, the value of $r_\triangle$ decreases, i.e., the stiffer the braced frame, the larger the reduction of $r_\triangle$. This occurs due to the fact that the inter-story drift response at a given story is directly dependent on the stiffness of the story, and adding a brace with higher stiffness results in lower inter-story drifts.

For the friction-damped structures, as the activation force decreases (which is to say lesser values of c_f), it is observed that in general the value of $r_\triangle$ decreases, but not in a monotonic manner. Further, as it will be emphasized later, this reduction is not as significant as the reduction due to lesser values of c_k.

In Table 4.1, values of $r_\triangle$ are shown for the braced structure ($c_f = 1.0$) considering a uniform height-wise distribution of brace stiffness. In the same table, values of $r_\triangle$ are shown for the corresponding optimal friction-damped structure ($c_f < 1.0$) considering a uniform height-wise distribution of the activation force, being the optimal the one for which the inter-story drift response is minimized. When Table 4.1 is examined, it is clear

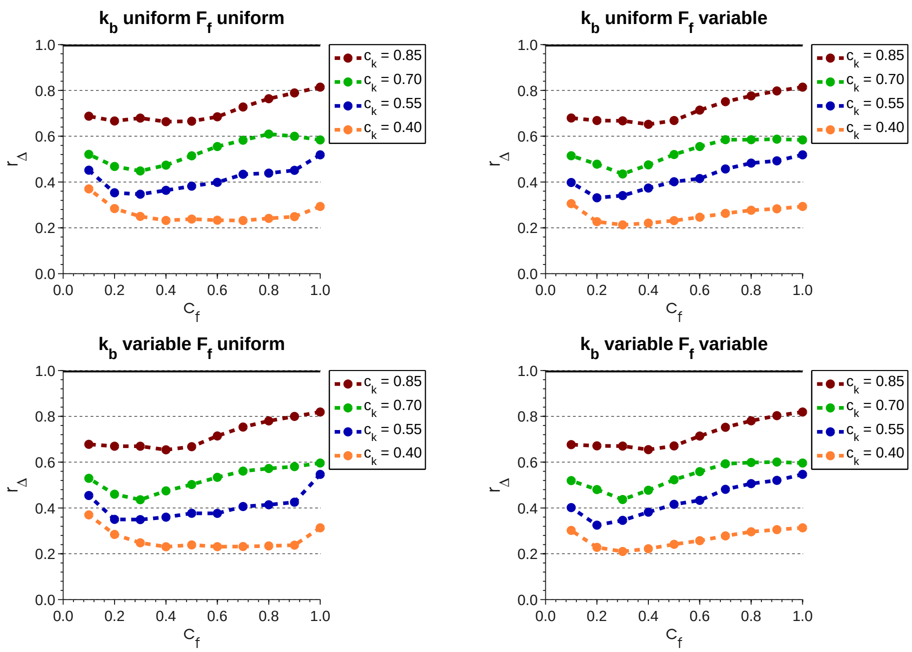

(a) Maule Earthquake seismic set

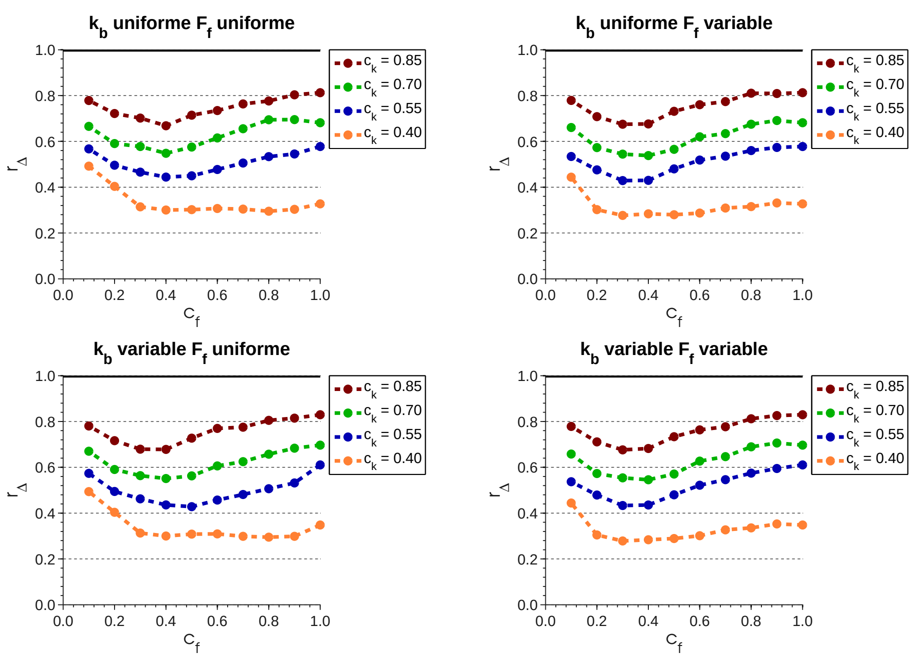

(b) FEMA Far Field seismic set

Figure 4.1: Normalized response $r_\triangle$, 3-story structure

that the additional reduction of the inter-story drift response due to the addition of a friction device to an already braced structure is 5 % to 66 % less than the reduction due to the sole addition of an elastic brace to the base structure. Furthermore, it is observed that for a given braced structure, lesser values of r_Δ can generally be obtained by increasing the brace stiffness (i.e., lesser value of c_k) rather than by the addition of a friction device (i.e., lesser value of c_f), even when the activation force of the latter is the optimal. For instance, when $c_k = 0.85$, the minimum value of r_Δ that can be obtained with a friction-damped structure is 0.6634, which is greater than the value ($r_\Delta = 0.5837$) of a stiffer braced structure (e.g., $c_k = 0.70$).

Table 4.1: Normalized response r_Δ for braced 3-story structure and optimum friction-damped 3-story structure (Uniform height-wise distribution of F_f and k_b)

	$c_k = 0.85$	$c_k = 0.70$	$c_k = 0.55$	$c_k = 0.40$
$r_\Delta^{c_f=1.0}$	0.8141	0.5837	0.5186	0.2932
$r_{opt\Delta}^{c_f<1.0}$	0.6634	0.4482	0.3468	0.2321
$r_\Delta^{c_f=1.0} - r_{opt\Delta}^{c_f<1.0}$	0.1507	0.1355	0.1718	0.0611

For a given value of c_k the additional reduction of r_Δ due to the addition of a friction device to an already braced structure can be evaluated by the difference $r_\Delta^{c_f=1.0} - r_{opt\Delta}^{c_f<1.0}$. It can also be seen in Table 4.1 that the addition of a friction device to an already braced structure results in a further reduction of r_Δ in the range of 0.06-0.15, which is less than the 0.19-0.71 reduction that can be obtained solely from adding an elastic brace to the base structure. Clearly, the inter-story drift response of the friction-damped structures is then predominantly influenced by the brace stiffness, and the influence of the activation force is of much lesser significance.

For the braced structures it is not surprising to observe that $r_a > 1.0$, indicating that the floor acceleration response of the braced structures increases with respect to that of the

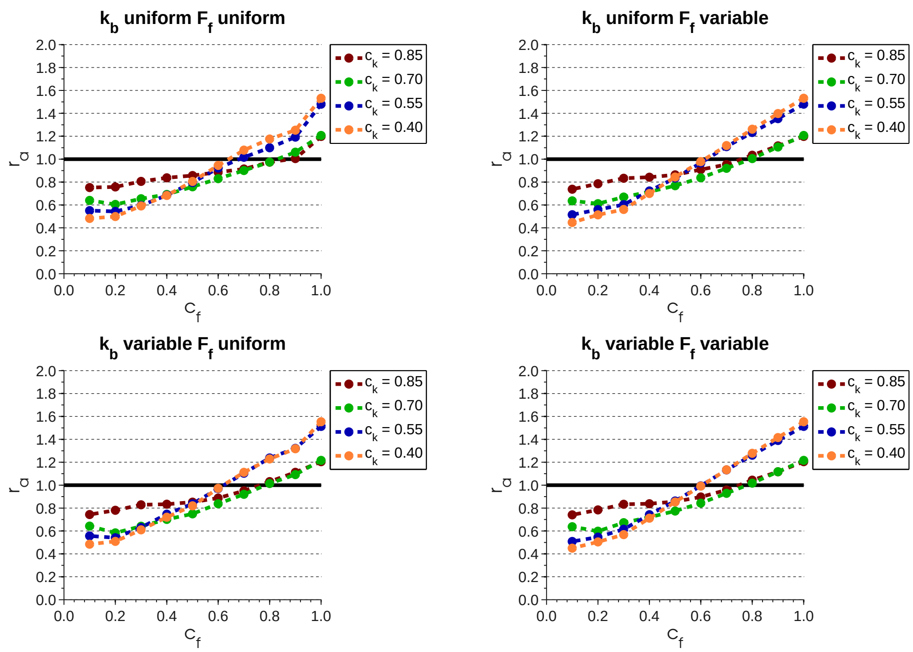

(a) Maule Earthquake seismic set

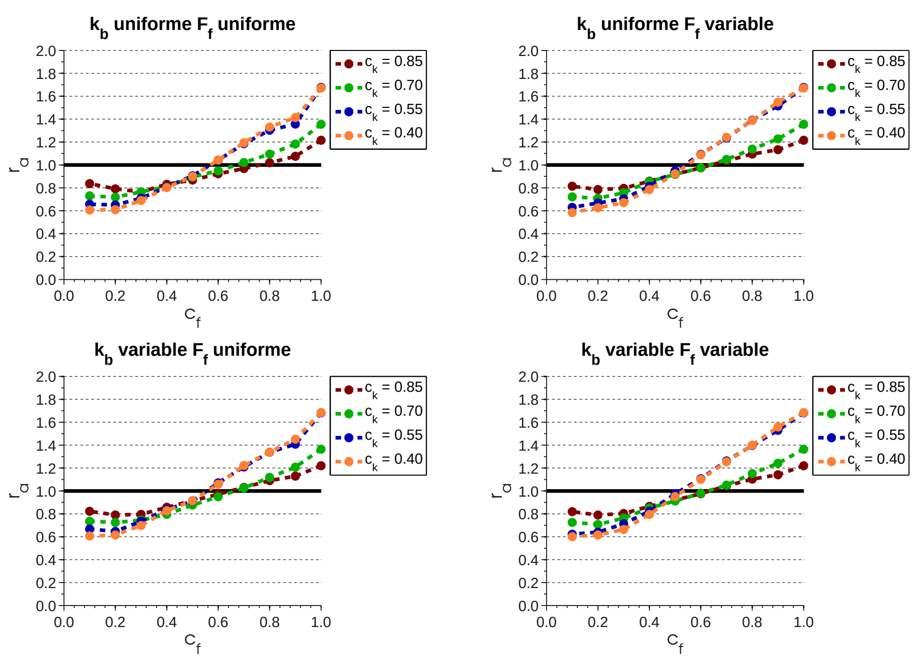

(b) FEMA Far Field seismic set

Figure 4.2: Normalized response r_a, 3-story structure

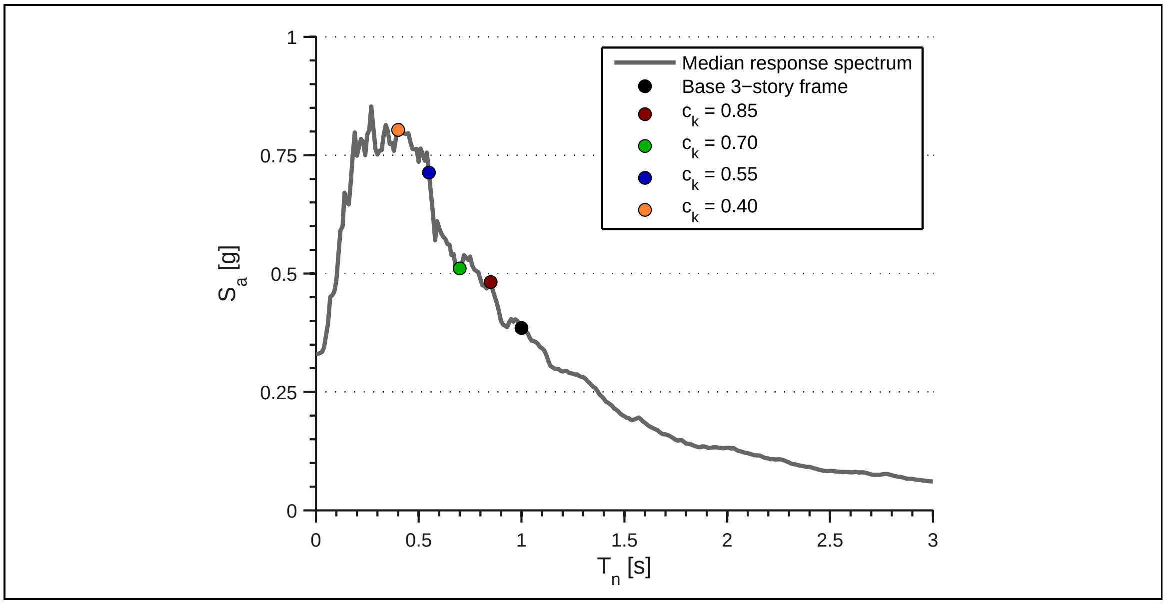

Figure 4.3: Maule set median Response spectra

base structure (Figure 4.2). A braced structure with stiffer bracing has a lower fundamental period, and for the 3-story structure this implies a greater first-mode spectral ordinate (Figure 4.3).

As the value of c_f decreases, so does the value of r_a (Figure 4.2), indicating that, due to the effect of the friction device, the floor acceleration response of friction-damped structures is less than that of the corresponding braced structures, and even less than that of the corresponding base structures if the value of c_f is sufficiently small. The lesser the activation force (which implies greater slip displacement), the greater the effective flexibility of the structure, which results in larger effective periods of oscillation (Pall and Marsh, 1982). From Figure 4.3 it is clear that if the period of a braced structure increases, the acceleration response decreases. For this same reason, it is observed in Figure 4.2 that there are greater reductions of r_a (at very low values of c_f) for higher values of c_k, i.e., the reduction of the spectral ordinate is greater for structures that are more rigid (Figure 4.3).

The minimum (i.e., optimal) values of r_a range from 0.75 for $c_k = 0.85$ to 0.45 for $c_k = 0.40$. These values are achieved when $c_f = 0.1$ or $c_f = 0.2$, regardless of the value of c_k and of the height-wise distribution of the activation force and/or the brace stiffness.

The relationship between the mechanical properties of friction dampers and the axial force in the central columns (Figure 4.4) is analogous to that between the same properties and the floor acceleration response. This occurs due to the fact that, as floor accelerations increase, so do story shears, resulting in greater axial forces on the central columns. The maximum values of r_c occur for the braced structures, and the higher the stiffness the higher the values of r_c, though the relationship is not necessarily linear. In particular, when $c_k = 0.55$ and $c_k = 0.40$, the value of r_c approaches 100 (Figure 4.4), appearing to imply that, as a result of bracing, the central columns of the braced structures must resist axial loads that are approximately 100 times greater than the axial loads on the same columns of the base structure. However, this result is somewhat misleading because the axial forces on the central columns of the base structures, due solely to seismic actions, are close to zero. Recalling that $r_c = \frac{c_{fk}}{c_o}$, where c_o is the axial force in the central columns of the base structure, it is clear that if this value is close to zero, r_c will take very large values.

Figure 4.5 shows values of factor r_{cg}, which is the same as r_c but considering axial forces due to both seismic and gravity loads. It is observed that for the braced structures r_{cg} takes values between 4.0 and 16.0 depending on the value of c_k. The redistribution of forces as a consequence of adding the braces leads to significant axial forces on the central columns when the structure is subjected to seismic actions, hence $r_{cg} > 1.0$ in almost all cases. As expected, the lower the value of c_f, the lower the values of r_{cg}. This means that the minimum values of r_{cg} occur for $c_f = 0.1$, regardless of the height-wise distribution of the activation force and the brace stiffness, and regardless of the value of c_k. The minimum values of r_{cg} range from 1.0 ($c_k = 0.85$) to approximately 2.5 ($c_k = 0.40$).

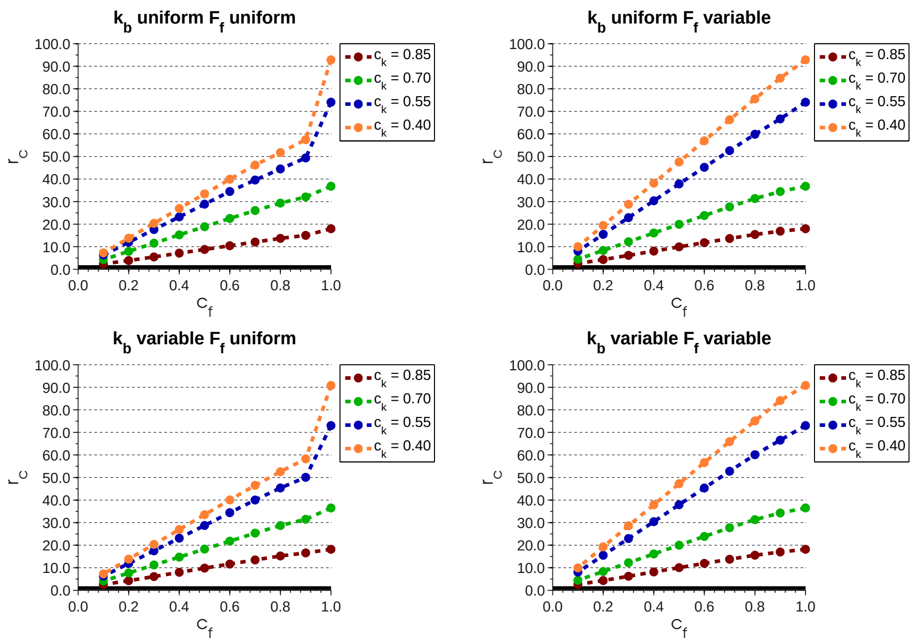

(a) Maule Earthquake seismic set

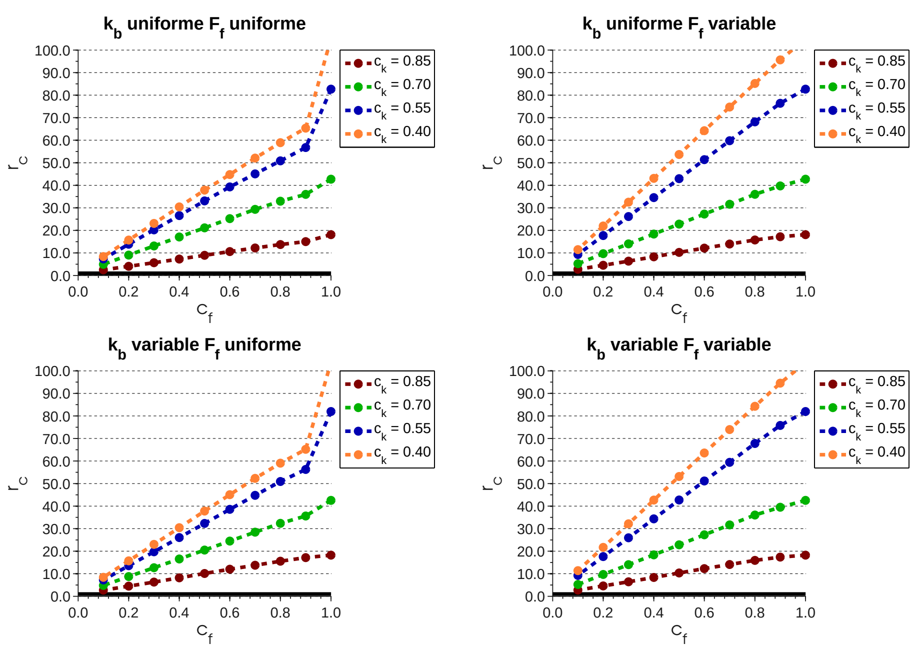

(b) FEMA Far Field seismic set

Figure 4.4: Normalized response r_c, 3-story structure

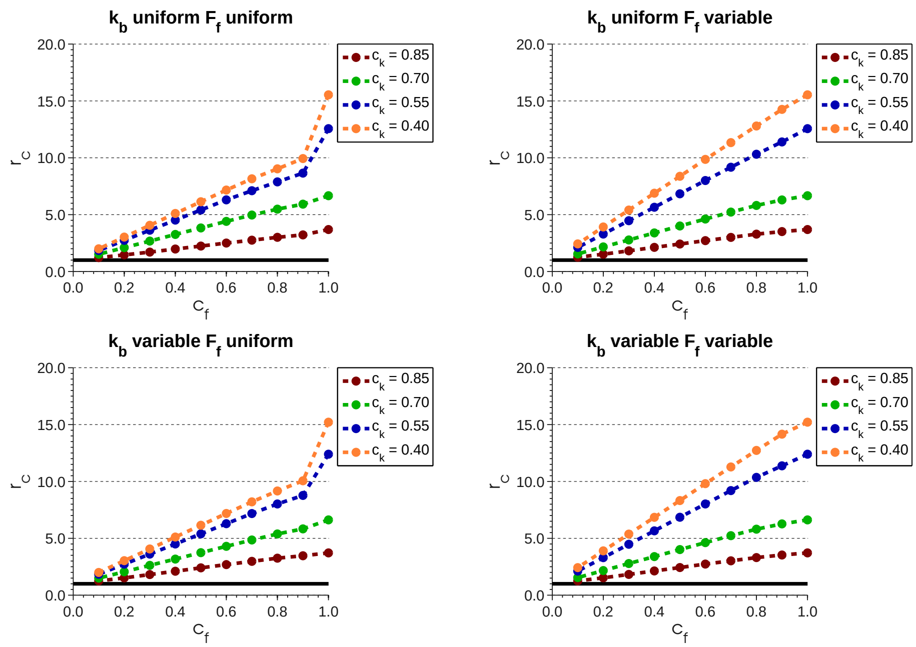

(a) Maule Earthquake seismic set

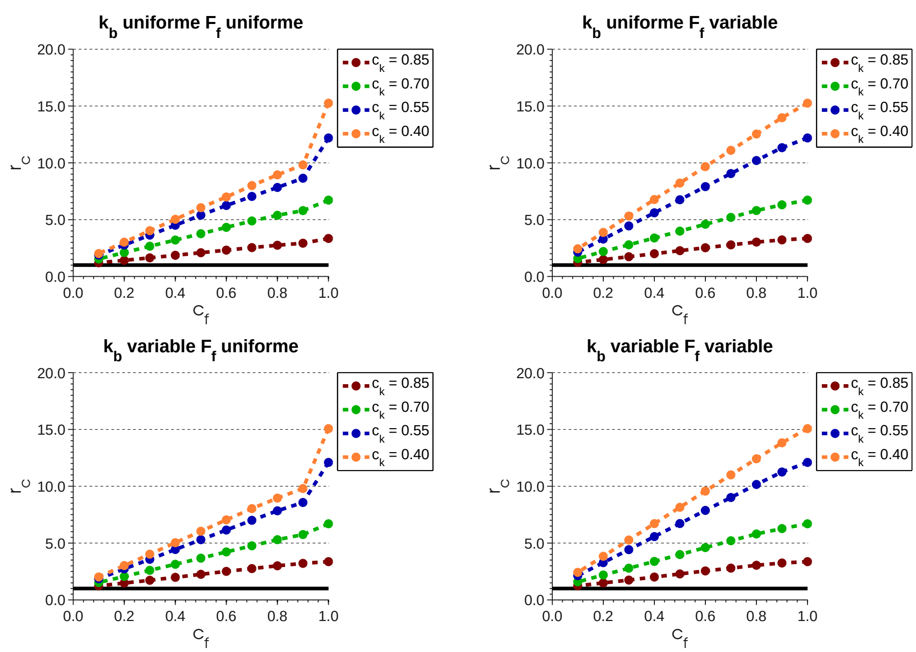

(b) FEMA Far Field seismic set

Figure 4.5: Normalized response r_{cg}, 3-story structure

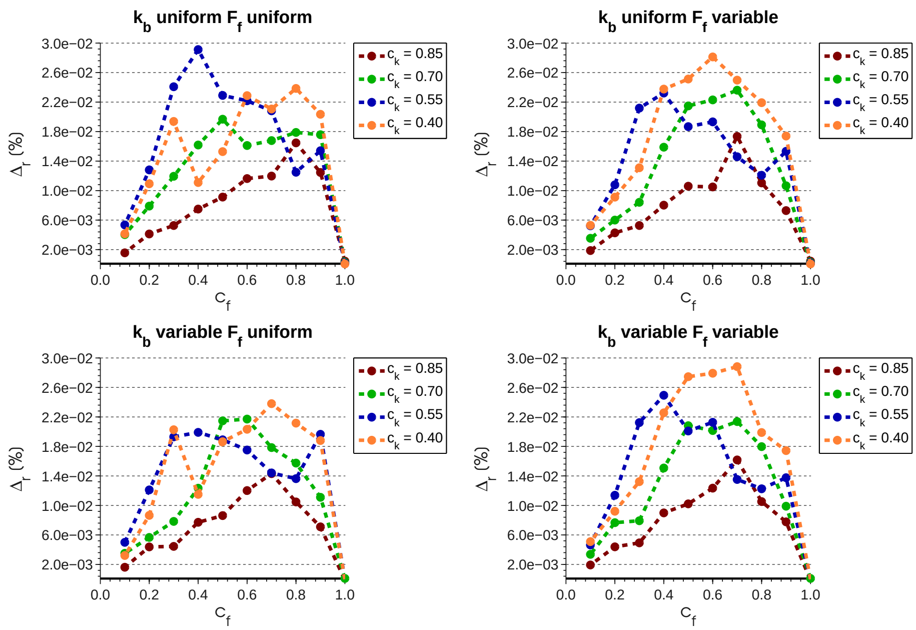

(a) Maule Earthquake seismic set

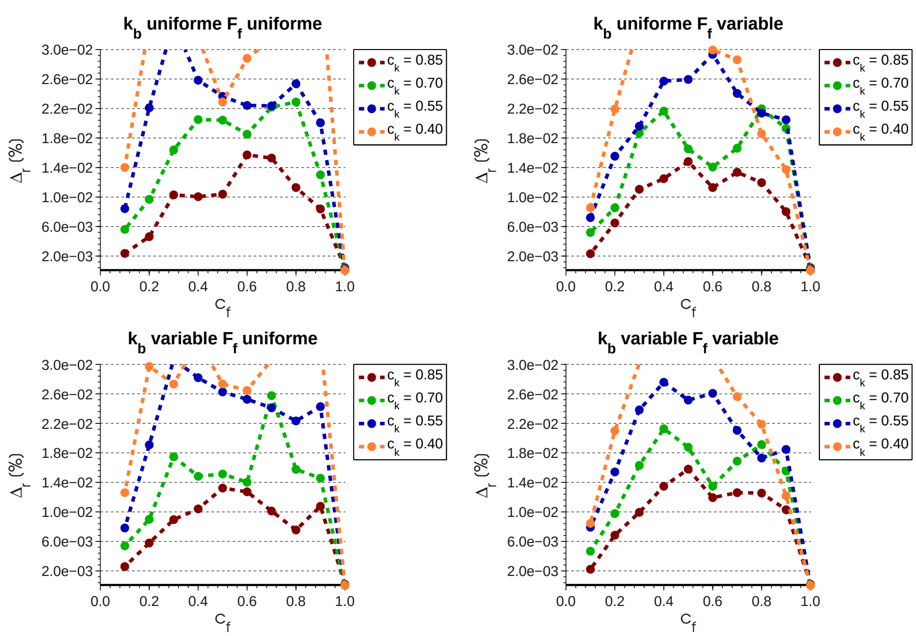

(b) FEMA Far Field seismic set

Figure 4.6: Response Δ_r,3-story structure

Regarding the residual inter-story drift response, it is important to recall that the response values Δ_r are not normalized because the base structures are linearly elastic and are not affected by residual deformations (i.e., $\Delta_{ro} = 0$). It is observed in Figure 4.6 that, regardless of the value of c_k, maximum values of Δ_r occur when c_f takes moderate values, between 0.4 and 0.6. This is explained by the fact that the structure becomes more flexible as the value of c_f decreases, and the behavior of the friction-damped structures approaches that of an elastic system of very low stiffness as c_f approaches zero, which explains why the values of Δ_r are close to zero when the value of c_f is very low. Hence, the response is elastic when $c_f = 1.0$ and seemingly elastic when c_f is very low, and residual deformations reach maximum values at intermediate values of c_f.

It is also apparent in Figure 4.6 that values of Δ_r are in all cases too low (less than $0.1\ \%$) to have any real structural significance. As it will be shown later, the residual inter-story drift response of the 6- and 9-story structures is very similar to that of the 3-story structure, thus no further comments will be made unless deemed necessary.

4.2. Response of the 6-Story structure

The inter-story drift response of the 6 story structure (Figure 4.7) is very different from that of the 3-story structure (Figure 4.1). This difference is due to the fact that for the 6-story structure it becomes apparent that the friction device has a larger impact on the reduction of r_Δ compared to that for the 3-story structure.

Table 4.2: Normalized response r_Δ for braced 6-story structure and optimum friction-damped 6-story structure (Uniform height-wise distribution of F_f and k_b)

	$c_k = 0.85$	$c_k = 0.70$	$c_k = 0.55$	$c_k = 0.40$
$r_\Delta^{c_f=1.0}$	0.9096	0.7853	0.6404	0.5849
$r_{opt\Delta}^{c_f<1.0}$	0.7111	0.5393	0.4062	0.2010
$r_\Delta^{c_f=1.0} - r_{opt\Delta}^{c_f<1.0}$	0.1985	0.2460	0.2342	0.3839

From Table 4.2, it is apparent that, for the 6-story structure, the reduction of the inter-story drift response due to the addition of a friction device to an already braced structure is comparable to the reduction due solely to the addition of elastic braces to the base structure. This contrasts with what was observed in Table 4.1, where the reduction due to the addition of a friction device was found less significant. The influence of the properties of friction dampers on the inter-story drift response of the 6-story differs from what has been previously observed in SDOF structures (Vergara, 2012). The minimum values of r_Δ that can be obtained are shown in Table 4.2, and range from 0.20 for $c_k = 0.40$, to 0.71 for $c_k = 0.85$.

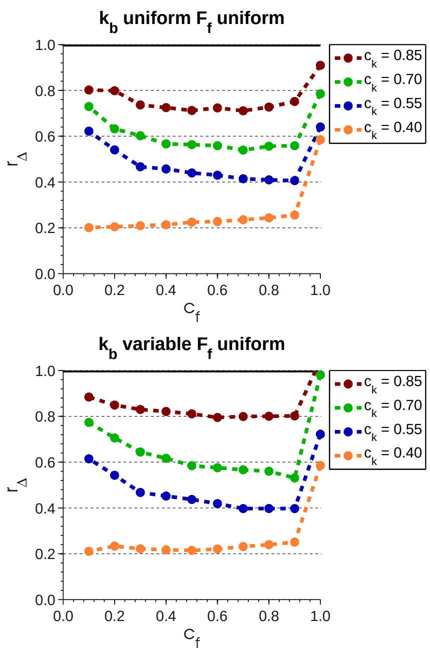

(a) Maule Earthquake seismic set

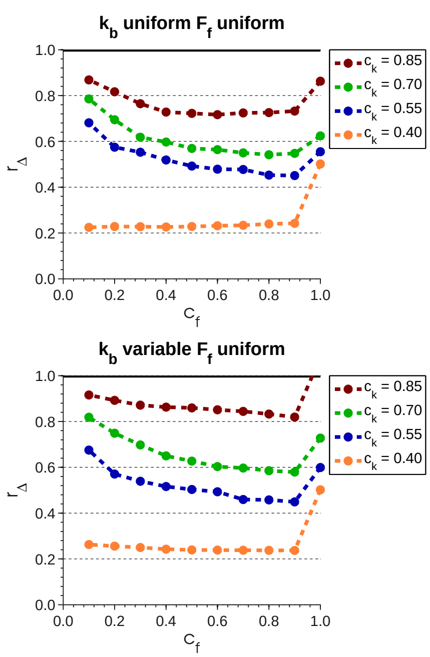

(b) FEMA Far Field seismic set

Figure 4.7: Normalized response r_Δ, 6-story structure

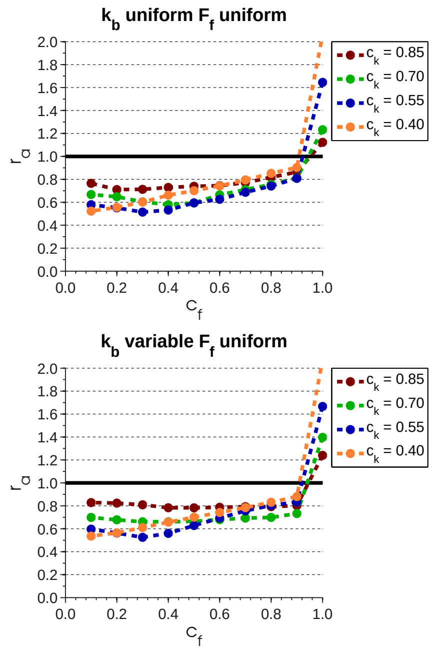

(a) Maule Earthquake seismic set

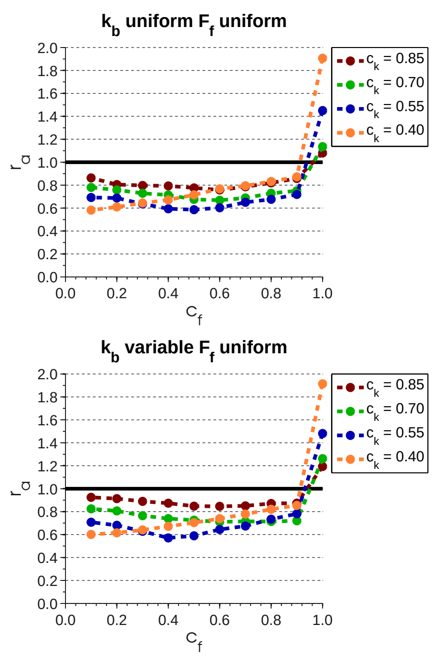

(b) FEMA Far Field seismic set

Figure 4.8: Normalized response r_a, 6-story structure

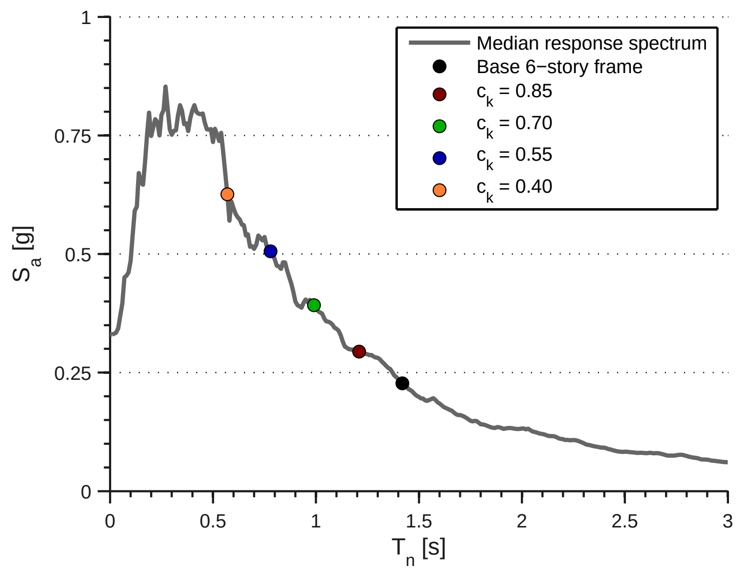

Figure 4.9: Maule set median Response spectra

The floor acceleration response (Figure 4.8) was found to be deeply influenced by the height-wise distribution of the activation force. In the case of the uniform distribution (left-side plots), the addition of a friction device to an already braced structure significantly reduces the floor acceleration response. The reduction is essentially insensitive to the value of c_f, and is such that $r_a < 1.0$ regardless of the height-wise distribution of the brace stiffness. Most notably, the level of reduction is already significant for $c_f = 0.9$, the highest value that still ensures that all the friction devices are activated. It can be observed from Figure 4.9, that the manner in which floor accelerations scale with the different stiffness of the braced structures is explained due to the median response spectrum of the ground motions used. Minimum values of r_a range from 0.55 for $c_k = 0.40$ to 0.80 for $c_k = 0.85$. In the case of the variable distribution of the activation force, on the other hand (right-side plots), the addition of a friction device to an already braced structure still reduces the floor acceleration response, but the level of reduction increases with decreasing values of c_f in an essentially monotonic manner, and r_a becomes less than unity only when the value of c_f is very low. As in the case of the uniform distribution of the activation force, the height-wise distribution of the brace stiffness is essentially irrelevant.

Similar observations apply to the axial force demand on the central columns (Figure 4.10). As previously stated, the relationship between r_{cg} and the parameters c_f and c_k is similar to the relationship between these parameters and r_a, which is due to the fact that axial forces on the columns are proportional to floor accelerations (Chopra, 1995). Figure 4.10 also indicates that when $c_k = 0.40$ axial forces on the central columns are much greater than those when c_k has greater values, which means that very stiff braces are counterproductive in the sense that they lead to very large columns. Minimum values or r_{cg}, ranging from 1.0 for $c_k = 0.85$ to 1.5, for $c_k = 0.55$, are achieved when $c_f = 0.1$ regardless of the value of c_k or the height-wise distributions of the properties of the friction dampers.

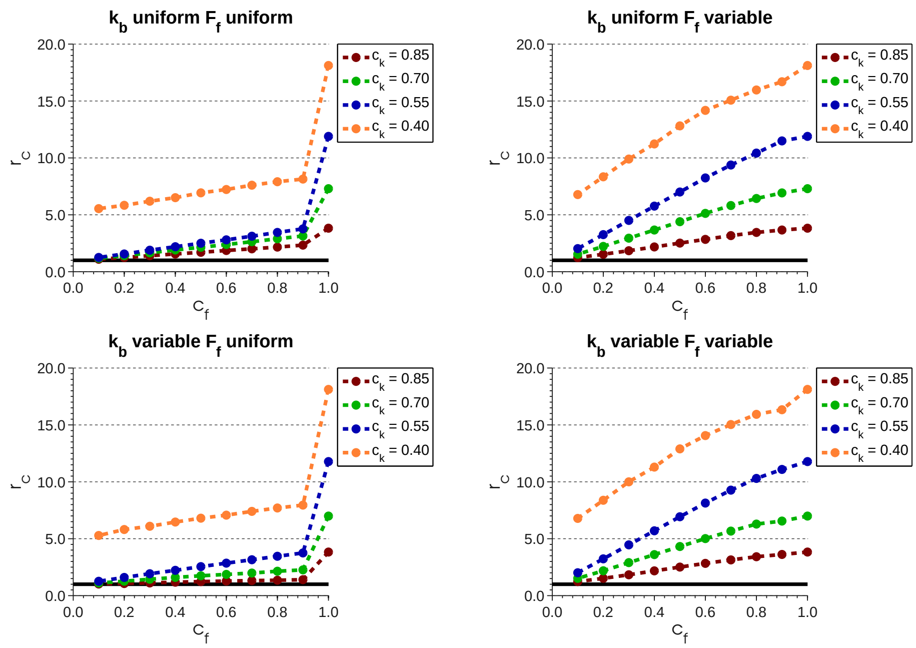

(a) Maule Earthquake seismic set

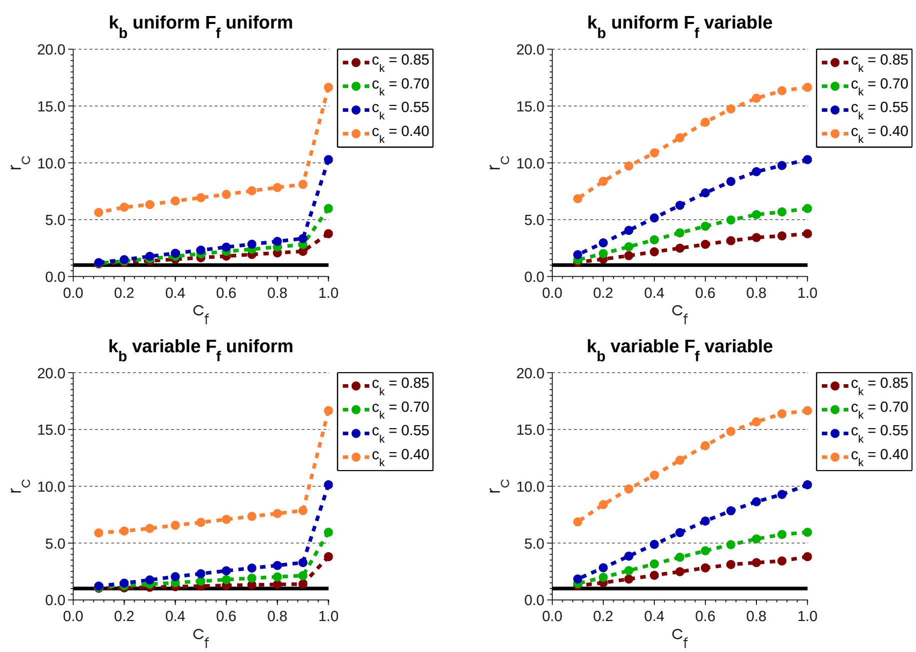

(b) FEMA Far Field seismic set

Figure 4.10: Normalized response r_{cg}, 6-story structure

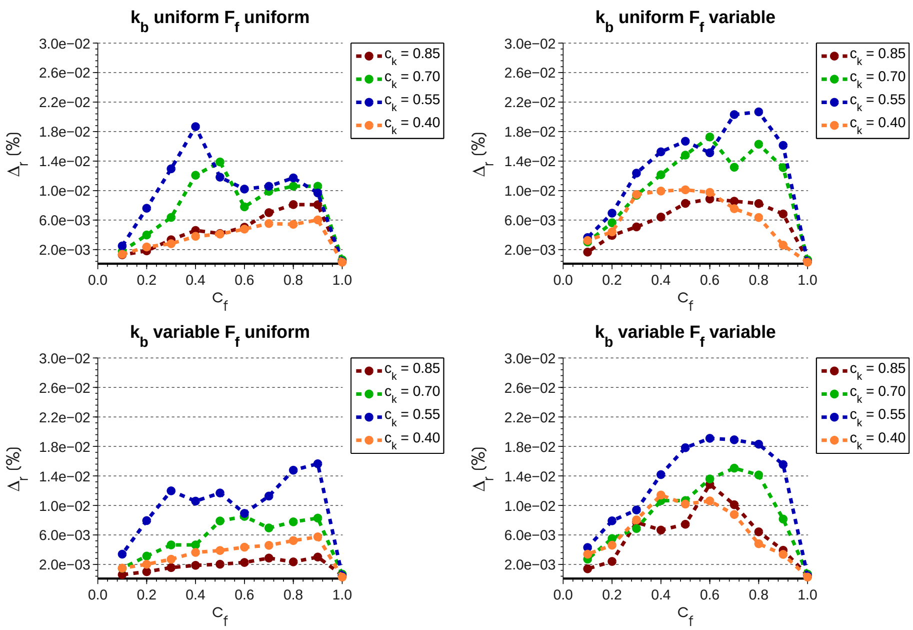

(a) Maule Earthquake seismic set

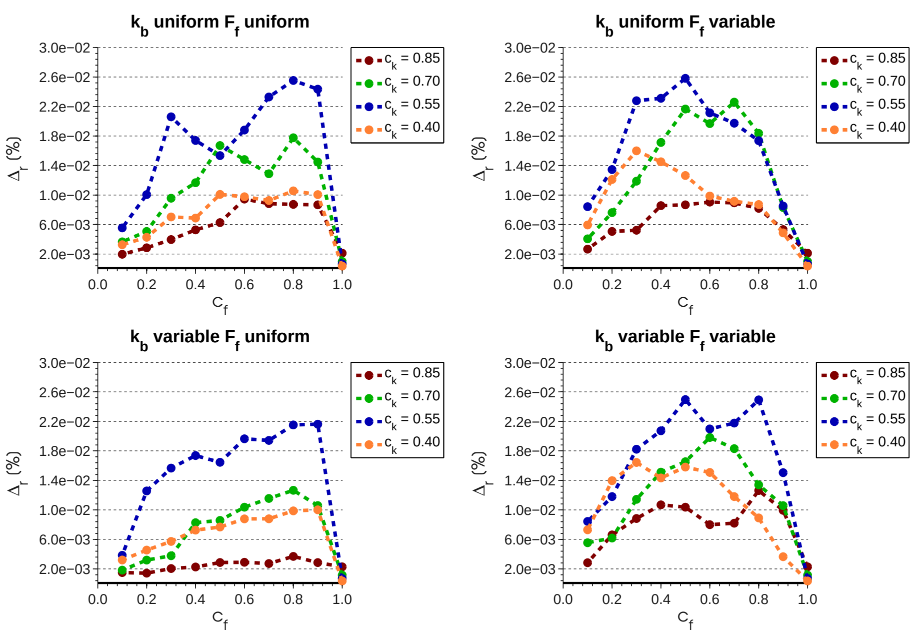

(b) FEMA Far Field seismic set

Figure 4.11: Response Δ_r, 6-story structure

4.3. Response of the 9-story structure

It is recalled that, due to the reasons mentioned in Section 3.3.2, the braced 9-story structures corresponding to $c_k = 0.40$ were not considered.

Table 4.3: Normalized response r_Δ for braced 9-story structure and optimum friction-damped 9-story structure (Uniform height-wise distribution of F_f and k_b)

	$c_k = 0.85$	$c_k = 0.70$	$c_k = 0.55$
$r_\Delta^{c_f=1.0}$	0.7080	0.6550	0.6463
$r_{opt\Delta}^{c_f<1.0}$	0.5389	0.3608	0.2810
$r_\Delta^{c_f=1.0} - r_{opt\Delta}^{c_f<1.0}$	0.1691	0.2942	0.3653

The inter-story drift response (Figure 4.13) appears to be similar to that of the 6-story structure (Figure 4.7). It can be seen in Table 4.3 that, similar to what was observed for the 6-story structure, the response reduction due to addition of friction devices to an already braced structure is similar to that due to the addition of braces to the base structure. Minimum values of r_Δ range from 0.54 ($c_k = 0.85$) to 0.28 ($c_k = 0.55$), and are obtained considering a uniform height-wise distribution of both brace stiffness and activation force.

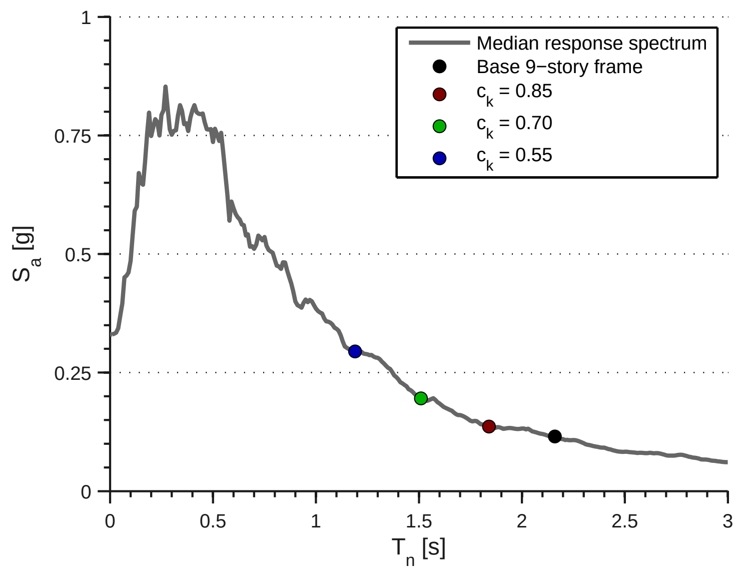

Figure 4.12: Maule set median Response spectra

The floor acceleration response (factor r_a, Figure 4.14) and the axial force demand on the central columns (factor r_{cg}, Figure 4.15) greatly resemble their counterparts corresponding to the 6-story structure. As seen in Figure 4.12, a similar relationship is seen between structure stiffness and the manner in which floor accelerations increase. In both cases the response reduction depends mainly on the activation force: in general, the lower the activation force, the greater the response reduction. Minimum values of r_a are reached when $c_f = 0.2$ or $c_f = 0.1$, ranging from 0.65 ($c_k = 0.85$) to 0.45 ($c_k = 0.55$): they are insensitive to the height-wise distribution of brace stiffness, and take slightly lesser values when the height-wise distribution of the activation force is uniform. Minimum values of r_{cg} are obtained for uniform height-wise distributions of both activation force and brace stiffness, and are reached when $c_f = 0.1$, ranging from 0.9 ($c_k = 0.85$) to 1.5 ($c_k = 0.55$).

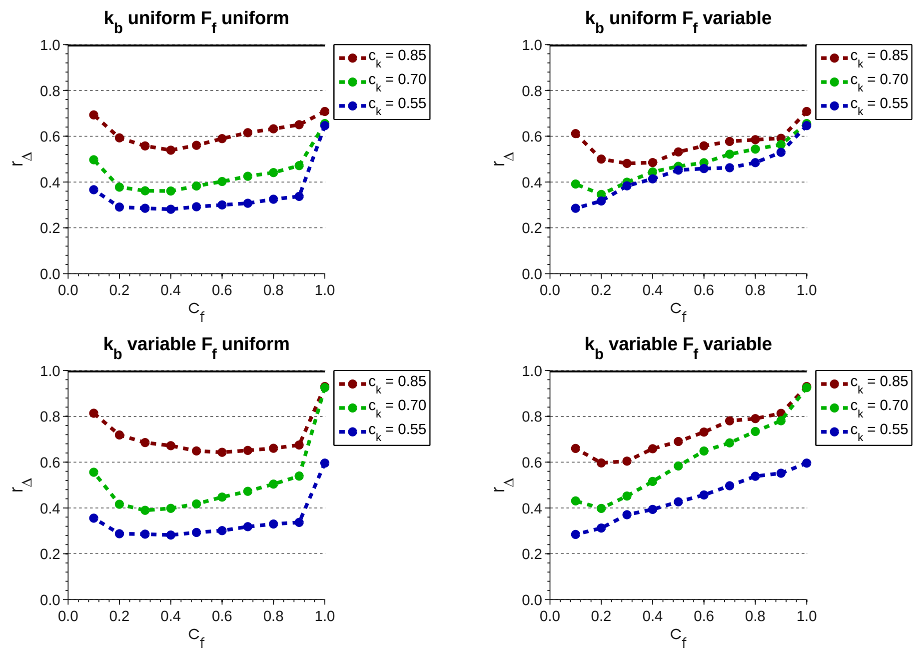

(a) Maule Earthquake seismic set

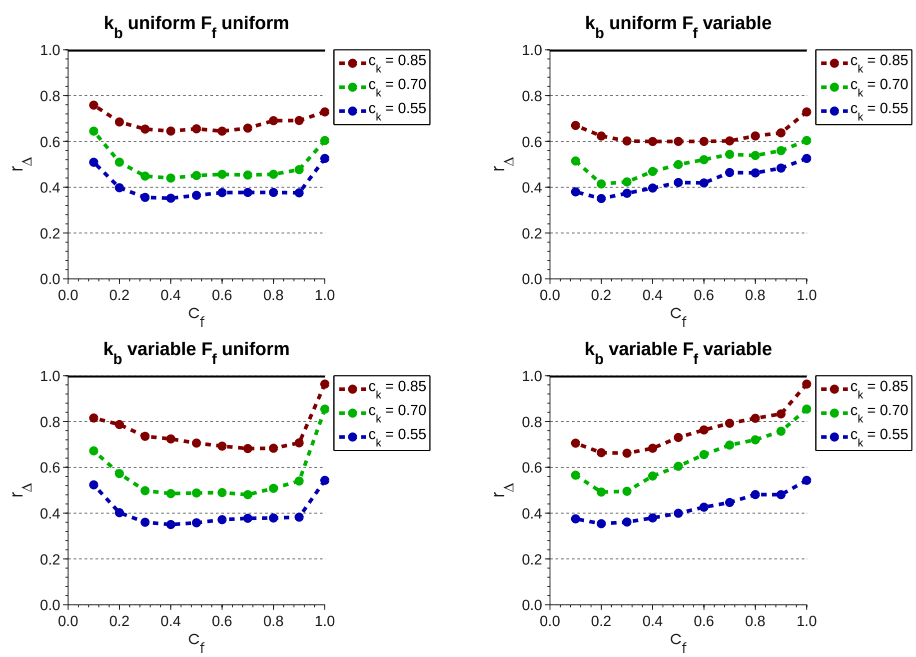

(b) FEMA Far Field seismic set

Figure 4.13: Normalized response r_Δ, 9-story structure

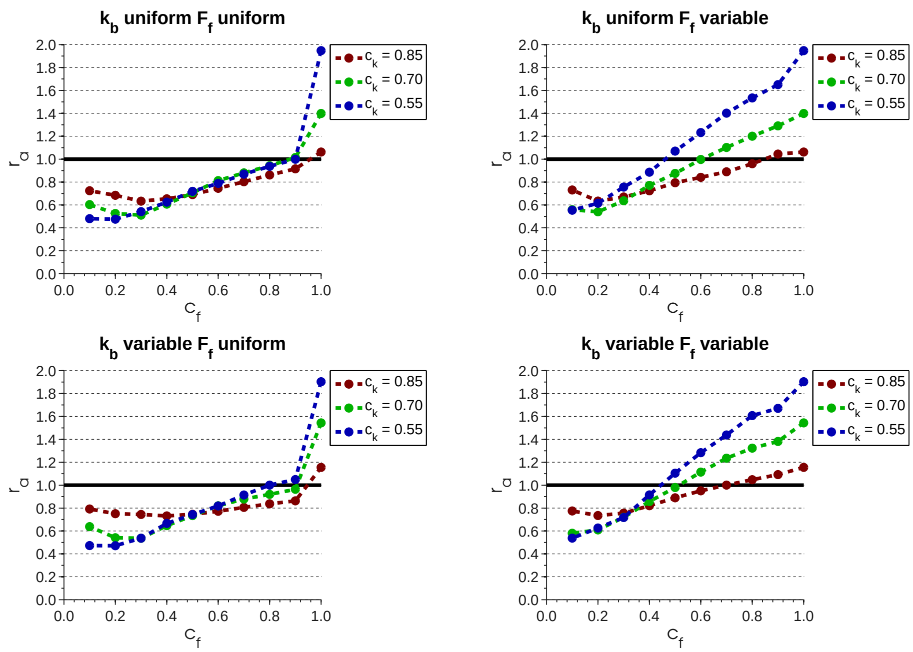

(a) Maule Earthquake seismic set

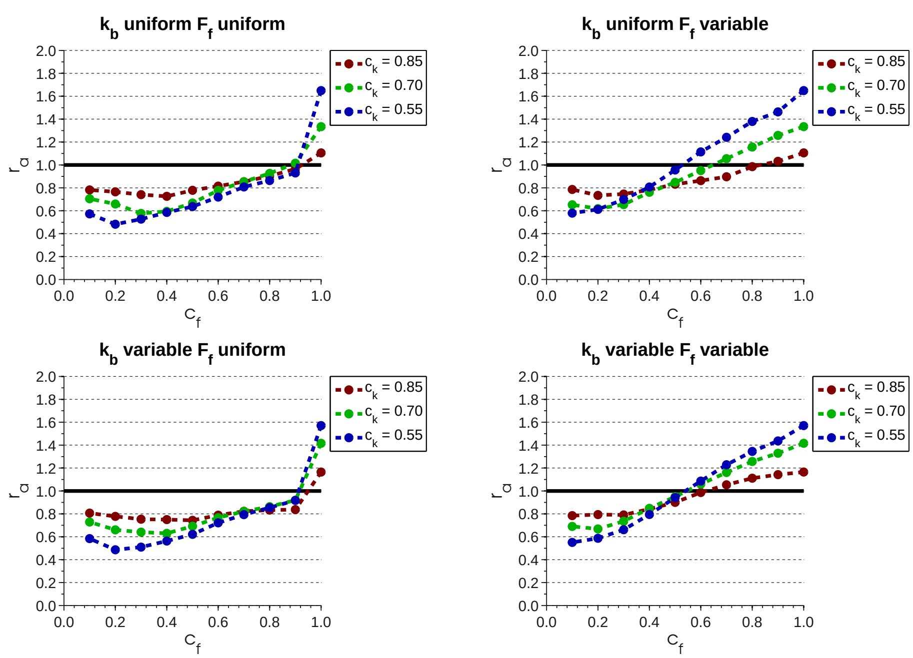

(b) FEMA Far Field seismic set

Figure 4.14: Normalized response r_a, 9-story structure

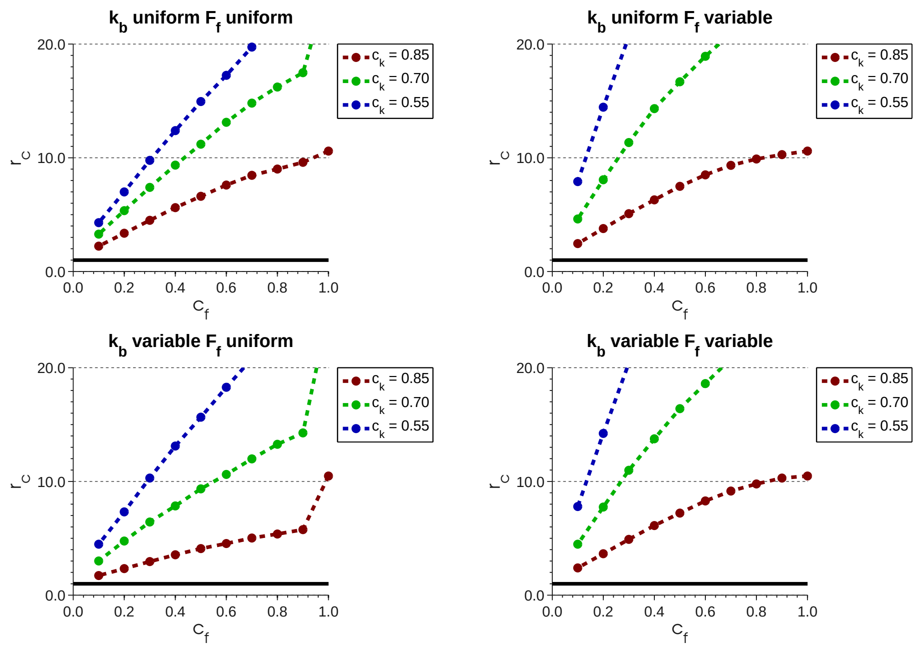

(a) Maule Earthquake seismic set

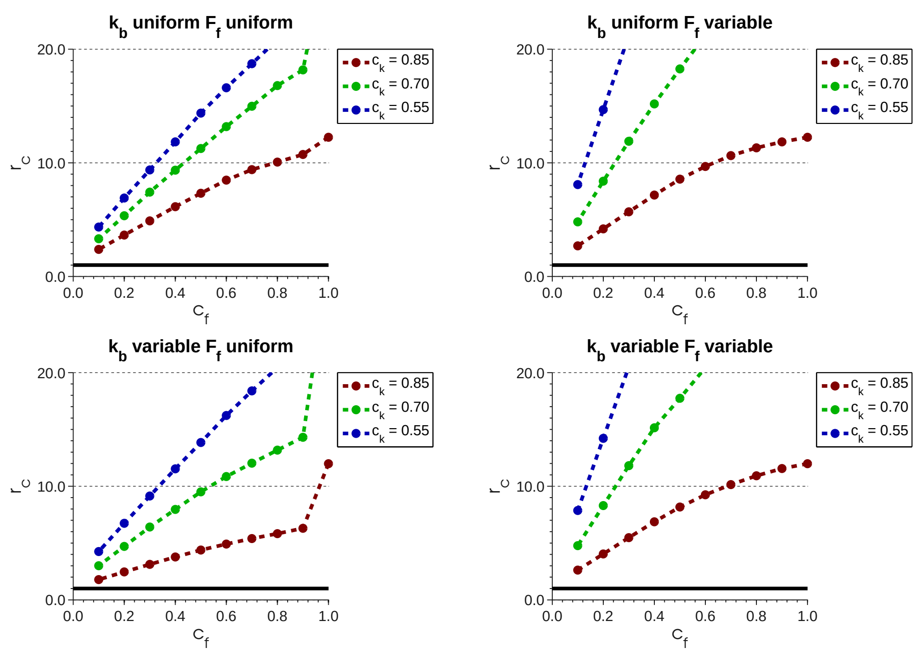

(b) FEMA Far Field seismic set

Figure 4.15: Normalized response r_{cg}, 9-story structure

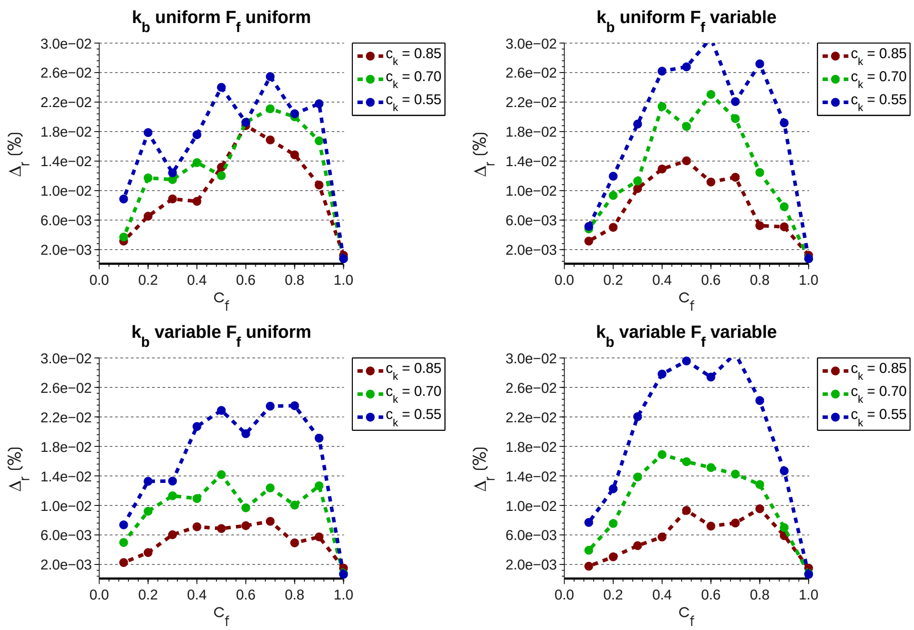

(a) Maule Earthquake seismic set

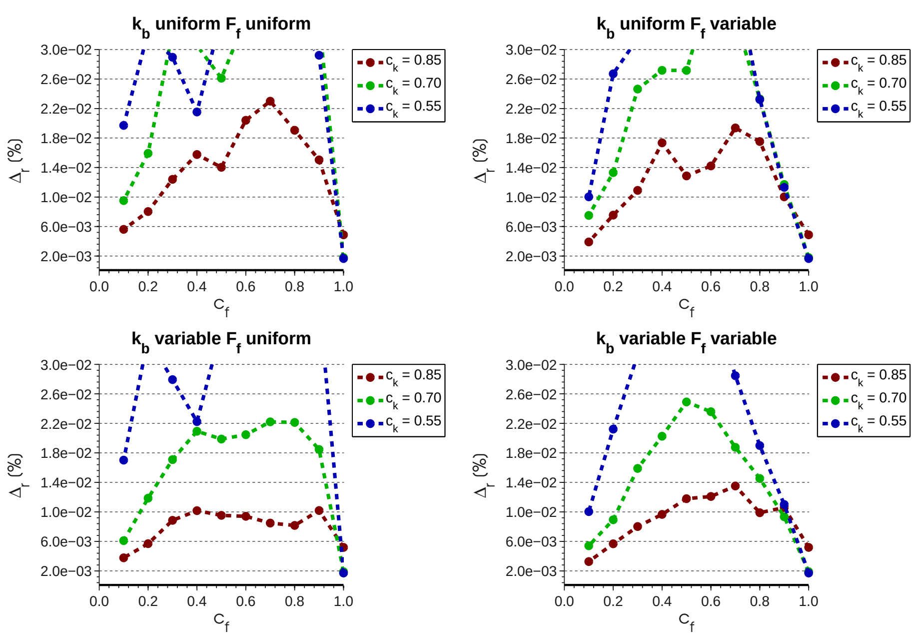

(b) FEMA Far Field seismic set

Figure 4.16: Response Δ_r, 9-story structure

4.4. Comparative analysis

In this section, a comparative analysis is carried out in order to more thoroughly determine how the seismic response of the friction-damped structures is affected by: 1) the number of stories of the structure; 2) the height-wise distribution of the mechanical properties of the friction dampers; and 3) the characteristics of the seismic excitation.

4.4.1. Influence of the number of stories

As a basis for comparison, the values of factor r_Δ shown in Figure 4.17 were obtained considering uniform height-wise distributions of both activation force and brace stiffness, and the Maule earthquake set.

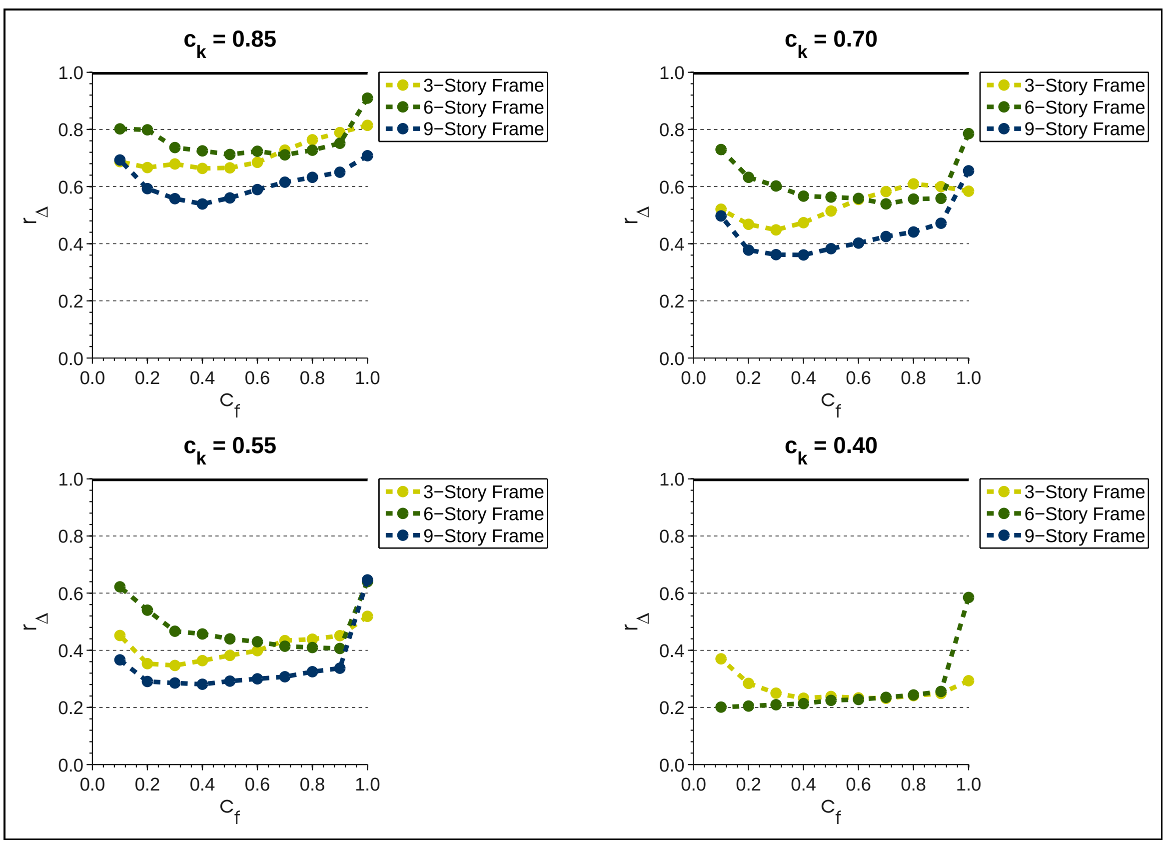

Figure 4.17: Normalized response r_Δ for frames with uniform height-wise distribution of activation force and brace stiffness

It is apparent in Figure 4.17 that the inter-story drift response is dependent on the number of stories. Adding elastic braces to the base 3-story structure results in a 19 % to 71 % response reduction, while the further addition of optimized friction devices results in a mere 6 % to 15 % additional reduction (Table 4.1). For the 6-story structure, however, the addition of elastic braces to the base structure results in a 10 % to 42 % response reduction, and the further addition of optimized friction devices results in a significant 20 % to 38 % additional reduction (Table 4.2). Similarly, adding elastic braces to the base 9-story structure results in a 30 % to 35 % response reduction, and the further addition of optimized friction devices results in a significant 17 % to 37 % additional reduction (Table 4.3). It is apparent that the inter-story drift response of the friction-damped 3-story structures is primarily controlled by the stiffness of the braces, and the influence of the friction devices is in general much less relevant. However, the inter-story drift response of the friction-damped 6- and 9-story structures is influenced by both the brace stiffness and the activation force, in roughly equal terms when the value of the activation force is the optimal value.

There is apparently no significant qualitative influence of the number of stories on the floor acceleration response (Figure 4.18). In quantitative terms, the influence of the number of stories is not negligible, but small in all cases. These observations are also applicable to the axial force demand on the central columns (factor r_{cg}, Figure 4.19), except than larger quantitative differences are observed for the 9-story structure.

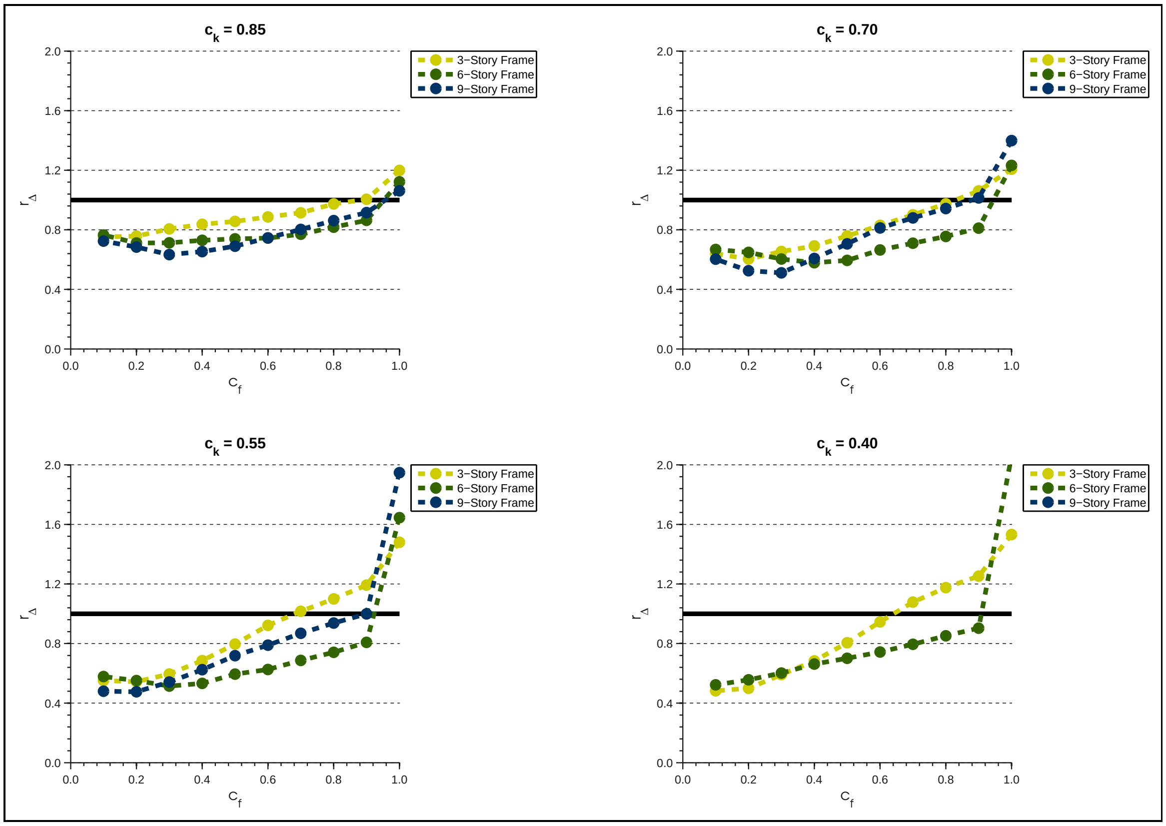

Figure 4.18: Normalized response r_a for frames with uniform height-wise distribution of activation force and brace stiffness

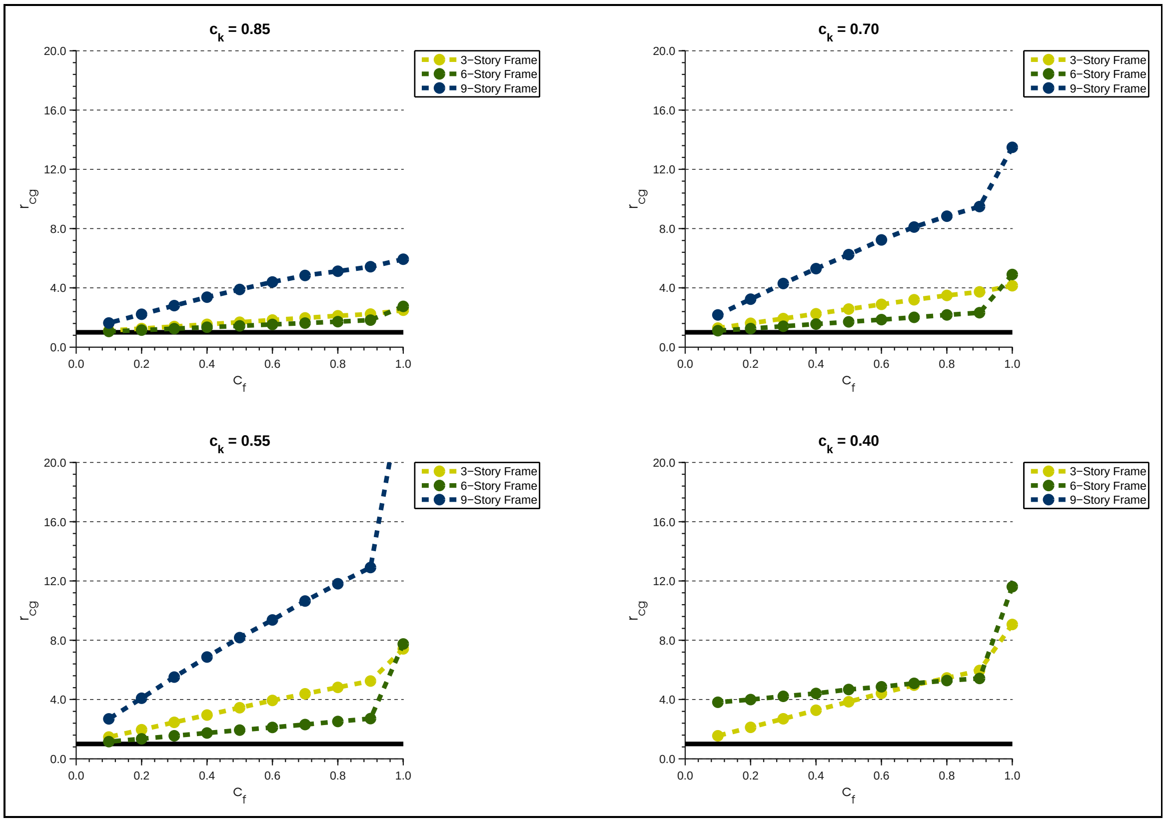

Figure 4.19: Normalized response r_{cg} for frames with uniform height-wise distribution of activation force and brace stiffness

4.4.2. Influence of the height-wise distributions of the properties of the friction-dampers

As a basis for comparison, values of factors r_Δ and r_a shown in this section were obtained considering the Maule earthquake set.

For the 3-story structure, it is clear that there is no significant influence of the height-wise distributions of either property of the friction dampers (Figure 4.20). The lack of influence of the distribution of the brace stiffness might be explained by the fact that the values of the variable brace stiffness are not very different from the ones of the uniform distribution (Table 3.3), which in turn is due to the fact that the first modal shape of the 3-story base structure is already similar to a straight line, hence the procedure described in Section 3.3.2 to set the values of the variable brace stiffness does not result in brace stiffness significantly different from those of the uniform distribution.

For the 6- and 9-story structures (Figure 4.21 and 4.22), it is observed that the height-wise distribution of the activation force does have an influence on the response, whereas the height-wise distribution of the brace stiffness again does not. At best, the latter has a very small influence on the floor acceleration response (Figure 4.21b and Figure 4.22b). This probably occurs due to the fact that even when the brace stiffness is variable, the height-wise variation of the story stiffness is still not very different from that when the brace stiffness is uniform. In the case of the inter-story drift response, however, the response for the variable height-wise distribution is somewhat greater than that for the uniform height-wise distribution (Figure 4.21a and Figure 4.22a). This is probably due to the fact that the procedure described in Section 3.3.2 considers only the first mode, and for the 6- and 9-story structures the contribution of higher modes is not negligible.

In Section 3.3.3 it was described that the uniform height-wise distribution of the activation force implies assigning an equal activation force F_f at every story, calculated as a fraction c_f of the minimum elastic demand min(F_e) on the braces of the braced structure. For all stories except for the one at the which the elastic demand is equal to min(F_e), the actual elastic demand will be larger than min(F_e), but since the activation force is the same at all stories, the activation force to elastic demand ratio is less than c_f, resulting in a damping effect that is larger than that suggested by the value of c_f. As a consequence, the response can be expected to be different from the one corresponding to the same value of c_f but with a variable distribution of the activation force. The latter distribution implies that the activation force to elastic demand ratio is the same at every story, which results in lesser damping effects.

The floor acceleration response of the 3-story structure is essentially insensitive to the height-wise distribution of the activation force. This is probably due to the small differences in the elastic demand on the braces of the braced structure, hence the variable activation forces are not very different from those of the uniform distribution. The floor acceleration response of the 6- and 9-story structures, on the other hand, is indeed influenced by the height-wise distribution of the activation force. This influence vary from very important at large values of c_f, and diminishes up to insignificant as the value of c_f tends to zero. For instance, when $c_f = 0.8$ and $c_k = 0.70$, $r_a \approx 1.1$ for the variable distribution whereas $r_a \approx 0.75$ for the uniform distribution. However, when $c_f = 0.3$ and $c_k = 0.70$, $r_a \approx 0.65$ for the variable distribution and $r_a \approx 0.60$ for the uniform distribution. The reason why the responses for both distributions tend to converge at small values of c_f is most likely due to the fact that at small values of c_f the ratio of activation force to elastic demand takes similar values at all stories, hence the variable distribution becomes somewhat similar to the uniform distribution.

The influence of the height-wise distribution of the activation force on the inter-story drift response is similar to that on the floor acceleration response when the value of c_f is relatively high. For instance, when $c_f = 0.8$ and $c_k = 0.70$, $r_\Delta \approx 0.8$ for the variable distribution whereas $r_\Delta \approx 0.55$ for the uniform distribution. When the value of c_f is small, however, the influence on r_Δ is different from that on r_a. For instance, when $c_f = 0.3$ and

$c_k = 0.70$, $r_\Delta \approx 0.5$ for the variable distribution whereas $r_\Delta \approx 0.62$ for the uniform distribution. This is related to the optimal value of c_f, optimal meaning the value for which the response is minimized. For the floor acceleration response, the optimal value of c_f is always a very low value, usually equal to 0.1 or 0.2, and essentially independent of the number of stories and the distribution of the activation force. For the inter-story drift response, on the other hand, the optimal value of c_f is greater than 0.1, 0.2 in almost all cases, exhibits a much larger range of possible values, and is highly dependent on the number of stories and the distribution of the activation force. Hence, the influence of the distribution of the activation on the inter-story drift response is still significant when the value of c_f is relatively small, and the uniform distribution does not always results in lesser responses.

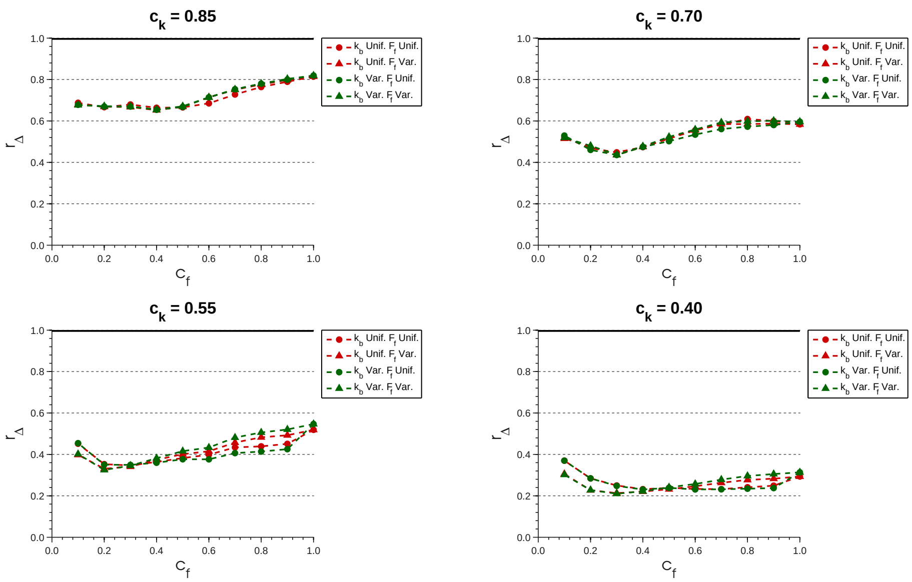

(a) Normalized response r_Δ for 3-story structure subjected to Maule seismic set

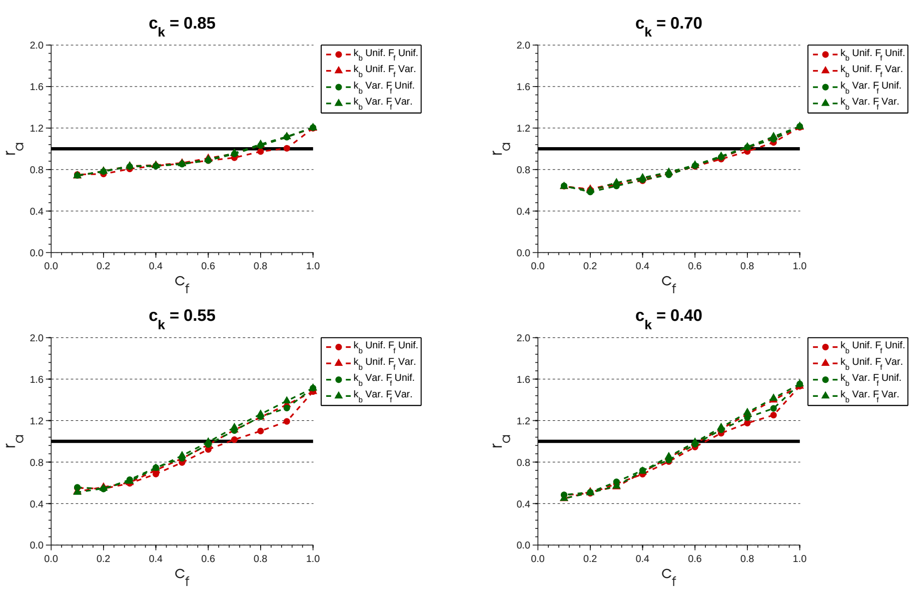

(b) Normalized response r_a for 3-story structure subjected to Maule seismic set

Figure 4.20: Normalized responses r_Δ and r_a for 3-story structure with different height-wise distributions of the mechanical properties of the friction dampers

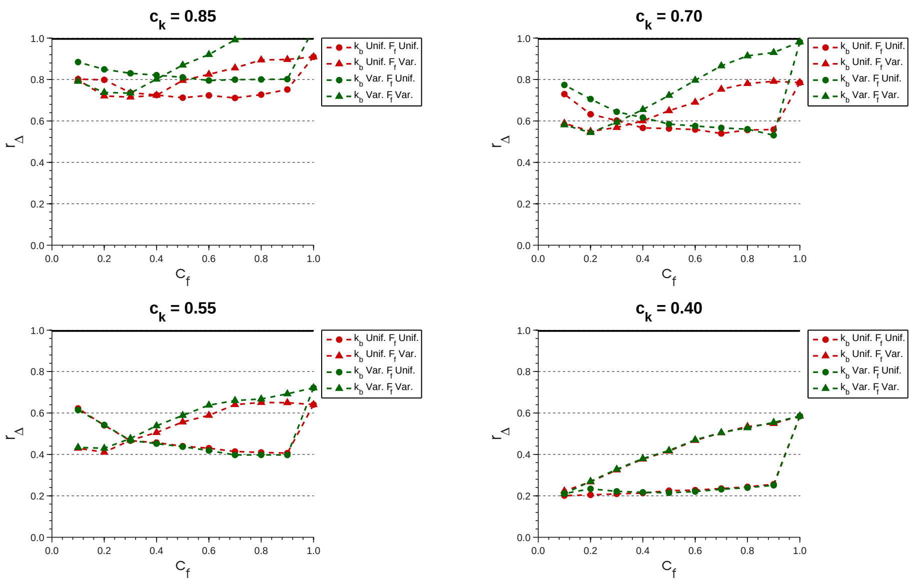

(a) Normalized response r_Δ for 6-story structure subjected to Maule seismic set

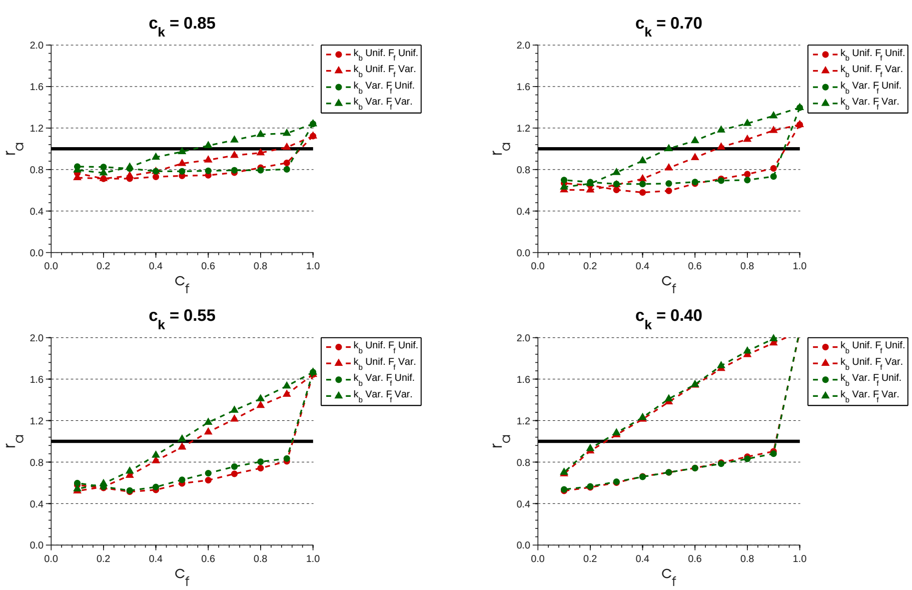

(b) Normalized response r_a for 6-story structure subjected to Maule seismic set

Figure 4.21: Normalized responses r_Δ and r_a for 6-story structure with different height-wise distributions of the mechanical properties of the friction dampers

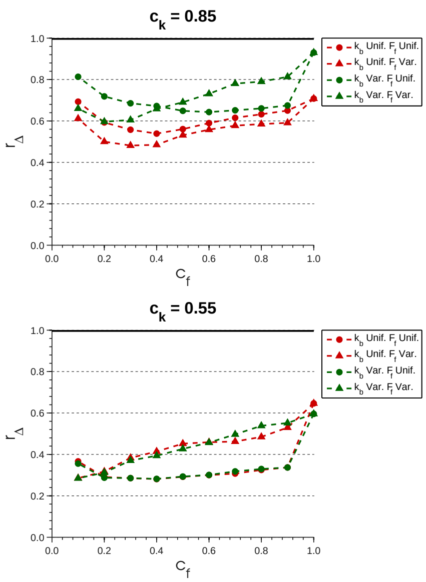

(a) Normalized response r_Δ for 9-story structure subjected to Maule seismic set

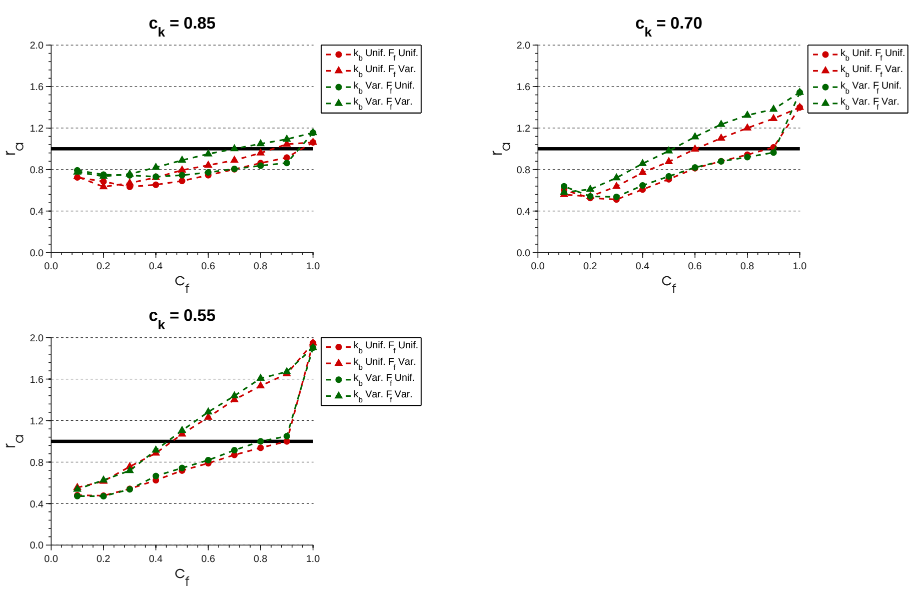

(b) Normalized response r_a for 9-story structure subjected to Maule seismic set

Figure 4.22: Normalized responses r_Δ and r_a for 9-story structure with different height-wise distributions of the mechanical properties of the friction dampers

4.4.3. Influence of the characteristics of the seismic excitation

As a basis for comparison, values of factors r_Δ and r_a shown in this section were obtained considering uniform height-wise distributions of both activation force and brace stiffness.

It is observed in Figures 4.23, 4.24 and 4.25 that the influence of the seismic excitation on the response is qualitatively insignificant, regardless of the number of stories. There exist slight quantitative differences, being the response to the FEMA P-695 set of records generally somewhat greater than that to the Maule set. While some difference is logical due to the fact that the sets are made up of records having very different characteristics, the difference turned out to be much less than expected, which is similar to the small differences that were observed between the median response spectra of both sets (Figure 3.4).

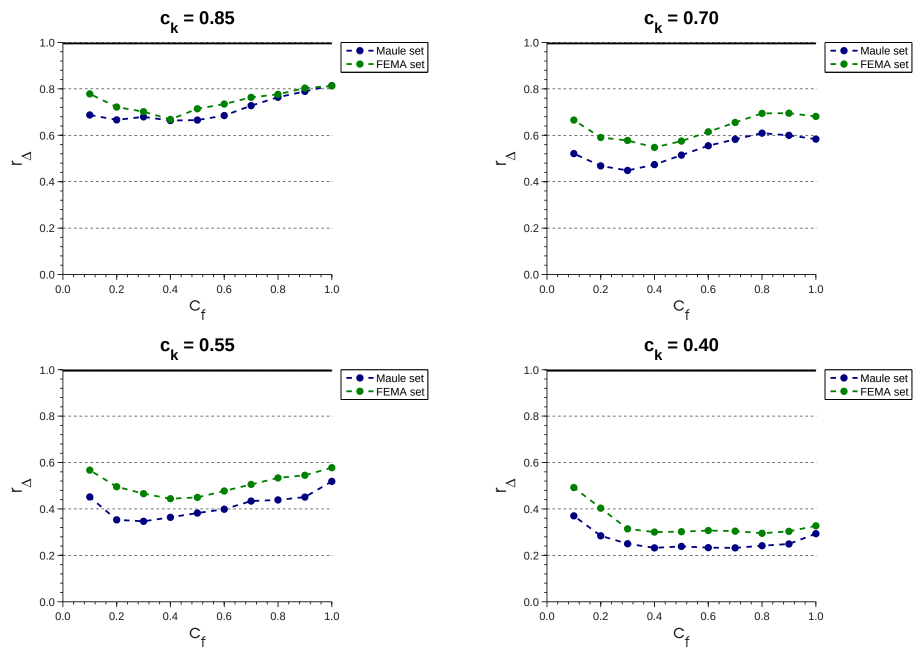

(a) Normalized response r_Δ for 3-story structure uniform height-wise distribution of brace stiffness and activation force

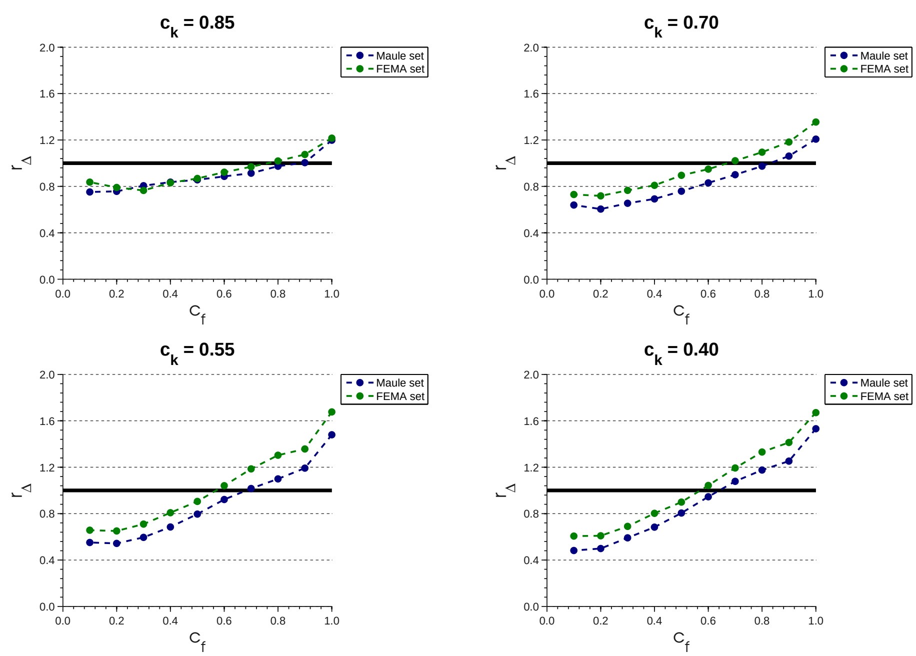

(b) Normalized response r_a for 3-story structure uniform height-wise distribution of brace stiffness and activation force

Figure 4.23: Normalized responses r_Δ and r_a for 3-story structure with different seismic excitations

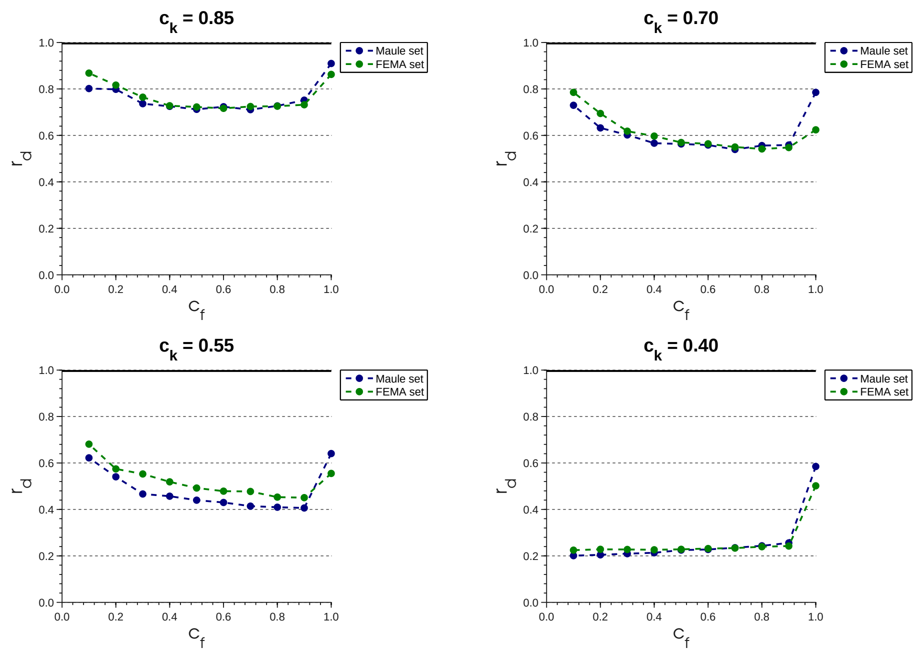

(a) Normalized response r_Δ for 6-story structure uniform height-wise distribution of brace stiffness and activation force

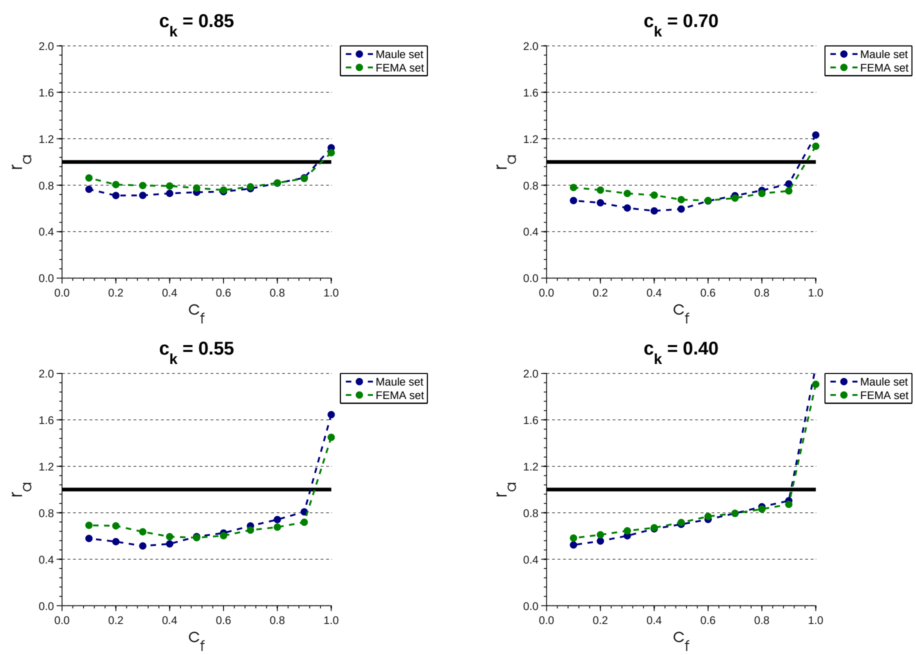

(b) Normalized response r_a for 6-story structure uniform height-wise distribution of brace stiffness and activation force

Figure 4.24: Normalized responses r_Δ and r_a for 6-story structure with different seismic excitations

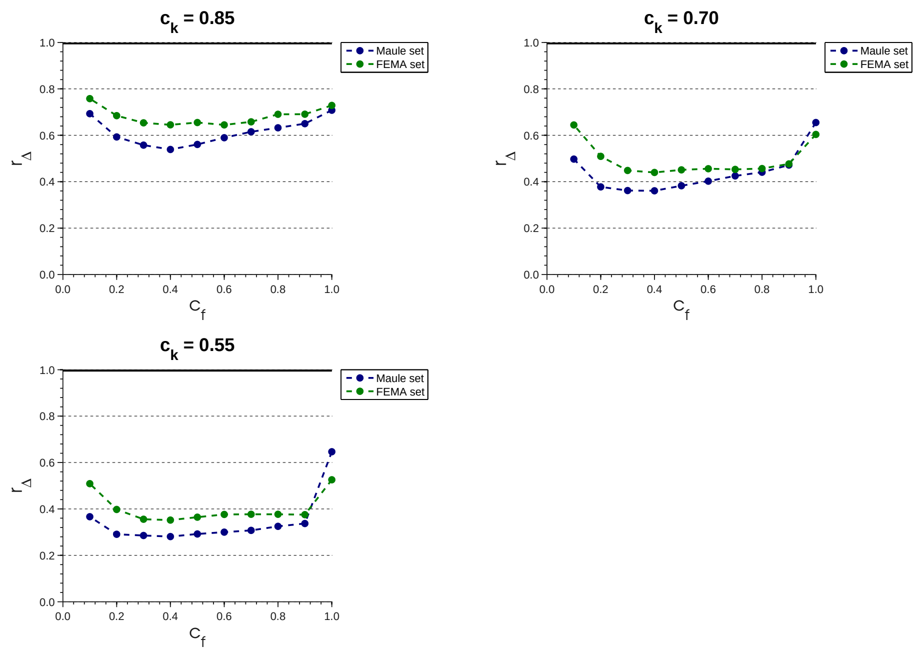

(a) Normalized response r_Δ for 9-story structure uniform height-wise distribution of brace stiffness and activation force

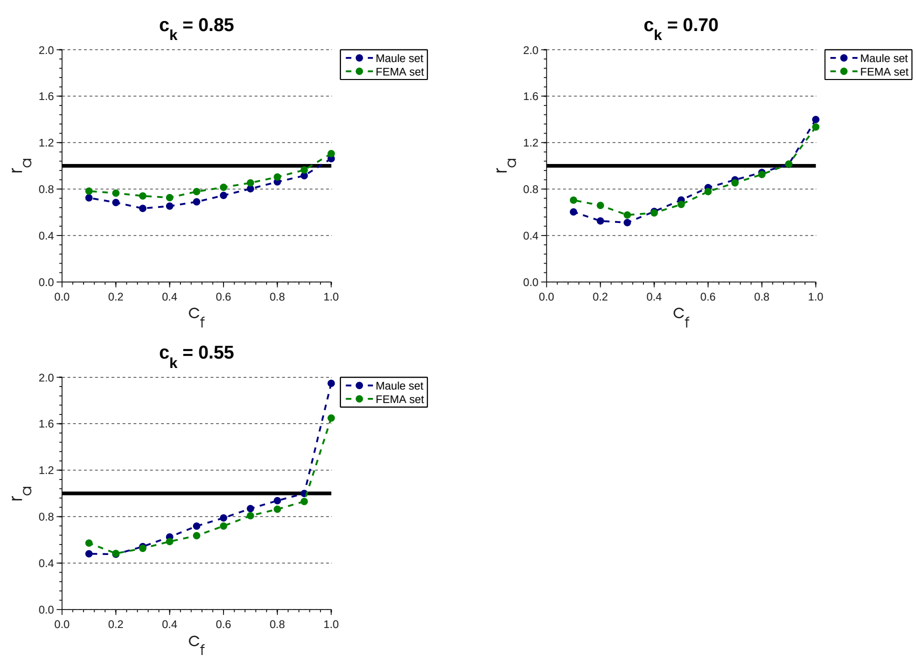

(b) Normalized response r_a for 9-story structure uniform height-wise distribution of brace stiffness and activation force

Figure 4.25: Normalized responses r_Δ and r_a for 9-story structure with different seismic excitations

5. FINAL REMARKS

In this study, the influence of the mechanical properties (brace stiffness and activation force) of friction dampers on the seismic response of three steel structures of 3, 6 and 9 stories was studied through nonlinear time-history analysis of these structures. The analysis was done considering two sets of real earthquake records obtained, respectively, from the 2010 Maule Earthquake and the FEMA P-695 far-field set. By comparing the response of the friction-damped structures to that of the base structures (i.e., the same structures but without friction dampers), the influence of the mechanical properties of the friction dampers on the seismic response was identified.

5.1. Conclusions

From previous studies on SDOF systems it is known that the brace stiffness mainly controls the inter-story drift response. The activation force controls the floor acceleration response, but has little influence on the inter-story drift response. This study concludes that the extension of such observations to MDOF structures greatly depends on the number of stories. For the 3-story structure considered in this study, the observations valid for SDOF systems still hold true, as this study shows that the addition of elastic braces to the base structure results in inter-story drift reductions that range from 20 % when $c_k = 0.85$ to 70 % when $c_k = 0.40$, while the further addition of optimal friction devices (i.e., with an activation force F_f that minimizes the response) to an already braced structure provides small additional reductions (6 % to 15 %). This however, does not apply to the 6- and 9-story structures, where adding elastic braces to the base structure results in inter-story drift response reductions of 9 % to 42 % for the 6-story structure, and 30 % to 35 % for the 9-story structure, and further adding optimal friction devices to the already braced structure results in further reductions of 20 % to 38 % for the 6-story structure and 17 % to 37 % for the 9-story structure. Therefore it is concluded that the influence of the activation force on the inter-story drift response is not independent of the number of stories of the structure:

it seems to increase as the number of stories increases.

This study also provides insight into the influence on the response of the height-wise distribution of brace stiffness and activation force. While the influence of the distribution of brace stiffness was found to be not significant, the influence of the distribution of the activation force turned out to range from not relevant for the 3-story structure to very important for the 6- and 9-story structures. The inter-story drift response of the latter structures is less when the distribution is uniform and the activation forces are relatively high, but the difference becomes less significant when the values of the activation forces are the optimal values. The floor acceleration response of these structures is also less when the distribution is uniform, but the difference becomes irrelevant only when the activation force is very small. These last observations are also applicable to the axial force demand on the central columns.

This study also concluded that for the seismic sets studied, the source and characteristics of the seismic records did not affect how the mechanical properties qualitatively influence the seismic response of the structures, notwithstanding some minor quantitative effects. This however cannot be generalized due to the surprising similarity that resulted between the median response spectra of both sets of records.

Based on the previous conclusions, this study also proposes practical design criteria and procedures to help design supplemental friction dampers. These criteria, especially useful for preliminary design, are based on the figures presented in Sections 4.1, 4.2 and 4.3, which show how the seismic response of the three structures studied change based on the values of the mechanical properties (brace stiffness and activation force) of the friction dampers. By determining the desired reduction of one specific response quantity, for example, inter-story drift, the bracing stiffness and the activation force can be determined. The resulting increments or decrements of other response quantities can be checked in order to ensure that they fall within acceptable ranges of design, and thus the mechanical properties of the friction dampers can be adjusted in order to satisfy all desired criteria. Further, based on the previously mentioned conclusions, it can be determined that the brace stiffness should uniformly distributed, and the height-wise distribution of the activation force is determined based on the number of stories and the response quantity that controls the design.

5.2. Future work

In order to better understand how the mechanical properties of friction dampers affect the seismic response of steel structures, a similar study with more consideration of the nonlinear behavior of the steel structure should be considered. Base structures similar to the ones considered in this study, but modeled considering inelastic behavior and other effects such as P-Δ or large deformations, may better determine if the observations found in this study still hold. A complementary study, or extension, of the previously described proposal might consider 3D models of the buildings. An extensive numerical analysis of such models might be computationally expensive, but based on the findings of this study, the range of values of the parameters of interest can be refined so that only the most relevant cases are analyzed. Most important is probably the study of structures having a greater number of stories.

Complementary to the previously mentioned studies, it is recommended that some of the analysis carried out in this study be experimentally reproduced. Due to the relatively limited amount of tests that are feasible to conduct, the results of this study could help select the number and characteristics of the seismic records to be used in the proposed study, and the values of interest of the activation force and brace stiffness to be considered. The previously considered studies in combination with this present study, could eventually lead to criteria and recommendations for Performance-Based Design (PBD).

BIBLIOGRAPHY

Aiken, I. D., Kelly, J., and Pall, A. (1988). Seismic response of a nine-story steel frame with friction damped cross-bracing. *Rep. No. UCB/EERC*, 88:17.

Aiken, I. D., Nims, D., and Kelly, J. M. (1992). Comparative study of four passive energy dissipation systems. *Bull. New Zealand Nat. Soc. For Earthquake Engrg*, 25(3):175–192.

Aiken, I. D., Nims, D. K., Whittaker, A. S., and Kelly, J. M. (1993). Testing of passive energy dissipation systems. *Earthquake spectra*, 9(3):335–370.

Barrientos, S. (2010). Terremoto cauquenes 27 febrero 2010. *Servicio Sismologico. Universidad de Chile (www. sismologia. cl)*.

Chopra, A. K. (1995). *Dynamics of structures*, volume 3. Prentice Hall New Jersey.

Christopoulos, C., Filiatrault, A., and Bertero, V. V. (2006). *Principles of passive supplemental damping and seismic isolation*. IUSS Press.

Colajanni, P. and Papia, M. (1995). Seismic response of braced frames with and without friction dampers. *Engineering structures*, 17(2):129–140.

Constantinou, M., Mokha, A., and Reinhorn, A. (1990). Teflon bearings in base isolation ii: Modeling. *Journal of Structural Engineering*, 116(2):455–474.

Constantinou, M. C. and Symans, M. (1992). *Experimental and analytical investigation of seismic response of structures with supplemental fluid viscous dampers*. National Center for earthquake engineering research.

FEMA P-695 (2009). Quantification of building seismic performance factors.

Filiatrault, A. and Cherry, S. (1987). Performance evaluation of friction damped braced steel frames under simulated earthquake loads. *Earthquake Spectra*, 3(1):57–78.

Filiatrault, A. and Cherry, S. (1988). Comparative performance of friction damped systems and base isolation systems for earthquake retrofit and aseismic design. *Earthquake engineering & structural dynamics*, 16(3):389–416.

Fitzgerald, T., Anagnos, T., Goodson, M., and Zsutty, T. (1989). Slotted bolted connections in aseismic design for concentrically braced connections. *Earthquake Spectra*, 5(2):383–391.

Geschwindner, L. F. (2002). A practical look at frame analysis, stability and leaning columns. *Engineering Journal*, 39(4):167–181.

Grigorian, C. E., Yang, T.-S., and Popov, E. P. (1993). Slotted bolted connection energy dissipators. *Earthquake Spectra*, 9(3):491–504.

Gupta, A. and Krawinkler, H. (1999). *Seismic demands for the performance evaluation of steel moment resisting frame structures*. PhD thesis, Stanford University.

Hall, J. F. (1995). Parameter study of the response of moment-resisting steel frame buildings to near-source ground motions.

Hamburger, R. O., Krawinkler, H., Malley, J. O., and Adan, S. M. (2009). *Seismic design of steel special moment frames: a guide for practicing engineers*.

Mazzoni, S., McKenna, F., Scott, M. H., Fenves, G. L., and Jeremic, B. (2006). Open system for earthquake engineering simulation (opensees). *Berkeley, California*.

Moreschi, L. and Singh, M. (2003). Design of yielding metallic and friction dampers for optimal seismic performance. *Earthquake engineering & structural dynamics*, 32(8):1291–1311.

Ohtori, Y., Christenson, R., Spencer Jr, B., and Dyke, S. (2004). Benchmark control problems for seismically excited nonlinear buildings. *Journal of Engineering Mechanics*, 130(4):366–385.

Pall, A. S. and Marsh, C. (1982). Response of friction damped braced frames. *Journal of Structural Engineering*, 108(9):1313–1323.

Popov, E. P., Yang, T.-S., and Grigorian, C. E. (1993). New directions in structural seismic designs. *Earthquake Spectra*, 9(4):845–875.

Sabelli, R., Mahin, S., and Chang, C. (2003). Seismic demands on steel braced frame buildings with buckling-restrained braces. *Engineering Structures*, 25(5):655–666.

Towashiraporn, P., Park, J., Goodno, B., and Craig, J. (2002). Passive control methods for seismic response modification. *Progress in Structural Engineering and Materials*, 4(1):74–86.

Venuti, W. J. (1976). Energy absorbtion of high strength bolted connections. *Test Report*.

Vergara, L. J. (2012). Respuesta sísmica de estructuras equipadas con disipadores de fricción.

Vulcano, A. and Mazza, F. (2000). Comparative study of the seismic performance of frames using different dissipative braces. In *Proceedings of the 12th World Conference on Earthquake Engineering*.

Youssef, N. F., Bonowitz, D., and Gross, J. L. (1995). *A survey of steel moment-resisting frame buildings affected by the 1994 Northridge earthquake*. US National Institute of Standards and Technology.

APPENDIX

A. ACTIVATION FORCES

The activation forces of the friction devices of the friction-damped structures depend on several factors. As described in the main body of the thesis, for each of the three base structures, there are two possible braced structures, with a uniform or variable height-wise distribution of brace stiffness. For each of those two possible braced structures, there are two possible friction-damped structures, with uniform or variable height-wise distribution of activation force. In other words there are 4 possible friction-damped structures for each of the three base structures. Since the activation force is calculated as a fraction of the elastic demand of the braces, the value of the activation force F_f also depends on the seismic set used, this results in a total of 8 combination of possible activation forces for each structure, i.e., a total of 24 set of friction-damped structures. The activation forces F_f shown here were obtained for each of the four possible friction-damped structures of the three base structures calculated using the Maule set.

Table A.1: Activation force F_f [kgf] (Uniform height-wise distribution based on Maule set)

	$c_k = 0.85$	$c_k = 0.70$	$c_k = 0.55$	$c_k = 0.40$
3-Story Frame	1.772×10^5	3.753×10^5	5.695×10^5	6.556×10^5
6-Story Frame	0.665×10^5	1.0781×10^5	1.414×10^5	1.8216×10^5
9-Story Frame	2.219×10^5	4.079×10^5	5.645×10^5	7.160×10^5

Table A.2: Activation force F_f [kgf] (Variable height-wise distribution based on Maule set)

	$c_k = 0.85$	$c_k = 0.70$	$c_k = 0.55$	$c_k = 0.40$
1st Floor	0.177×10^6	0.3897×10^6	0.8248×10^6	1.103×10^6
2nd Floor	0.218×10^6	0.422×10^6	0.834×10^6	1.032×10^6
3rd Floor	0.206×10^6	0.375×10^6	0.570×10^6	0.656×10^6

Table A.3: Activation force F_f [kgf] (Variable height-wise distribution based on Maule set)

	$c_k = 0.85$	$c_k = 0.70$	$c_k = 0.55$	$c_k = 0.40$
1st Floor	0.171×10^6	0.3992×10^6	0.754×10^6	1.202×10^6
2nd Floor	0.135×10^6	0.301×10^6	0.558×10^6	0.873×10^6
3rd Floor	0.129×10^6	0.291×10^6	0.490×10^6	0.755×10^6
4th Floor	0.122×10^6	0.268×10^6	0.421×10^6	0.610×10^6
5th Floor	0.105×10^6	0.208×10^6	0.339×10^6	0.458×10^6
6th Floor	0.067×10^6	0.108×10^6	0.141×10^6	0.182×10^6

Table A.4: Activation force F_f [kgf] (Variable height-wise distribution based on Maule set)

	$c_k = 0.85$	$c_k = 0.70$	$c_k = 0.55$	$c_k = 0.40$
1st Floor	0.321×10^6	1.010×10^6	2.048×10^6	2.600×10^6
2nd Floor	0.264×10^6	0.780×10^6	1.646×10^6	2.106×10^6
3rd Floor	0.249×10^6	0.653×10^6	1.448×10^6	1.883×10^6
4th Floor	0.226×10^6	0.581×10^6	1.170×10^6	1.569×10^6
5th Floor	0.227×10^6	0.592×10^6	1.033×10^6	1.265×10^6
6th Floor	0.222×10^6	0.579×10^6	1.025×10^6	1.059×10^6
7th Floor	0.270×10^6	0.630×10^6	1.064×10^6	1.216×10^6
8th Floor	0.283×10^6	0.601×10^6	0.954×10^6	1.069×10^6
9th Floor	$0..225 \times 10^6$	0.408×10^6	0.565×10^6	0.716×10^6

B. SEISMIC RECORDS

Two set of seismic records were used to simulate the seismic excitation with which the numerical simulations of this study were carried out: one obtained from records obtained from the Maule earthquake of 2010, and the other from the FEMA P-695 far-field set. Basic information of the two set of seismic records, the Maule set and the far-field set, used in this study is included as follows.

Table B.1: Data of the Maule set of seismic records

Record information		
Rec. Station	PGA_{max} [g]	PGV_{max} [cm/s^2]
Angol	0.93	38
Campus Antumapu	0.27	25
Cerro Calán	0.22	30
Constitución	0.63	69
Curicó	0.48	33
Hualañe	0.45	39
Llolleo	0.56	31
Matanzas	0.34	43
Melipilla	0.77	78
Papudo	0.42	25
Santiago Centro	0.31	26
Santiago La Florida	0.19	15
Santiago Maipú	0.56	44
Santiago Peñalolen	0.30	29
Santiago Puente Alto	0.27	31
Talca	0.47	33
Valparaíso Almendral	0.27	29
Valparaíso UTFSM	0.30	16
Viña del Mar Centro	0.33	33
Viña del Mar El Salto	0.35	45

Table B.2: Data of the FEMA Far-field set of seismic records

Seismic event			Record information		
M_w	Year	Event Loc.	Rec. Station	PGA$_{max}$ [g]	PGV$_{max}$ [cm/s^2]
6.7	1994	Northridge, USA	Beverly Hills- Mullhol	0.52	63
6.7	1994	Northridge, USA	Canyon Country-WLC	0.48	45
7.1	1999	Duzce, Turkey	Bolu	0.82	62
7.1	1999	Hector Mine, USA	Hector	0.34	42
6.5	1979	Imperial Valley, USA	Delta	0.35	33
6.5	1979	Imperial Valley, USA	El Centro Area #11	0.38	42
6.9	1995	Kobe, Japan	Nishi-Akashi	0.51	37
6.9	1995	Kobe, Japan	Shin-Osaka	0.24	38
7.5	1999	Kocaeli, Turkey	Duzce	0.36	59
7.5	1999	Kocaeli, Turkey	Arcelik	0.22	40
7.3	1992	Landers, USA	Yermo Fire Station	0.24	52
7.3	1992	Landers, USA	Coolwater	0.42	42
6.9	1989	Loma Prieta, USA	Capitola	0.53	35
6.9	1989	Loma Prieta, USA	Gilroy Array #3	0.56	45
7.4	1990	Manjil, Iran	Abbar	0.51	54
6.5	1987	Superstition Hills, USA	El Centro Imp, Co.	0.36	46
6.5	1987	Superstition Hills, USA	Poe Road (temp)	0.45	36
7.0	1992	Cape Mendocino, USA	Rio Dell Overpass	0.55	44
7.6	1999	Chi-Chi, Taiwan	CHY101	0.44	115
7.6	1999	Chi-Chi, Taiwan	TCU045	0.51	39
6.5	1971	San Fernando, USA	LA-Hollywood Stor	0.21	19
6.5	1976	Friuli, Italy	Tolmezzo	0.35	31

C. MODAL SHAPES OF BRACED STRUCTURES

The first modal shape of each braced structure of 3, 6 and 9 stories are shown. This comparison allows to observe the difference in modal shape between using a uniform or variable height-wise distribution of brace stiffness. As a reference value, the linear mode shape is included, as one of the objectives of the procedure used for obtaining the values of brace stiffness for the variable height-wise was to obtain a modal shape which diverged less from the linear mode.

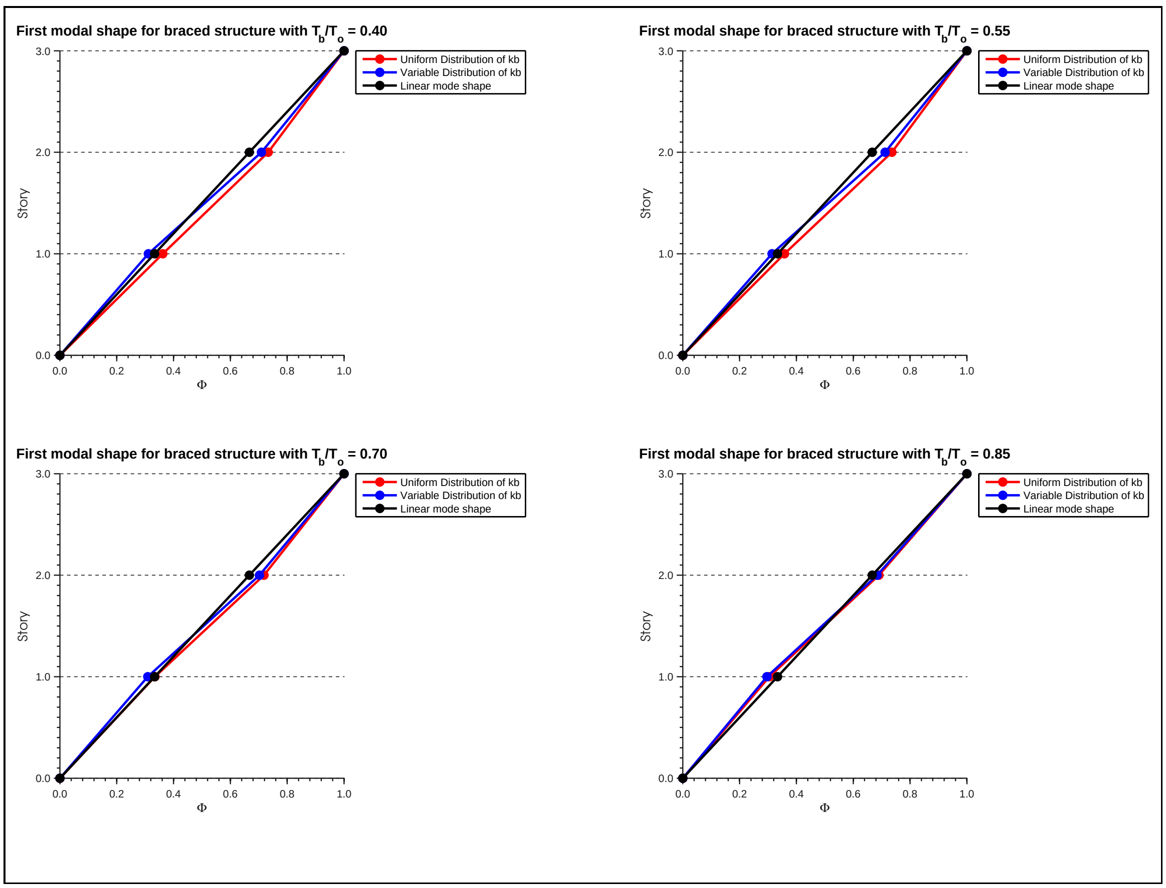

Figure C.1: First modal shape of the braced 3-story structure

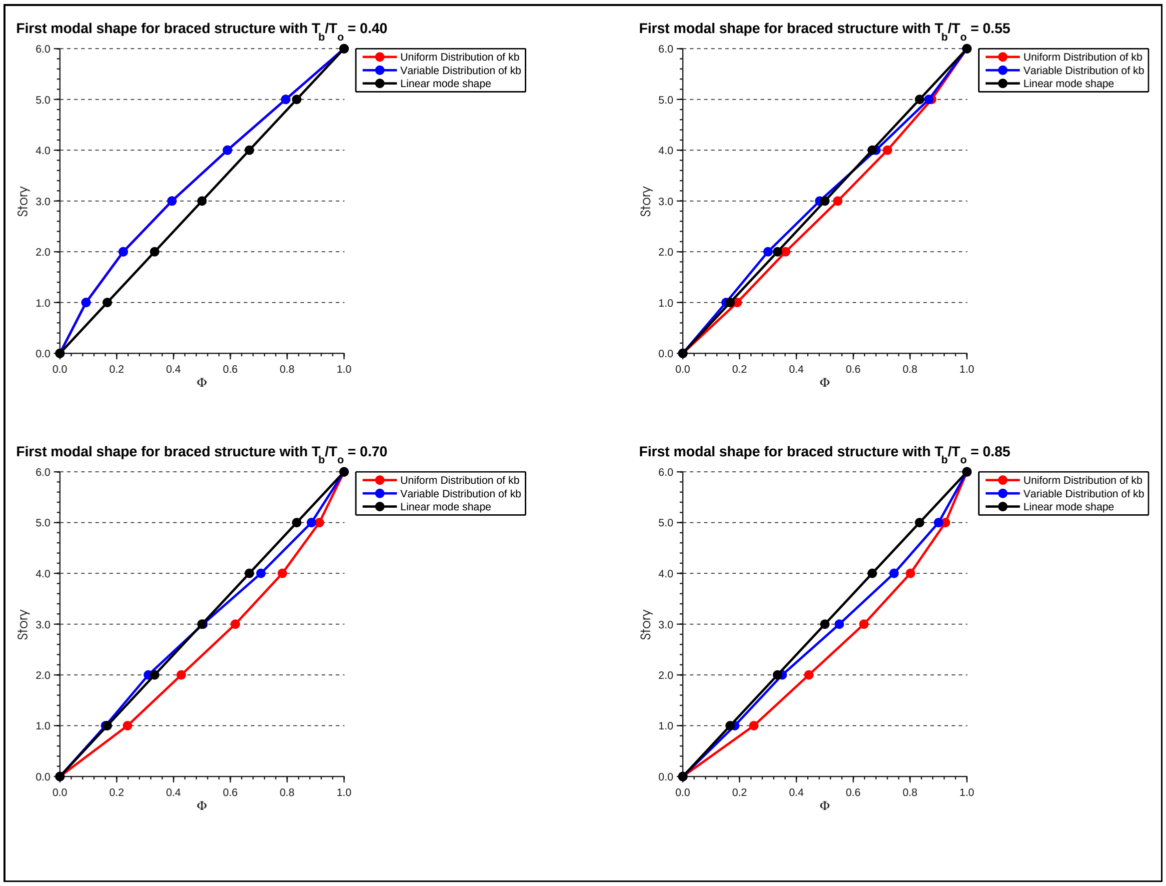

Figure C.2: First modal shape of the braced 6-story structure

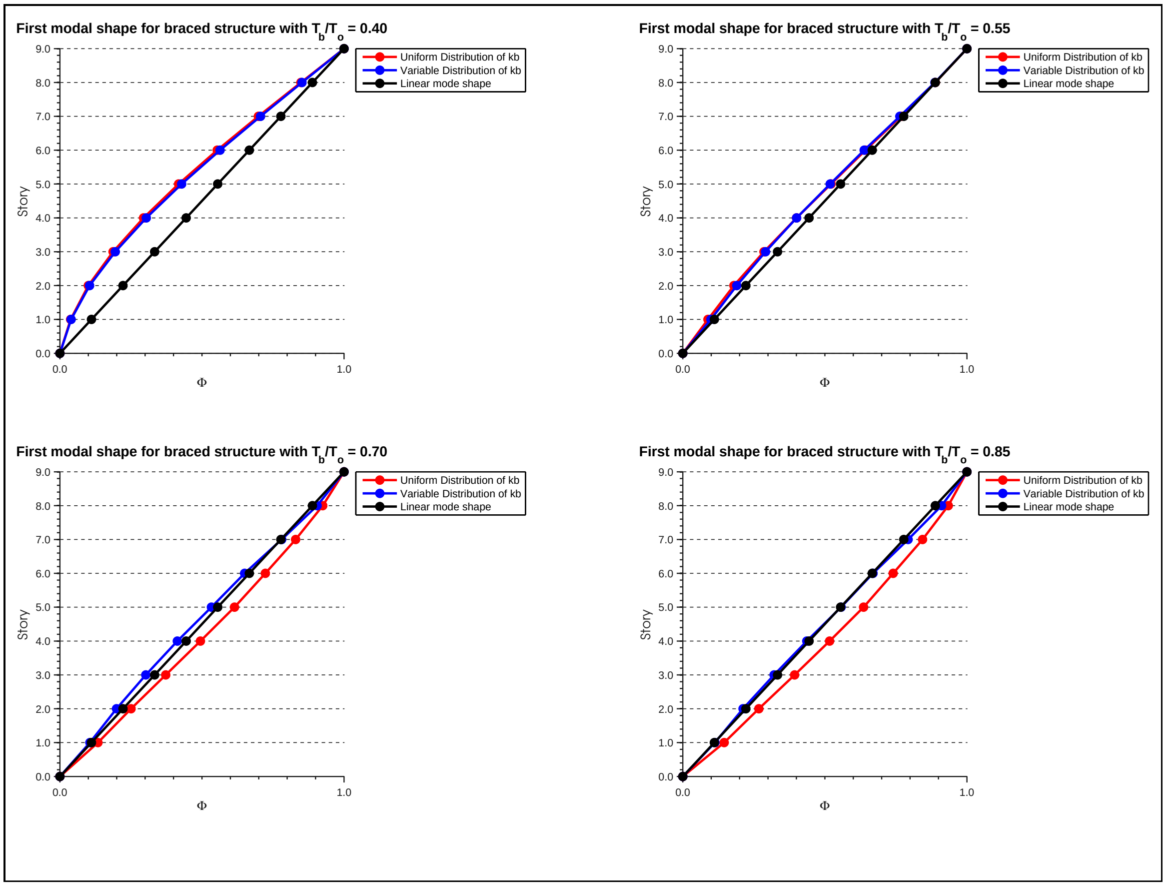

Figure C.3: First modal shape of the braced 9-story structure